

**Structural Limitations in the  
Scale-up of Anode Supported  
SOFCs**

**Final Report to DOE NETL**

**October 9th, 2002**

TIAX, LLC.  
Acorn Park  
Cambridge, Massachusetts  
02140-2390

75570-00

# Outline of Final Report

---

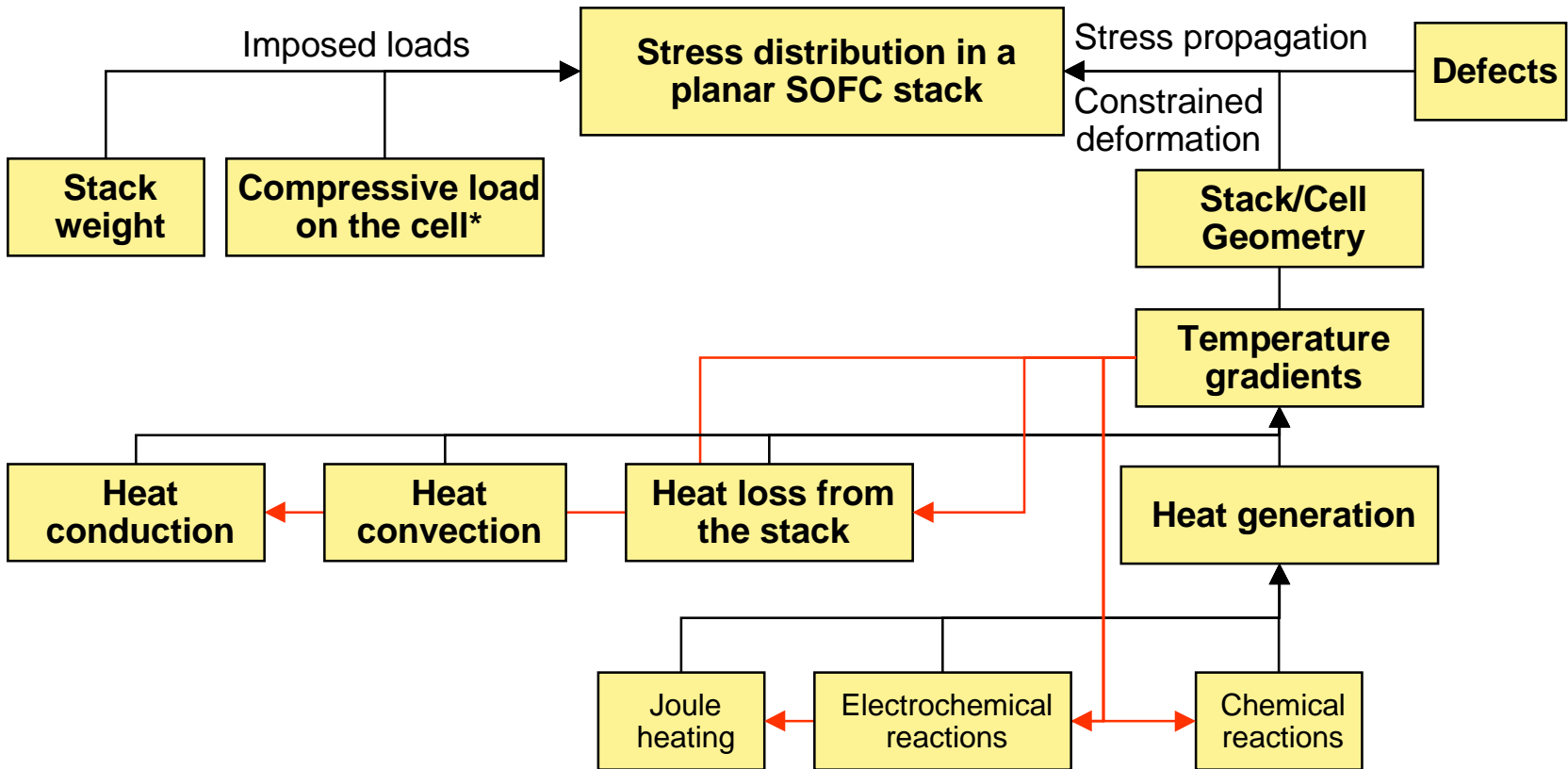
<b>0</b>	<b>Executive Summary</b>
<b>1</b>	<b>Background &amp; Objectives</b>
<b>2</b>	<b>Approach &amp; Scope</b>
<b>3</b>	<b>Model Development</b>
<b>4</b>	<b>Single Channel SOFC Results</b>
<b>5</b>	<b>Multi Channel SOFC Results</b>
<b>6</b>	<b>Limitations for Cell Size</b>
<b>7</b>	<b>Summary</b>
<b>A</b>	<b>Appendix</b>



**This study was intended to help identify any fundamental thermo-mechanical limitations that might limit stack scale-up.**

- The SECA strategy is to develop cost-effective modular planar SOFC stack technology that could be applied to a broad range of applications:
  - Application of similar stack design to multiple applications would accelerate stack cost reduction
  - Applications range from small-capacity applications (< 10 kW) with 1-4 stacks, to larger power plants (> 250 kW) with hundreds of stacks.
- Scale-up of individual stacks would offer economy of scale benefits and considerably simplify manifolding in larger systems.
- Single stack capacity is determined by the power density, the number of cells, and by the unit cell active area.
- Power density and number of cells are limited by unit cell performance and mechanical and flow-distribution considerations.
- Developers have found that when scaling up planar cells much beyond 100 cm<sup>2</sup> active area they become prone mechanical failure.

**The mechanical stress distribution in a planar SOFC is governed by a combination of design parameters and operating conditions.**



\* necessary for sealing and electrical interconnection in many planar stack designs

**The non-linear interactions among these phenomena make purely empirical characterization impractical and one-by-one analysis difficult.**



**The aim of this study was to develop a structural model to assess impact of operating conditions and scale-up on SOFC thermo-mechanical stresses.**

### **Deliverables**

- Profiles of temperature and mechanical stresses for normal operation of a typical planar anode supported SOFC with cross-flow of reactants.
- Sensitivity of these profiles to relevant operating and design variables

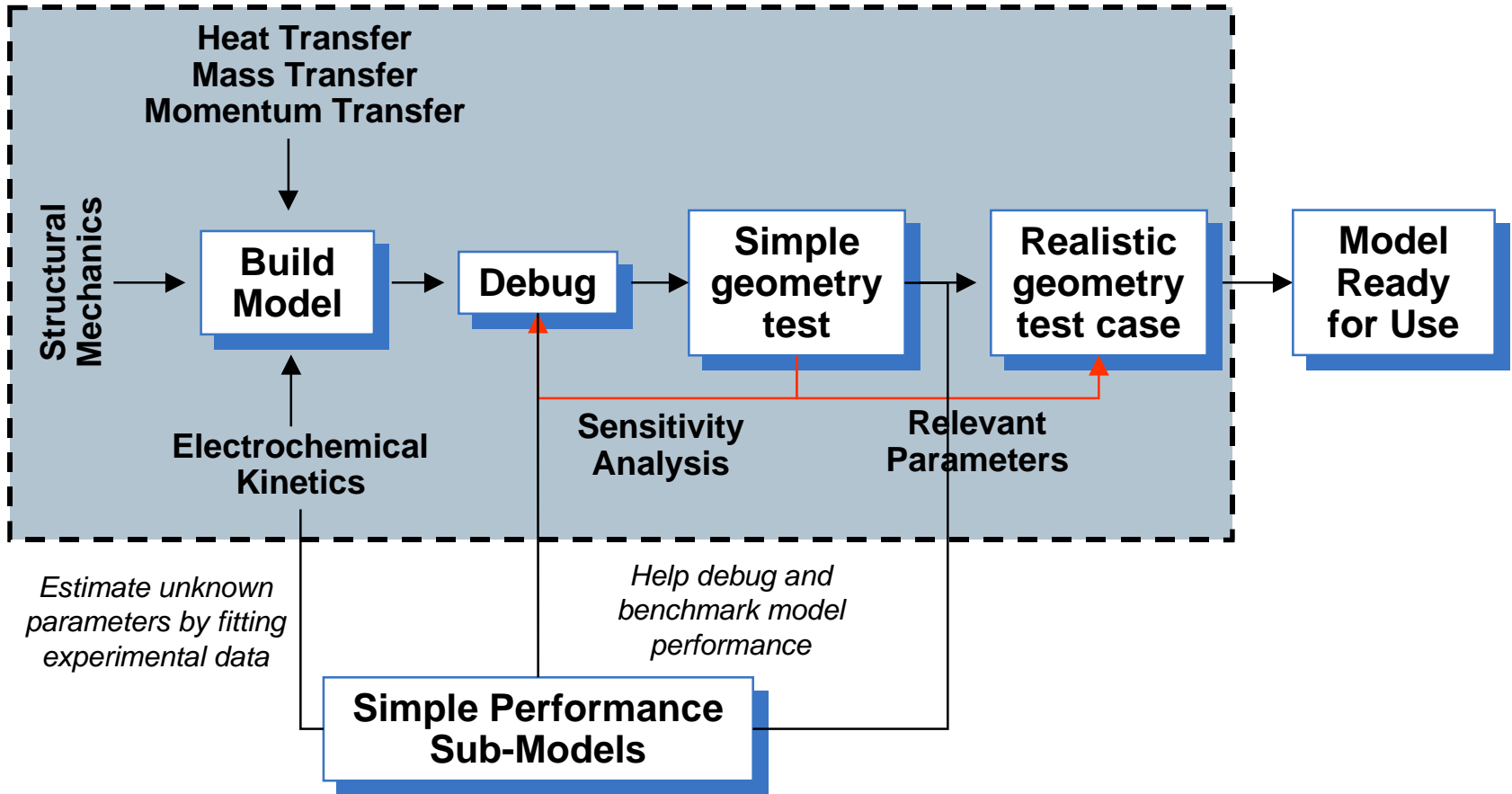
### **Questions to answer**

- Under normal operating conditions, what is the relative contribution to the stress distribution from: compressive load and temperature gradients?
- How does the stress distribution in the cell depend on the design parameters?
  - Cell size (area)
- How does the stress distribution in the cell depend on the operating conditions?
  - Temperature and stoichiometry of the inlet cathode stream
  - Cell voltage

**The resulting model is a multi-purpose engineering model that can be used to analyze other aspects of SOFC performance.**



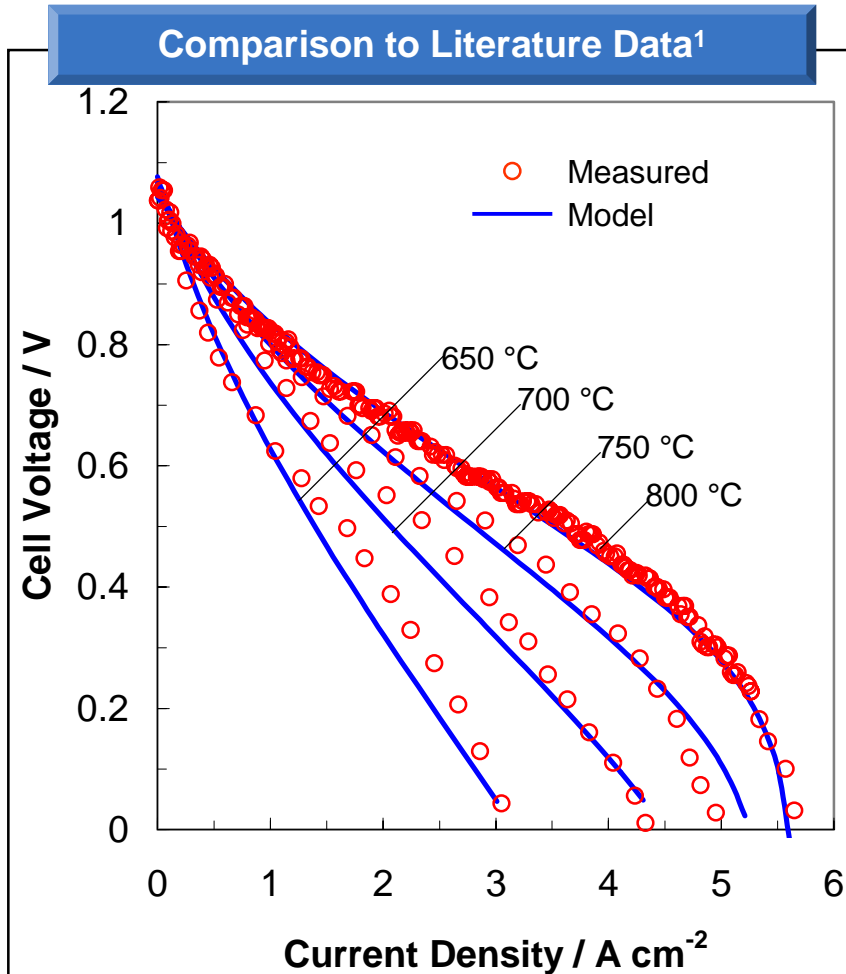
**Model development and validation was accomplished in a four-step process, including explicit validation of simple performance sub-models.**



**Each type of SOFC model developed here, has a different level of detail, and has a unique use in this project.**

Model	Cell Configuration simulated	Highlights	Primary uses	output
1-D Performance Model	<ul style="list-style-type: none"> <li>• Isothermal</li> <li>• Small area cell,</li> <li>• Negligible fuel utilization</li> </ul>	<ul style="list-style-type: none"> <li>• Flow channels are well mixed</li> <li>• 1-d diffusion in porous electrodes</li> <li>• Reaction + diffusion in the reaction zone</li> </ul>	<ul style="list-style-type: none"> <li>• Estimate unknown parameters by fitting experimental data, subsequently used in 3-d model</li> <li>• Understand and explain the trends observed in ‘model’ experiments from the literature</li> </ul>	<ul style="list-style-type: none"> <li>• Polarization curves</li> <li>• Overpotentials, electrolyte resistance, current distribution in the reaction zone</li> </ul>
2-D Performance Model	<ul style="list-style-type: none"> <li>• Isothermal</li> <li>• Large area cell</li> <li>• High fuel utilization</li> </ul>	<ul style="list-style-type: none"> <li>• Plug flow in the flow channels</li> <li>• 1-d diffusion in porous electrodes</li> <li>• Reaction + diffusion in the reaction zone</li> </ul>	<ul style="list-style-type: none"> <li>• Calculate cell performance at high fuel utilization</li> <li>• Help debug the more complicated 3-d model</li> <li>• Answer simple ‘what-if’ questions, such as effect of changes in operating conditions, cell dimensions, etc.</li> </ul>	<ul style="list-style-type: none"> <li>• Current density and overpotentials along the cell length and as a function of fuel utilization</li> </ul>
3-D Structural Model	<ul style="list-style-type: none"> <li>• Non-isothermal</li> <li>• Large area 3-d cell</li> <li>• Low and high fuel utilization</li> </ul>	<ul style="list-style-type: none"> <li>• Adiabatic or steady heat loss from outer edges</li> <li>• Plug flow in flow channels</li> <li>• 2-d diffusion in porous electrodes</li> <li>• Reaction only in the reaction zone</li> </ul>	<ul style="list-style-type: none"> <li>• Understand effects of operating conditions and cell design on performance: Identify hot spots, regions of low current, high stress and potential failure mechanisms</li> <li>• Answer ‘what-if’ questions, such as effect of changes in operating conditions, dimensions, etc.</li> </ul>	<ul style="list-style-type: none"> <li>• Spatial and temporal distribution of temperature, current density, stress, species concentrations, overpotentials, etc., for given design and operating conditions</li> </ul>

The parameters in the 1-d model were first fitted, and then validated by comparing with temperature-dependent experimental measurements.



Details of the Simulations

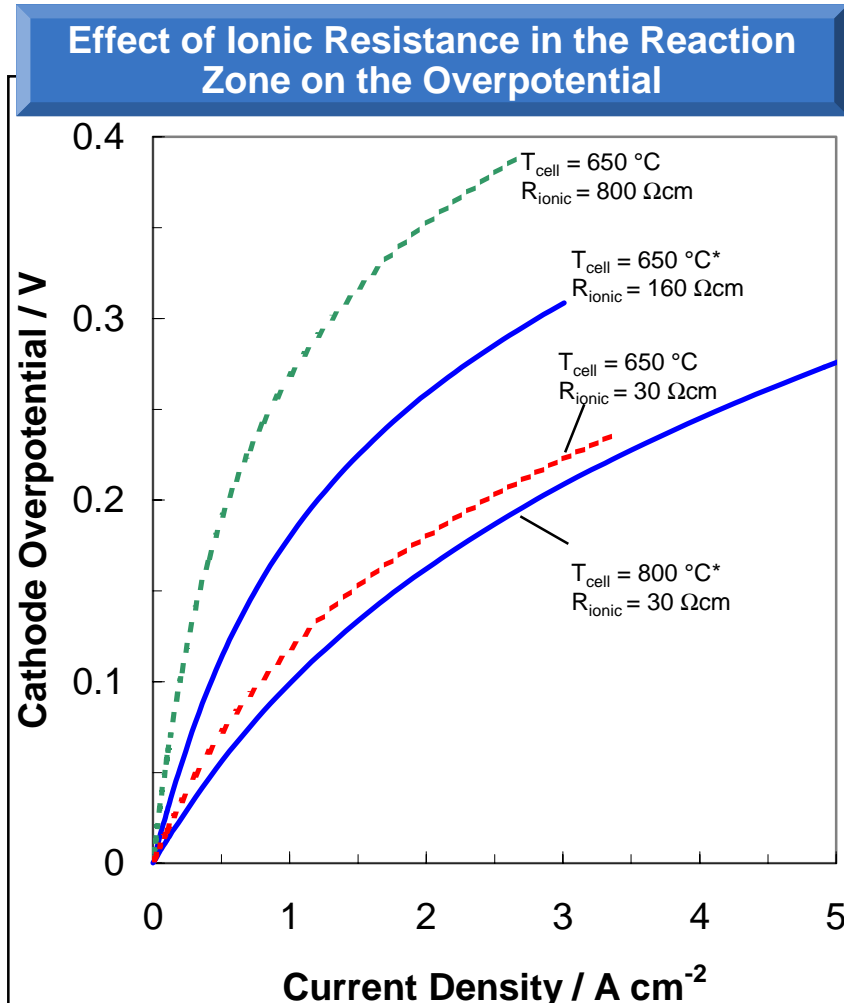
- Literature values were used for temperature dependent ionic conductivity of the electrolyte and the electronic conductivities of the anode and cathode.
- 800 °C data was fit by adjusting 6 parameters:
  - tortuosity factors (2)
  - exchange current densities (2)
  - transfer coefficients in the BV eqn. (2)
- Comparisons to data at other temperatures were obtained without further adjustment to the parameters
- Operating Conditions & Cell Design
  - Reactants: Anode: 95 % H<sub>2</sub>, 5 % H<sub>2</sub>O, Cathode: Air
  - Thickness: Anode: 750 μm, Cathode: 200 μm, Electrolyte 10 μm
- Assumptions
  - Isothermal Operation
  - Low utilization of reactants
  - The reaction zones were 10 μm thick
  - The electrolyte occupied 50 % of the volume of the solid phase.
  - 30 kJ/mol activation energy for anode and cathode.

<sup>1</sup> J-W Kim, A. Virkar, K-Z Fung, K. Mehta, S. Singhal, *J. Electrochem. Soc.*, 146 (1999) 69-78.





**1-d model showed that reducing ionic resistance of the cathode TPB# is essential for good cell performance at low temperatures.**



**Notes**

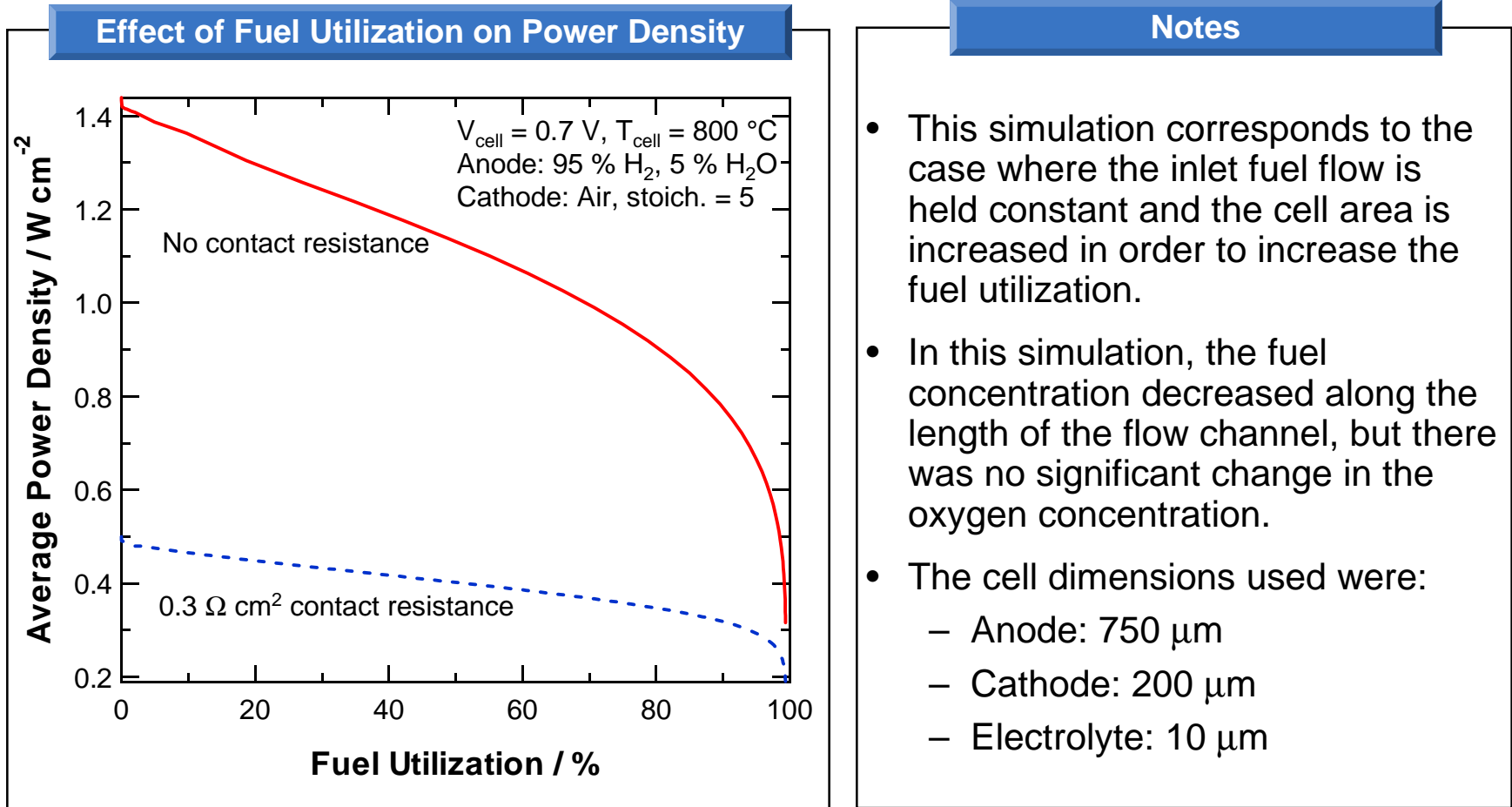
- The results presented here separate the effect on the overpotential of inherent kinetics and ionic resistance in the electrode:
  - Model results show that kinetics improvement alone reduces the overpotential by 20 mV at 1 Am cm<sup>-2</sup> (R<sub>ionic</sub> is constant at 30 Ω cm in going from 650 to 800 °C).
  - Whereas, improvement in the ionic resistance alone reduces the overpotential by 80 mV at 1 A cm<sup>-2</sup> (R<sub>ionic</sub> decreases from 160 Ωcm to 30 Ωcm at 650 °C).



# TPB: Three phase boundary

\* - base case parameters, R<sub>ionic</sub> = ionic resistivity of the electrolyte in the cathode reaction zone,

**The 2-d model allows studying the effect of fuel utilization on performance. For example: performance drops with increasing utilization ...**



**... but drop is less pronounced when the internal resistance of the cell is high.**



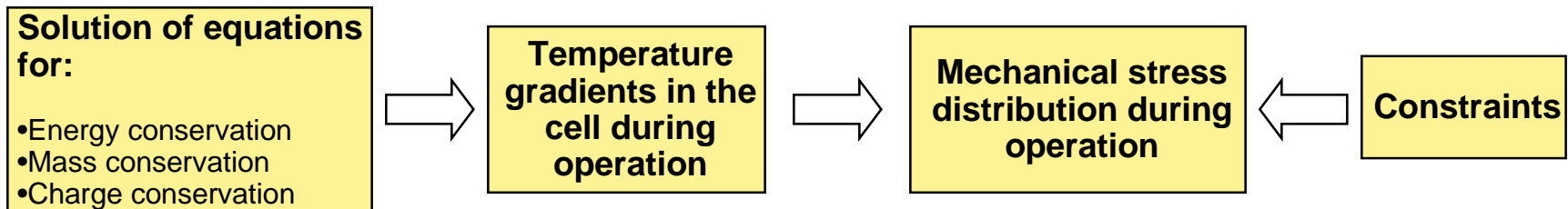
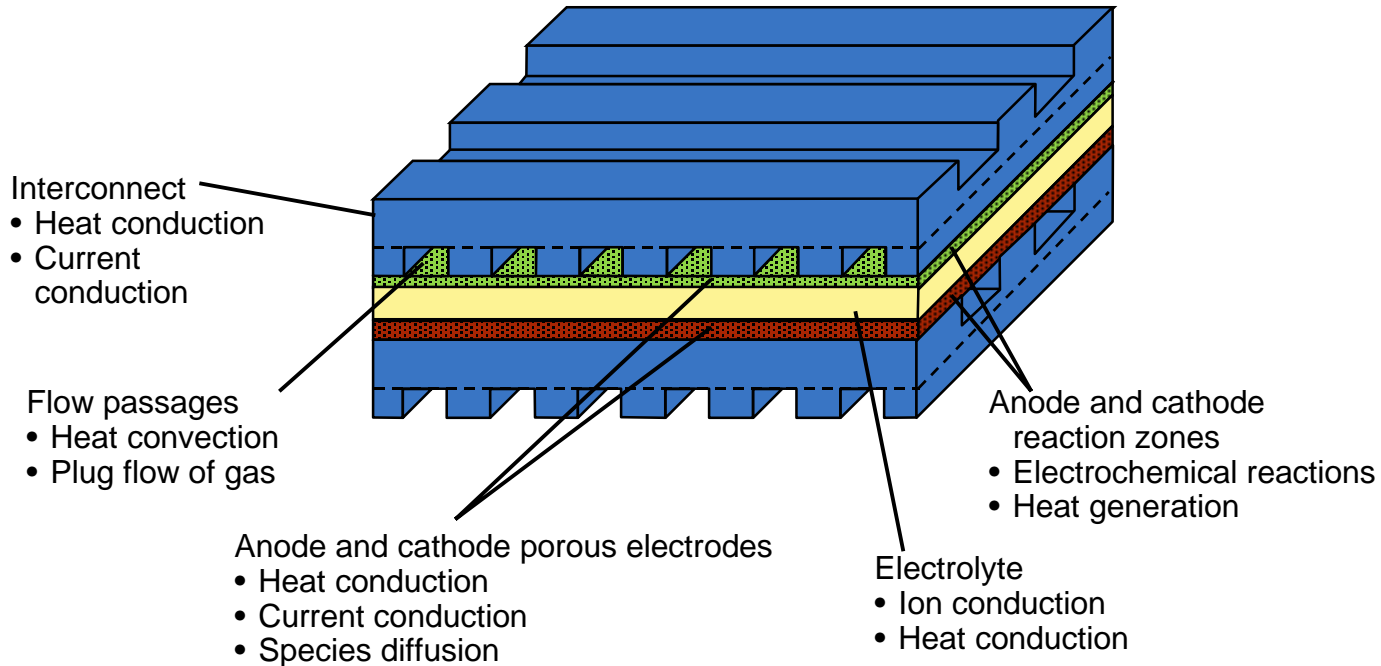
**We developed an ‘as simple as possible’ model using ABAQUS, a commercial finite element analysis (FEA) package.**

- Developed a 1-D electrochemistry module to work with our FEA package.
- Developed material property database based on (limited) available information.
- The commercial FEA package allows discretization of any complex cell / stack geometry into a **finite** number of **elements**.
- The code thus allows the analysis of any type of SOFC stack, including rectangular planar, circular planar, and non-planar designs.

**If necessary, the key modules developed here can be adapted to work with other FEM or CFD codes in the future.**

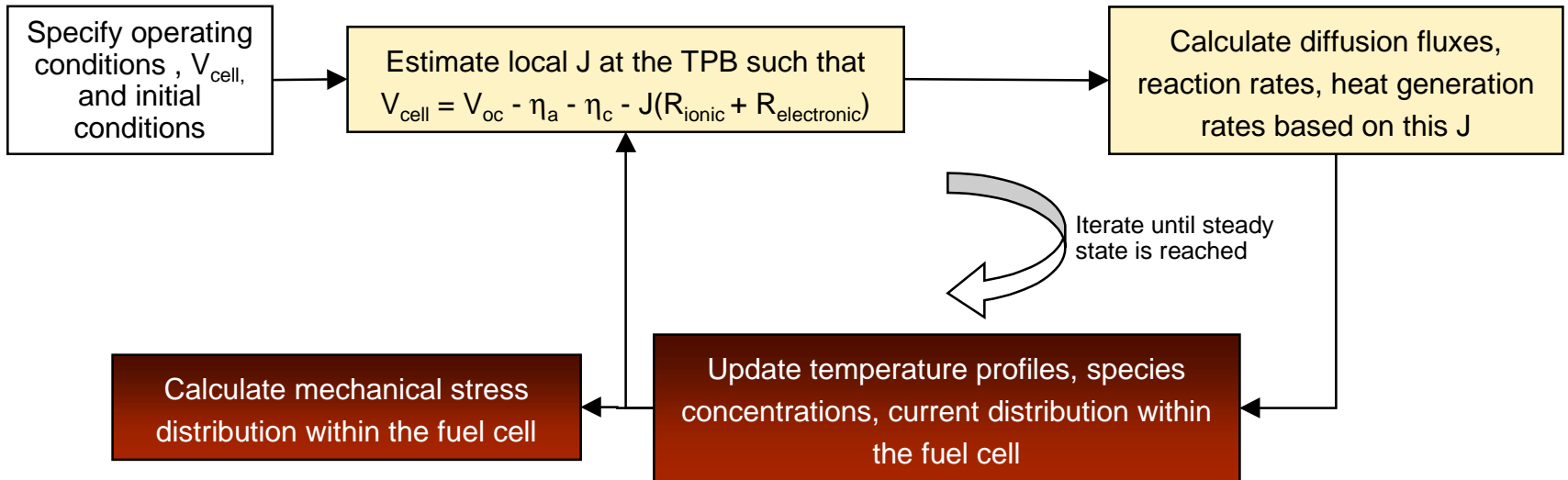


**The structural model accounts for all the relevant electro-chemo-thermo-mechanical phenomena, which influence cell performance.**



The temperature profiles were first calculated using an iterative procedure and then the stress distribution in the cell.

### Overview of GROVE™ Algorithm to be Implemented in ABAQUS



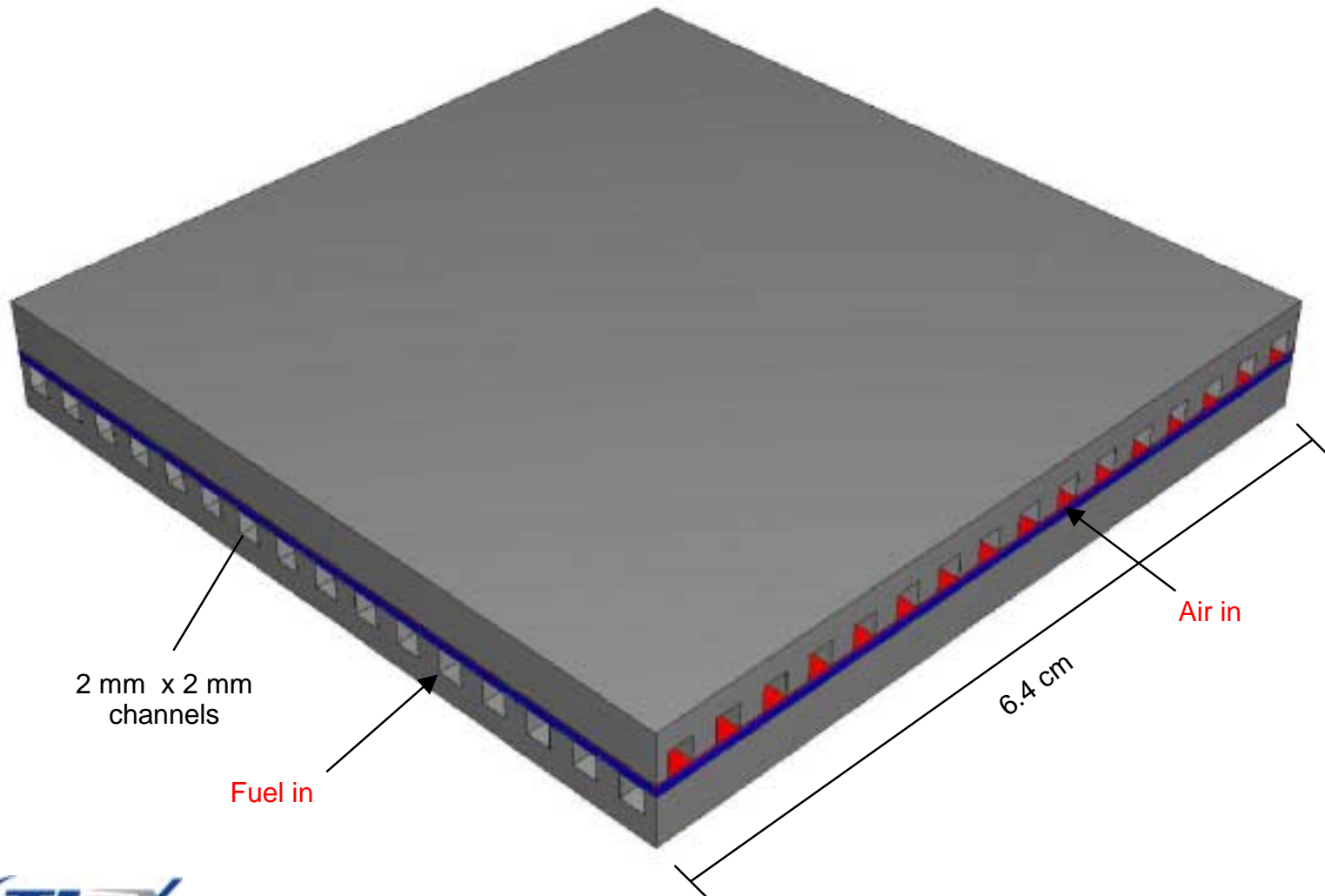
#### Nomenclature

- $V_{cell}$ : Cell voltage
- $V_{OC}$ : Open circuit voltage
- $\eta_a$ : Cathode overpotential
- $\eta_c$ : Anode overpotential
- $J$ : Current density
- $R_{ionic}$ : Area specific resistance of the electrolyte
- $R_{electronic}$ : Area specific resistance of the electrodes and interconnect

- Calculations by 1-d EC module
- Calculations by 3-d ABAQUS

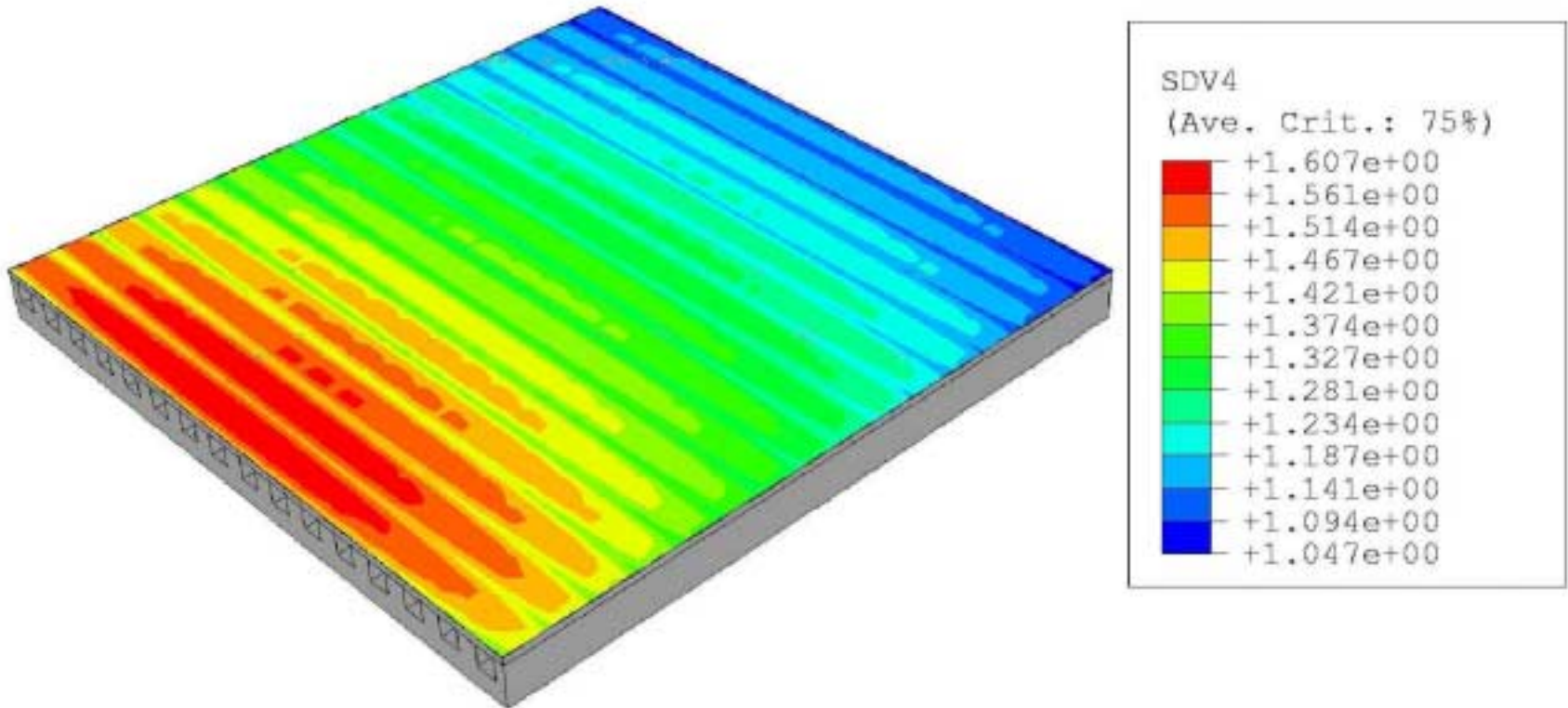


To evaluate the impact of cell size, we use a cross-flow configuration.



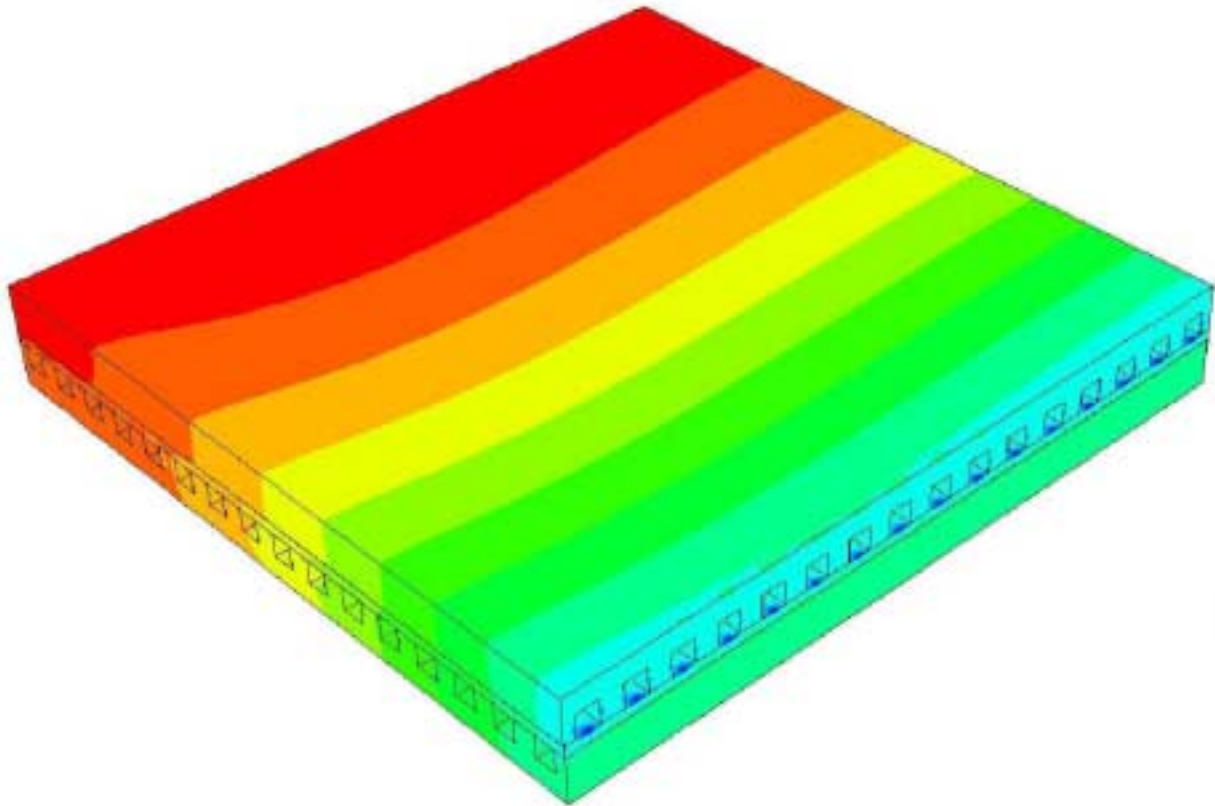
**The structural model calculates the time-dependent current density distribution during cell operation.**

Cell voltage = 0.7 V  
Steady state current density distribution, average = 1.3 A/cm<sup>2</sup>

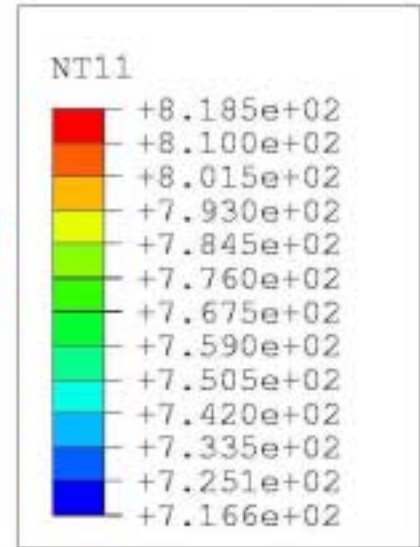


**The larger cell dimensions lead to wider temperature distribution, but similar temperature gradients compared to the 3.2-cm cell.**

Cell voltage = 0.7 V  
Steady state temperature distribution



Temperature / C





## A manufacturing procedure was assumed to calculate the residual stress distribution at room temperature.

### Procedure for residual stress calculations

#### Step 0: Sintering Ceramics

- Assume that all the ceramic layers in the MEA are stress-free at the co-sintering temperature of 1400 °C.
- The component layers in the ceramic MEA are assumed to be fused together.
- Assume interconnects are stress free at room temperature

#### Step 1: Cool Down to Room Temperature

- Calculate the stresses in the ceramic layers when the MEA is cooled down to room temperature (residual stresses).

#### Step 2: Flatten Ceramics

- Apply appropriate confining pressure to flatten the MEA (this is needed to ensure sealing and electric contact).
- Assemble flat MEA between interconnects

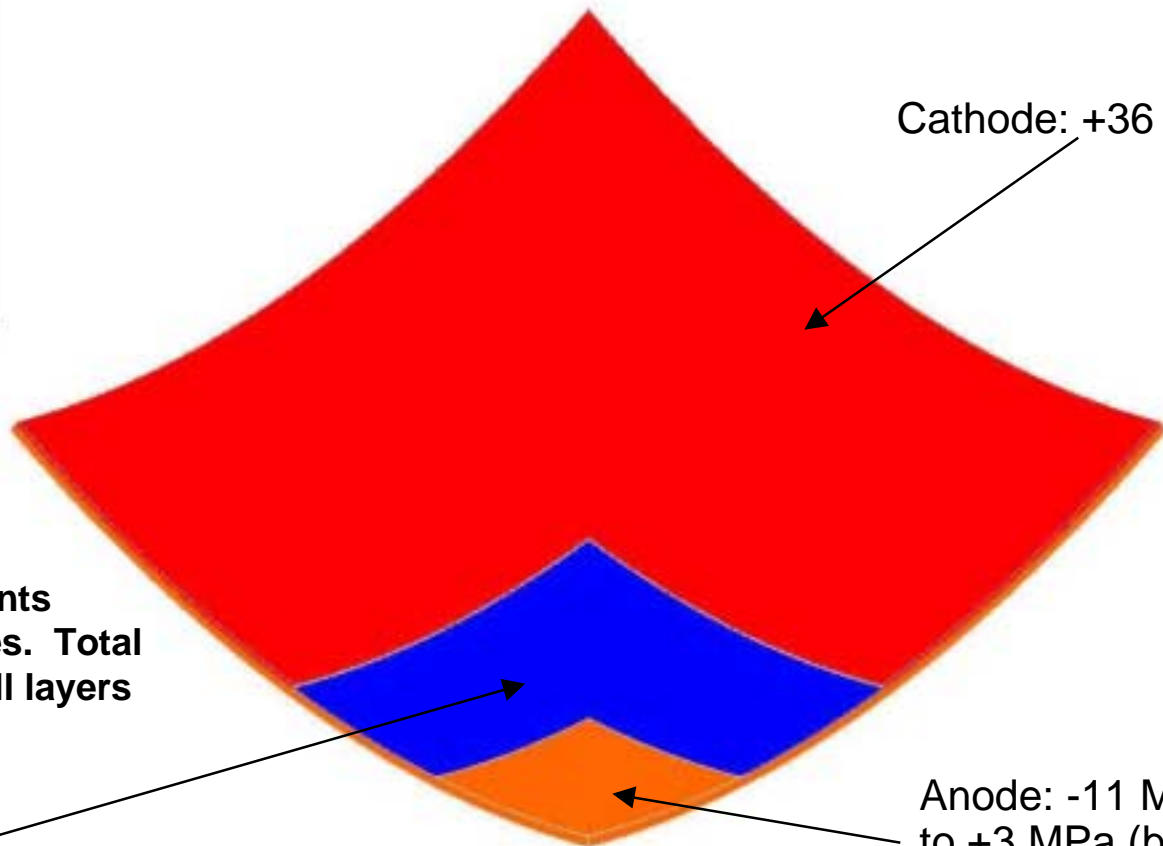
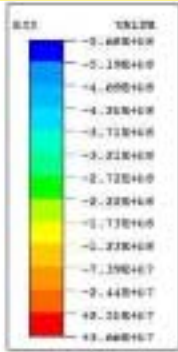
#### Step 3: Heat Up to Operating Temperature

- Assume no-slip condition between interconnect and ceramics
- Calculate stress distribution by applying the steady temperature gradients calculated for cell operation

**In the ensuing calculations, we assume that the ceramic MEA is defect free.**

## In Step 1, uncompensated bending stresses lead to warping of the MEA.

### Residual stresses and warping in the ceramic layers at room temperature



Cathode: +36 MPa

Anode: -11 MPa (top) to +3 MPa (bottom)

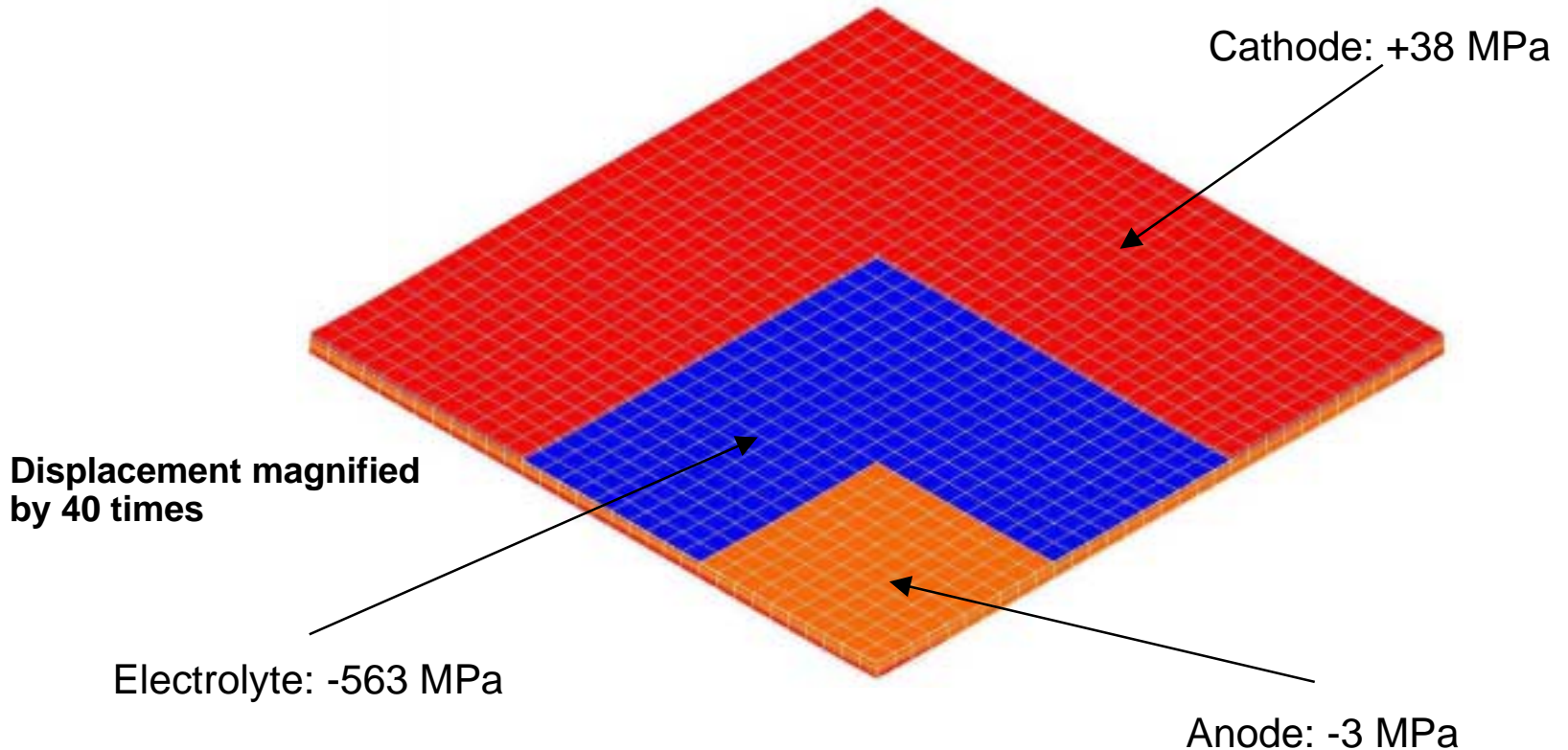
Note: displacements magnified 40 times. Total warping of the cell layers equals 0.12 mm.

Electrolyte: -567 MPa



In step 2 a confining pressure (0.4 MPa ) flattens the MEA and removes the anode bending stress but does not alter the cathode or electrolyte stresses.

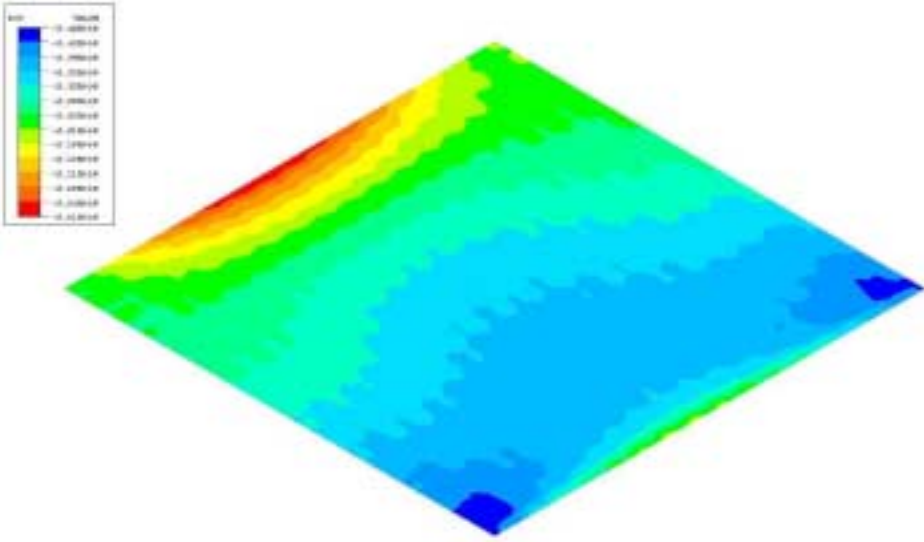
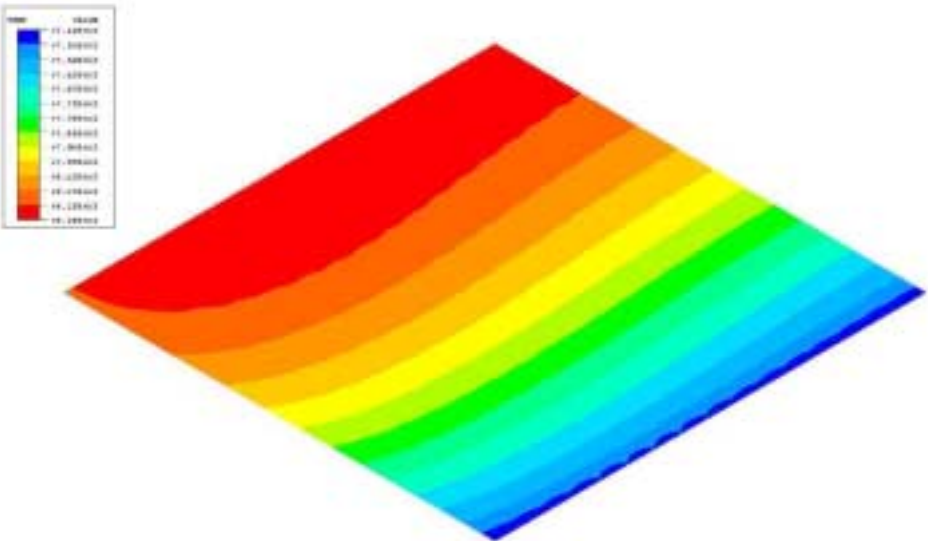
Stress in the ceramic MEA layers after 'flattening' between interconnects at room temperature



**Applying the steady state temperature profile shows that the stress distribution is much less severe than at room temperature.**

Electrolyte temperature varies from 744 °C (blue) to 818 °C (red) for operation at 0.7 V

Electrolyte stress varies from -246 MPa (blue) to -201 MPa (red) for operation at 0.7 V



## **Stress calculations show that, absent defects, the ceramics are unlikely to fail due to temperature gradients during cell operation.**

- For conditions we have simulated so far, the most severe stress state for the ceramics occurs at room temperature and not during cell operation.
- Severe residual stresses were built-up in the ceramic layers of the MEA during cool down from the stress-free sintering temperature.
  - Bending stresses, which arose to balance the moments created by anode/cathode TCE mismatch, caused warping of the ceramic MEA layers.
  - The warped MEA was ‘flattened’ by the application of a small confining pressure.
- At the steady state operating temperatures (650 - 850 °C), the residual stresses were relieved to some extent because the temperatures were closer to the stress-free sintering temperature (1400 °C).
- Under conditions simulated in this study, the temperature gradients during steady state operation did not generate severe stresses
  - The high thermal conductivity of the thick metallic interconnect lead only to modest temperature gradients
  - Also, the temperature gradients through the thickness of the ceramic layers were negligible

## **Increasing the cell size increases the total CTE-mismatch-related strains but does not significantly affect the stress state or flatness of the MEA.**

- To test the effects of cell area, the results of models representing 3.2-cm, 6.4-cm, and 10-cm square single cells were compared.
- Without application of the confining pressure, the total warping of the ceramic layer varies linearly with the cell area.
- Application of the 0.4 MPa confining pressure reduces the through-thickness displacement variation in the ceramic to below 2 microns for each of the cell sizes examined.
- The most severe stress state for the MEA is at room temperature, rather than under operating conditions, regardless of cell size.
- The average stresses in the MEA layers at room temperature do not depend strongly on the cell area.
- Increasing the cell area produces larger geometric incompatibilities along cell edges, possibly leading to seal failures.

**We are currently exploring more realistic operating conditions (not considered in this study) for determining cell-size limitations.**

- Potential causes for cell-size limitations not considered in this study:
- **Defects**
  - Ceramic MEAs are known to have defects. The defect density will clearly be higher for larger cells making them prone to failure.
- **Larger temperature gradients**
  - Heat loss from the edges of the stack
  - Internal reforming
- **Seal failure**
  - With larger cells, the total mismatch in strains is also higher, which might increase the probability of seal failure.
- **Unequal application of compressive load**
  - With large area cells it becomes difficult to apply a uniform load on the cell active area.
  - Unequal compressive force can lead to localized high contact resistance, which in turn might lead to local hot-spots because of resistive heating.

# Outline of Final Report

---

0	Executive Summary
1	Background & Objectives
2	Approach & Scope
3	Model Development
4	Single Channel SOFC Results
5	Multi Channel SOFC Results
6	Limitations for Cell Size
7	Summary
A	Appendix

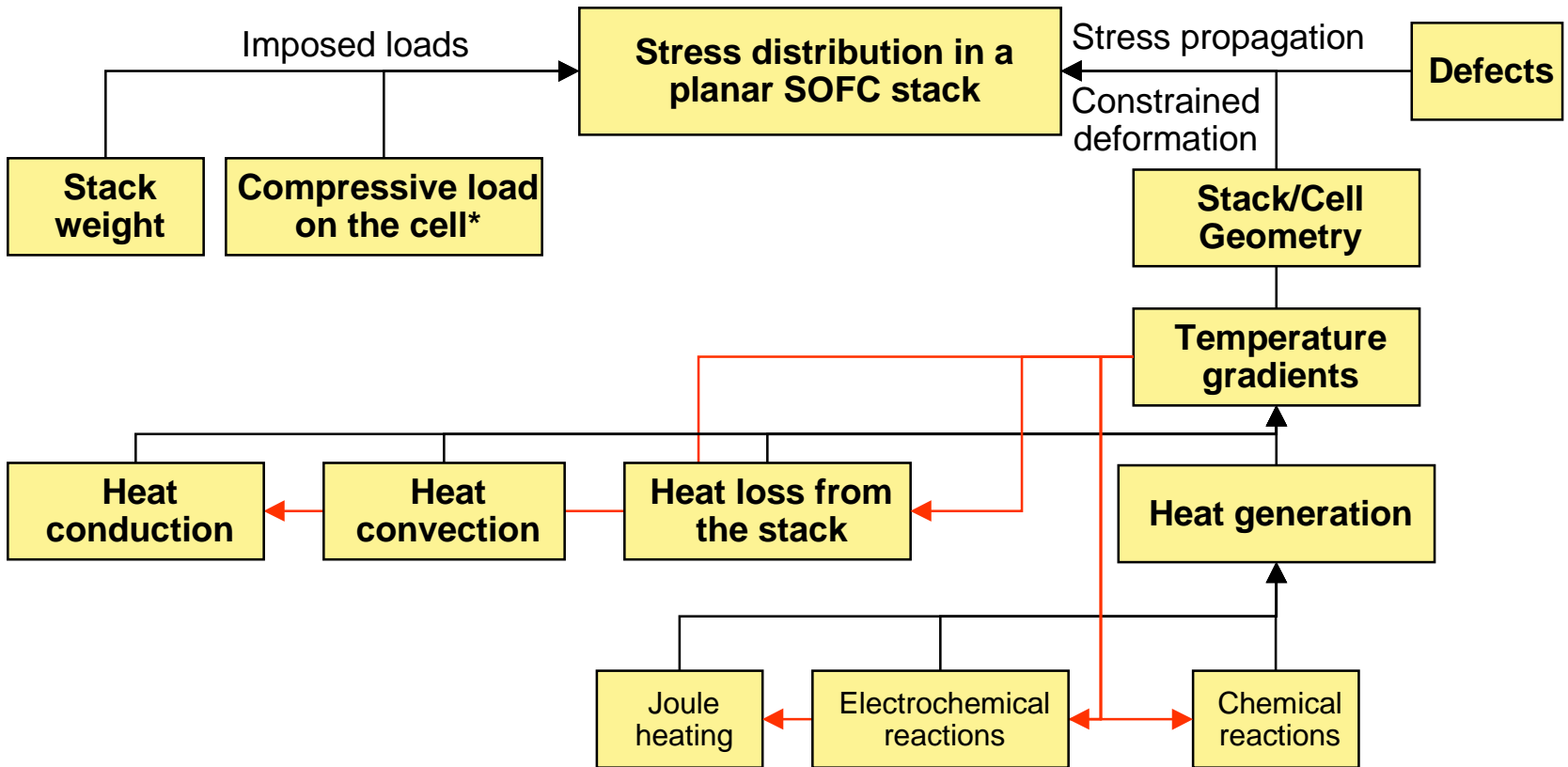




## **Thermo-mechanical stresses within planar SOFCs cells may limit stack scale-up, which is important for high-capacity applications.**

- The SECA strategy is to develop cost-effective modular planar SOFC stack technology that could be applied to a broad range of applications:
  - Application of similar stack design to multiple applications would accelerate stack cost reduction
  - Applications range from small-capacity applications (< 10 kW) with 1-4 stacks, to larger power plants (> 250 kW) with hundreds of stacks.
- Scale-up of individual stacks would offer economy of scale benefits and considerably simplify manifolding in larger systems.
- Single stack capacity is determined by the power density, the number of cells, and by the unit cell active area.
- Power density and number of cells are limited by unit cell performance and mechanical and flow-distribution considerations.
- Developers have found that when scaling up planar cells much beyond 100 cm<sup>2</sup> active area they become prone mechanical failure.
- This study is intended to help identify if there are any fundamental thermo-mechanical limitations that will limit stack scale-up

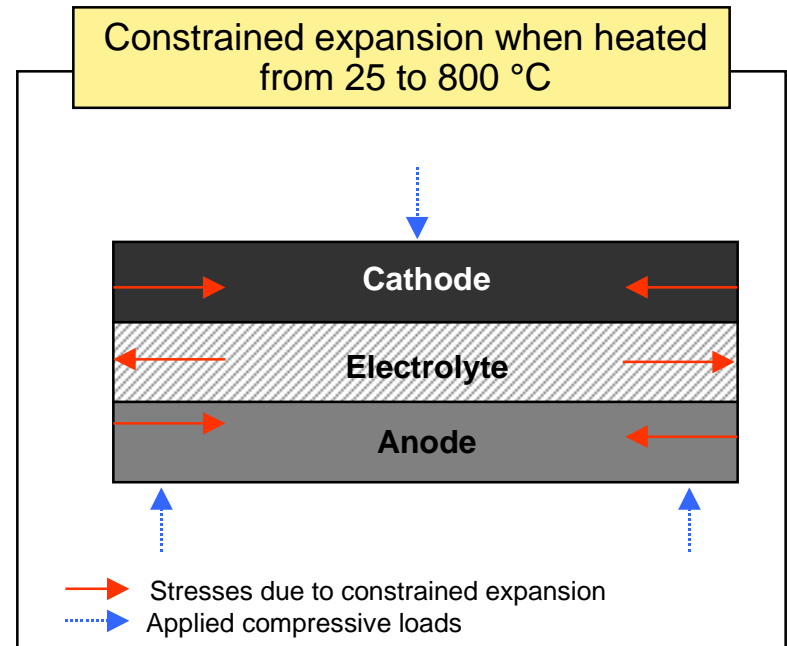
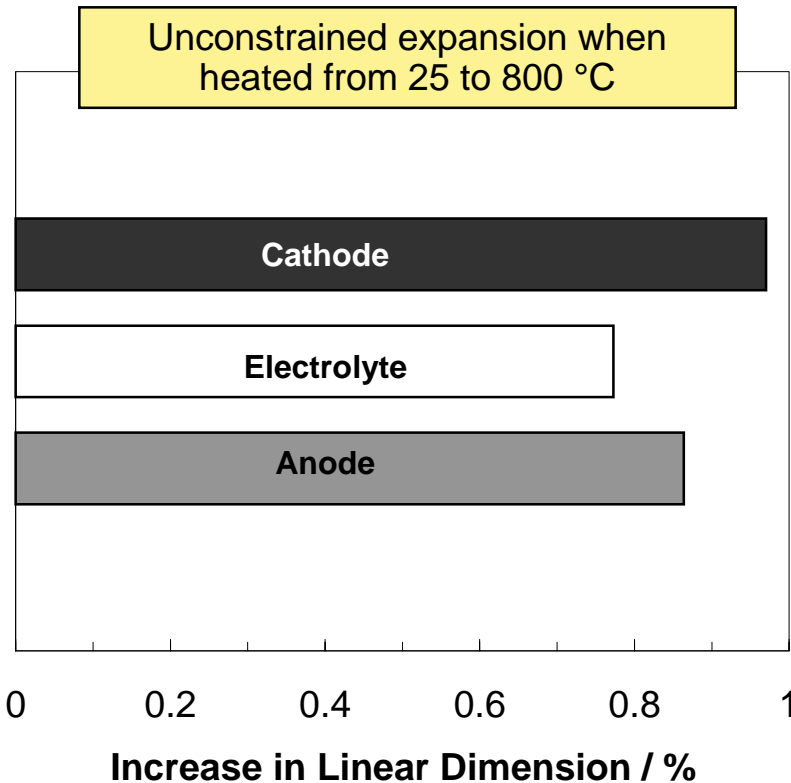
The mechanical stress distribution in a planar SOFC is governed by a combination of design parameters and operating conditions.



\* necessary for sealing and electrical interconnection in many planar stack designs

The non-linear interactions among these phenomena make purely empirical characterization impractical and one-by-one analysis difficult.

For example, differential thermal expansion leads to internal stresses in the cell layers during heat-up and cool-down.



<sup>1</sup> CTE: Coefficient of Thermal Expansion

Temperature gradients that occur during cell operation may help relieve or exacerbate these stresses depending on the local conditions.

**Significant advances are being made in detailed modeling of SOFC stacks based on both structural and computational fluid dynamics codes, ...**

### **Current Modeling Efforts**

- Development of basic science underlying SOFC operation
- Detailed electrochemical models of SOFC electrodes
- Incorporations of electrochemistry into structural and CFD codes
- High level of sophistication and modest to high level of complexity

**For feasibility studies and early design trade-offs, a simpler model representing the major trends is desirable:**

- Simple representation of flow
- Simple representation of (electro-)chemistry
- Uses thermal and structural capabilities of common structural code to allow rapid assessment of impact of design and operating condition changes on stresses

**... but a simple engineering model linking thermal, electrochemical, and mechanical system behavior is needed for feasibility and scoping studies.**

**This study aims to use a structural model to assess the impact of operating conditions and scale-up on SOFC thermo-mechanical performance.**

### **Deliverables**

- Profiles of temperature and mechanical stresses for normal operation of a typical planar anode supported SOFC with cross-flow of reactants.
- Sensitivity of these profiles to relevant operating and design variables

### **Questions to answer**

- Under normal operating conditions, what is the relative contribution to the stress distribution from: compressive load and temperature gradients?
- How does the stress distribution in the cell depend on the design parameters?
  - Cell size (area)
- How does the stress distribution in the cell depend on the operating conditions?
  - Temperature and stoichiometry of the inlet cathode stream
  - Cell voltage

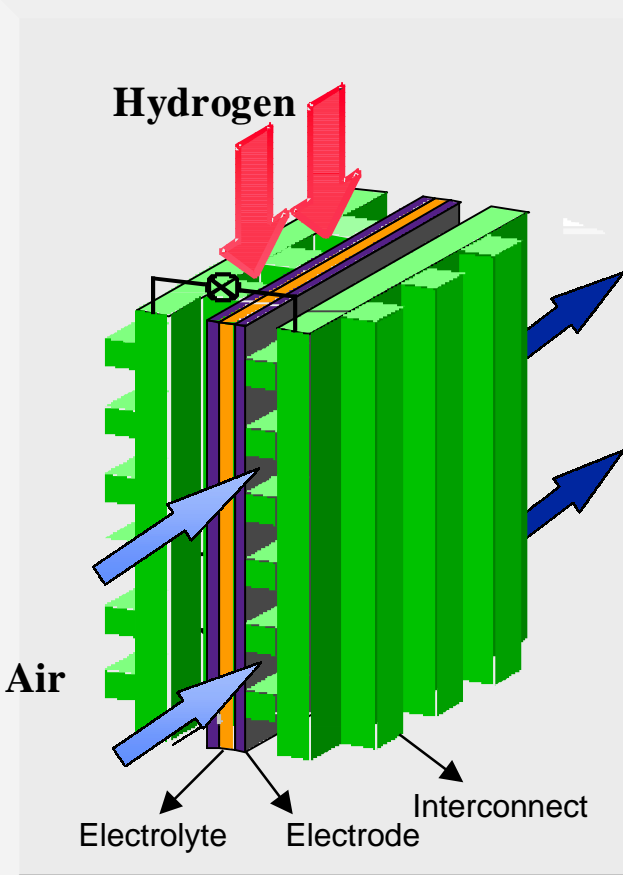
**The resulting model is a multi-purpose engineering model that can be used to analyze other aspects of SOFC performance.**

## Outline of Final Report

---

0	Executive Summary
1	Background & Objectives
2	Approach & Scope
3	Model Development
4	Single Channel SOFC Results
5	Multi Channel SOFC Results
6	Limitations for Cell Size
7	Summary
A	Appendix

**The model philosophy is to include the minimal representation of all relevant physical phenomena necessary for the intended analysis.**



The diagram illustrates a 3D view of a fuel cell stack. It shows multiple green rectangular cells stacked together. Red arrows labeled 'Hydrogen' point downwards into the top of the stack. Blue arrows labeled 'Air' point upwards into the bottom of the stack. The stack is composed of several layers: a central 'Electrolyte' layer, 'Electrode' layers on either side, and 'Interconnect' layers between the cells. A small circle with a cross inside is visible on the top surface of one of the cells.

- Each component in the stack has unique functions essential for good cell performance
- The key physical phenomena occurring in a stack span a wide range of characteristic length and time scales:
  - Charge transfer in an elementary reaction at the molecular level ( $\sim \text{\AA}$ ,  $\sim 10^{-13}$  s)
  - Diffusion through the porous electrodes ( $\sim \text{m}$ ,  $\sim 10^{-3}$  s)
  - Fluid mixing in flow channels at the macroscopic level ( $\sim \text{cm}$ ,  $10^{-2}$  s)
  - Changes in catalyst activity ( $\text{nm}$ ,  $10^{-1}$  -  $10^6$  s)
- The model must capture each of these phenomena in sufficient detail.
- The level of detail needed would depend on the objectives behind the model development.

**For example, for this study, detailed solution of the flow field in the channels is unnecessary - instead we used a simple plug-flow description.**

**We developed an ‘as simple as possible’ model using ABAQUS, a commercial finite element analysis (FEA) package.**

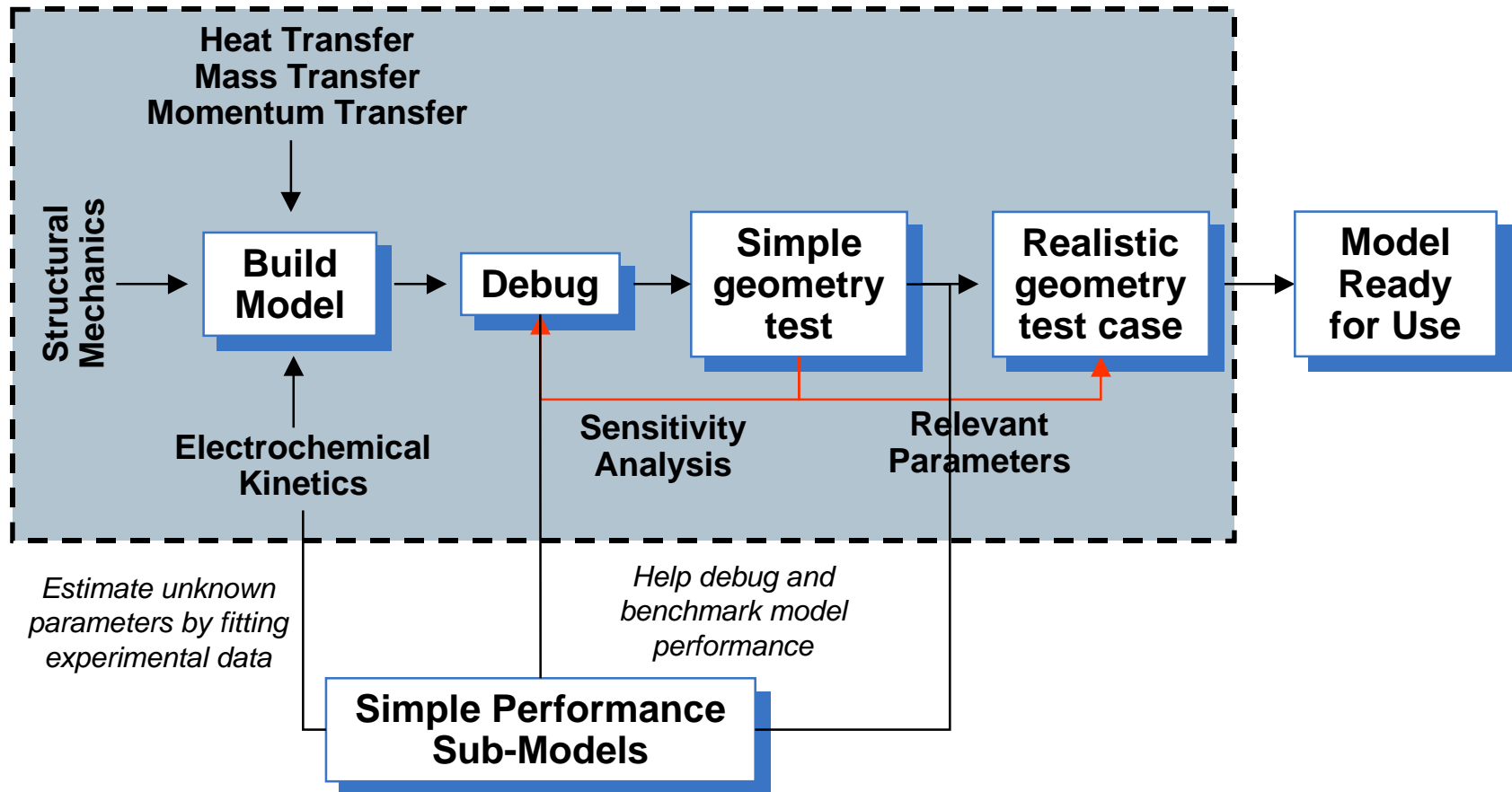
- Developed a 1-D electrochemistry module to work with our FEA package.
- Developed material property database based on (limited) available information.
- The commercial FEA package allows discretization of any complex cell / stack geometry into a **finite** number of **elements**.
- The code thus allows the analysis of any type of SOFC stack, including rectangular planar, circular planar, and non-planar designs.

**If necessary, the key modules developed here could be adapted to work with other FEM or CFD codes in the future.**





**Model development and validation was accomplished in a four-step process, including explicit validation of simple performance sub-models.**



# Outline of Final Report

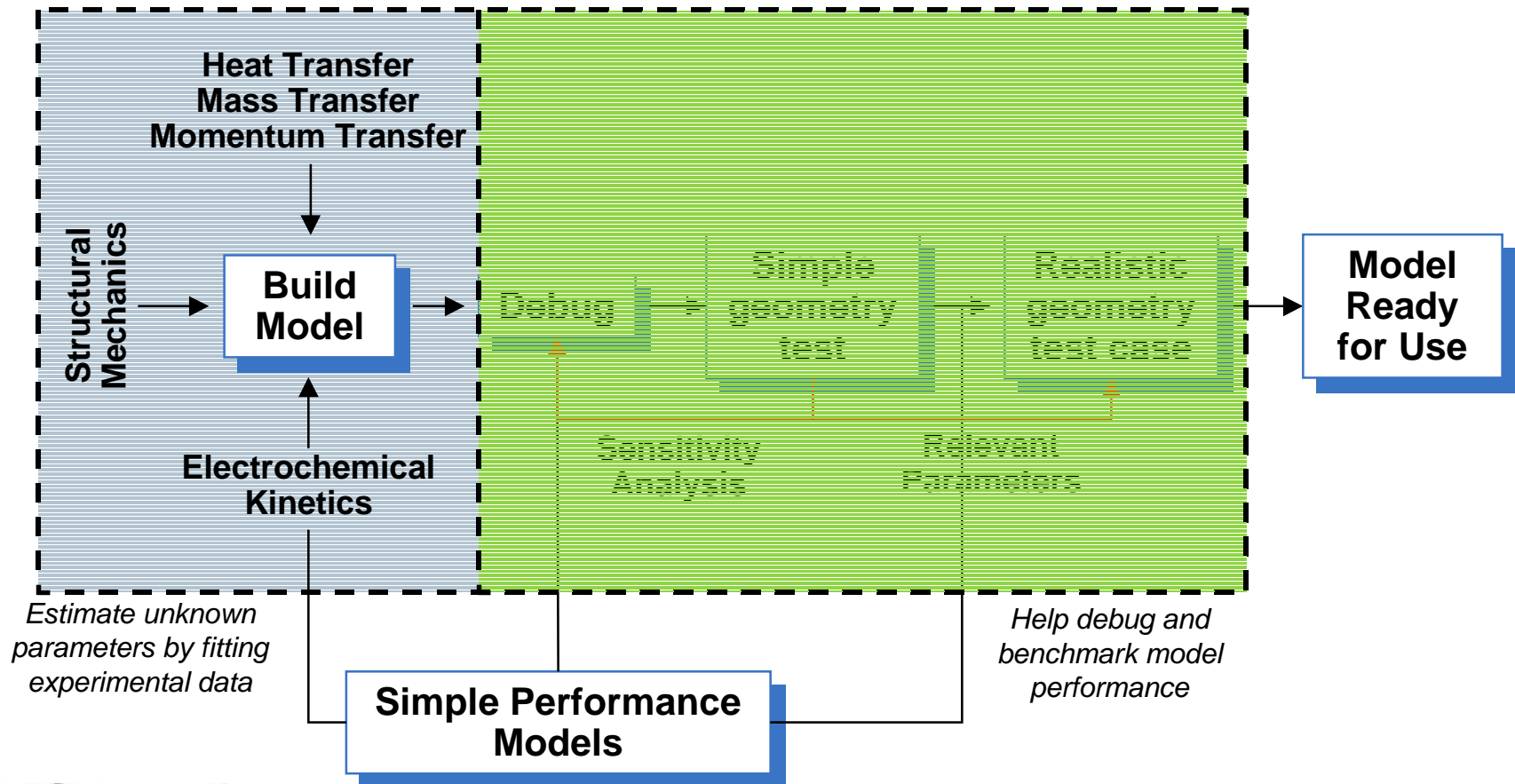
---

0	Executive Summary
1	Background & Objectives
2	Approach & Scope
3	Model Development
4	3a Structural Modeling Methodology
5	3b Simple Performance Model
5	Mu
6	Limitations for Cell Size
7	Summary
A	Appendix

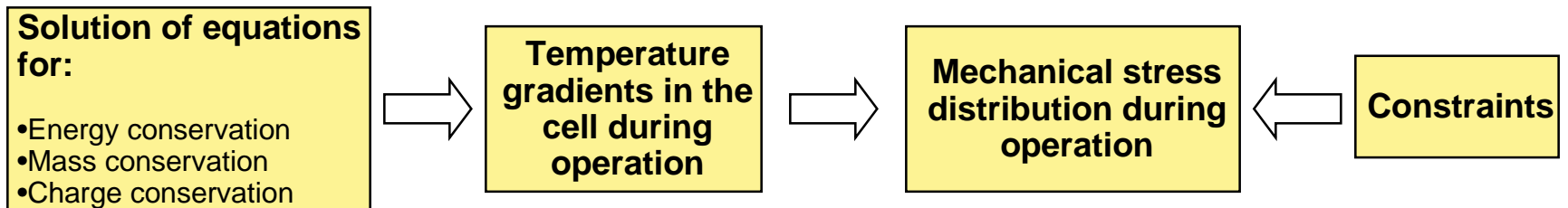
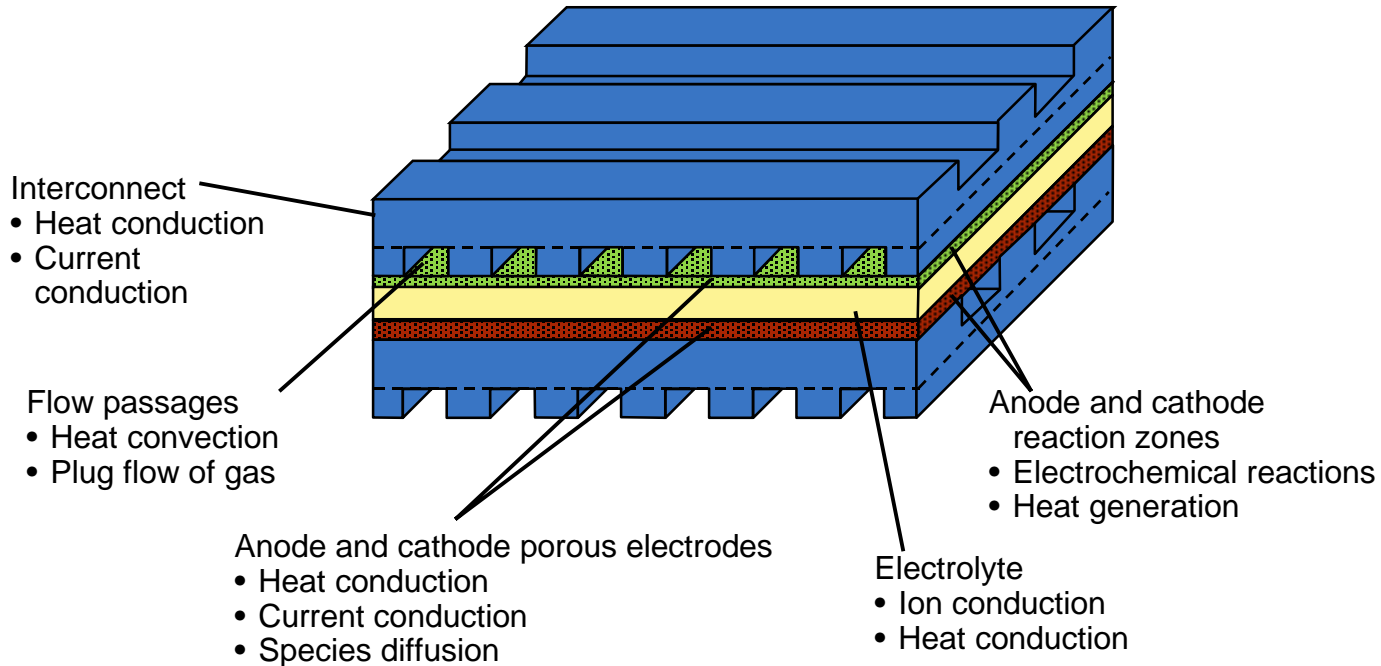


## Simple Performance Model Development

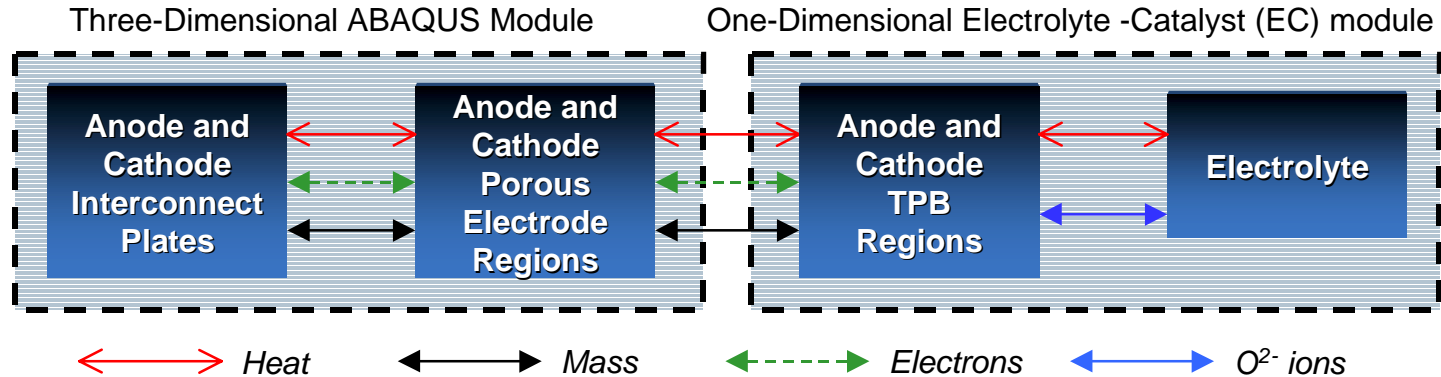
First, we developed the methodology for the structural model and developed the simple performance models.



The structural model accounts for all the relevant electro-chemo-thermo-mechanical phenomena, which influence cell performance.



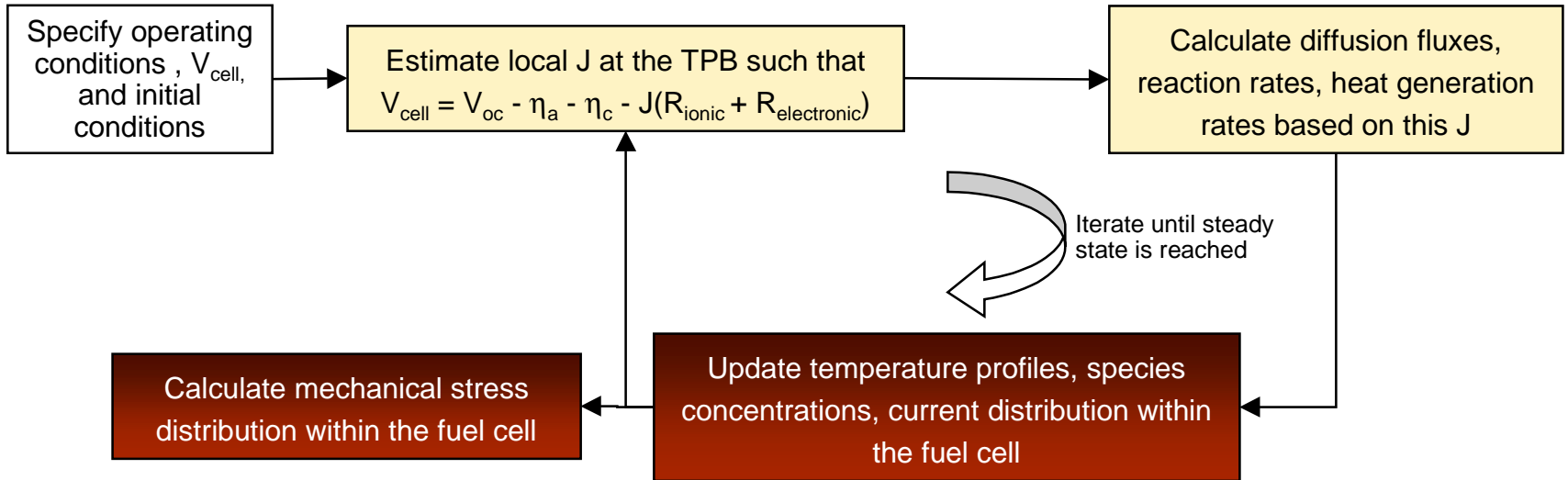
In this work, we use a modular algorithm to describe the relevant phenomena in the different regions of the cell.



- To develop the structural model, we are using ABAQUS, a commercially available Finite Element (FEM) code and supplementing it with the required subroutines.
- The 3-d ABAQUS model uses the temperature profiles to calculate the distribution of mechanical stresses in the stack.
- The EC module calculates the electrolyte resistance, rates of the electrochemical reactions, the anode and cathode overpotentials, and the heat generated due to reaction.
- If necessary, the key modules developed in this study could be converted for other FEM or CFD codes (outside the scope of the present study)

An iterative solution procedure is needed to solve the non-linear conservation equations.

**Overview of GROVE™ Algorithm to be Implemented in ABAQUS**



**Nomenclature**

- $V_{cell}$ : Cell voltage
- $V_{OC}$ : Open circuit voltage
- $\eta_a$ : Cathode overpotential
- $\eta_c$ : Anode overpotential
- $J$ : Current density
- $R_{ionic}$ : Area specific resistance of the electrolyte
- $R_{electronic}$ : Area specific resistance of the electrodes and interconnect

	Calculations by 1-d EC module
	Calculations by 3-d ABAQUS



**The model contains just enough detail to capture the salient impacts of cell design and operating conditions on internal stresses.**

- Simple Butler-Volmer kinetics were used to describe the electrochemical reactions for hydrogen and oxygen.
  - Internal reforming of hydrocarbon species is not considered in this phase.
  - Simple equilibrium reforming and shift reaction could easily be added.
- Test cases with simple planar rectangular geometries with straight flow channels and external manifolding were considered:
  - Non-rectangular geometries could easily be added
  - Internal manifolding could be added but a step-wise analysis may be more efficient, since typically the manifold areas are not active
- A single cell was simulated in a stack environment:
  - Considered symmetry of cells in stack.
  - Imposed compressive force as boundary conditions.
- Contact resistance between the different layers was ignored but could be added.

## Summary of Model Characteristics

**Each type of SOFC model developed here, has a different level of detail, and has a unique use in this project.**

Model	Cell Configuration simulated	Highlights	Primary uses	output
1-D Performance Model	<ul style="list-style-type: none"> <li>• Isothermal</li> <li>• Small area cell,</li> <li>• Negligible fuel utilization</li> </ul>	<ul style="list-style-type: none"> <li>• Flow channels are well mixed</li> <li>• 1-d diffusion in porous electrodes</li> <li>• Reaction + diffusion in the reaction zone</li> </ul>	<ul style="list-style-type: none"> <li>• Estimate unknown parameters by fitting experimental data, subsequently used in 3-d model</li> <li>• Understand and explain the trends observed in 'model' experiments from the literature</li> </ul>	<ul style="list-style-type: none"> <li>• Polarization curves</li> <li>• Overpotentials, electrolyte resistance, current distribution in the reaction zone</li> </ul>
2-D Performance Model	<ul style="list-style-type: none"> <li>• Isothermal</li> <li>• Large area cell</li> <li>• High fuel utilization</li> </ul>	<ul style="list-style-type: none"> <li>• Plug flow in the flow channels</li> <li>• 1-d diffusion in porous electrodes</li> <li>• Reaction + diffusion in the reaction zone</li> </ul>	<ul style="list-style-type: none"> <li>• Calculate cell performance at high fuel utilization</li> <li>• Help debug the more complicated 3-d model</li> <li>• Answer simple 'what-if' questions, such as effect of changes in operating conditions, cell dimensions, etc.</li> </ul>	<ul style="list-style-type: none"> <li>• Current density and overpotentials along the cell length and as a function of fuel utilization</li> </ul>
3-D Structural Model	<ul style="list-style-type: none"> <li>• Non-isothermal</li> <li>• Large area 3-d cell</li> <li>• Low and high fuel utilization</li> </ul>	<ul style="list-style-type: none"> <li>• Adiabatic or steady heat loss from outer edges</li> <li>• Plug flow in flow channels</li> <li>• 2-d diffusion in porous electrodes</li> <li>• Reaction only in the reaction zone</li> </ul>	<ul style="list-style-type: none"> <li>• Understand effects of operating conditions and cell design on performance: Identify hot spots, regions of low current, high stress and potential failure mechanisms</li> <li>• Answer 'what-if' questions, such as effect of changes in operating conditions, dimensions, etc.</li> </ul>	<ul style="list-style-type: none"> <li>• Spatial and temporal distribution of temperature, current density, stress, species concentrations, overpotentials, etc., for given design and operating conditions</li> </ul>



**Kinetic parameters for the electrocatalytic reactions have not been measured in fundamental, well-characterized experiments.**

Parameters required for Solving the Thermo-Electrochemical Problem		
	Availability	Comments
<b>Thermal conductivity</b>	Available, but not as a function of temperature	Temperature dependent data is unavailable. Used simplifying approximation that conductivity is independent of temperature
<b>Heat Capacity</b>	Available, but not as a function of temperature	Temperature dependent data is unavailable. Used simplifying approximation that specific heat is independent of temperature.
<b>Effective Mass Diffusivity</b>	Limited data available	Data available from Virkar's group, not published yet, used as a fitting parameter in 1-d model.
<b>Exchange current densities</b>	Available data is not for intrinsic Kinetics, estimated by fitting experimental results	Measurements from well-defined experiments are rare. Available data is from using lumped, global B-V kinetics and fitting experiments.
<b>Activation Energies</b>	Available data is not for intrinsic Kinetics, estimated by fitting experimental results	Measurements from well-defined experiments are rare. Available data is from using lumped, global B-V kinetics and fitting experiments.
<b>Transfer Coefficients</b>	Available data is not for intrinsic Kinetics, estimated by fitting experimental results	Measurements from well-defined experiments are rare. Available data is from using lumped, global B-V kinetics and fitting experiments.

**In this project, we estimated the kinetic parameters by fitting experimental data over a range of temperatures.**



**Most of the material properties of the stack components, needed for calculating the stress distribution, are not available.**

Parameters Required for Solving the Mechanical Problem		
<b>Thermal Expansion Coefficient</b>	Available, as a function of temperature	Temperature dependent measurements available for all of the cell components, but data limited to max of 1000 C.
<b>Young's Modulus</b>	-	Data unavailable
<b>Poisson's Ratio</b>	-	Data unavailable
<b>Residual Stress in Components</b>	Measurements for electrolyte in MEA available at room temperature	Data unavailable, residual stress calculated assuming that components were stress free at the sintering temperature.
<b>Interlayer Adhesion</b>	-	Data unavailable
<b>Fracture Resistance</b>	-	Data unavailable
<b>Compressive force on cells in a stack</b>	-	General data is available for the magnitude of the compressive force on a single cell in a stack.

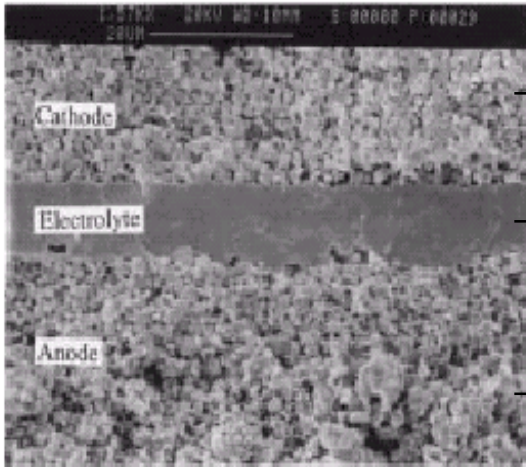
**We have developed simple performance models in order to help estimate kinetic parameters and help debug the more complicated 3-d model.**

- For simulating the cell performance in the 3-d structural model, we require:
  - kinetic parameters for the electrochemical reactions;
  - diffusion properties of the porous media.
- However, in the SOFC literature:
  - Measured data for intrinsic kinetics is scarce due to difficulty in measuring the electrolyte resistance in the electrode and its effect on the overpotential, the local gas concentration at the electrocatalyst, the length of the three-phase boundary, etc.
  - The measured diffusion coefficients are different from those predicted by molecular diffusion theories, and may vary from cell to cell<sup>a</sup>.
- Here, we propose to use simple models to facilitate in the construction of the 3-d model.
  - 1-d Performance Model: Fit experimentally obtained single cell polarization curves in order to estimate unknown parameters.
  - 2-d Performance Model: Help debug and benchmark the results from the more complicated 3-d model, particularly for the difficult case of high fuel utilization.

<sup>a</sup> J-W Kim, A. Virkar, K-Z Fung, K. Mehta, S. Singhal, *J. Electrochem. Soc.*, 146 (1999) 69-78,

For the performance models that follow, we assumed a simple microstructure to represent the details of the electrode/electrolyte interface<sup>a,b</sup>.

**SEM Image of the Structure of the Electrodes/Electrolyte Interface<sup>a</sup>**



*Porous cathode*  
LSM intermixed with YSZ

*Dense electrolyte*  
YSZ

*Porous anode*  
Ni particles intermixed with YSZ

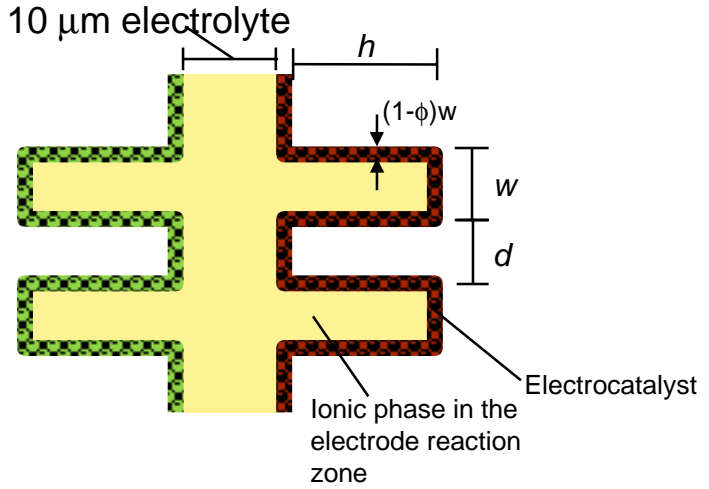
*Carthode*

*Electrolyte*

*Anode*

- LSM: Lanthanum Strontium Manganate
- YSZ: Yttrium Stabilized Zirconia
- Electrochemical reactions require, at the very least, an intersection of the electronic, ionic and gas phases.
- Therefore, inclusion of the ionic conductor YSZ in the electrodes increases the length of the three-phase boundary and hence improves cell performance.

**Assumed Microstructure for the Electrodes/Electrolyte Interface<sup>a,b</sup>**

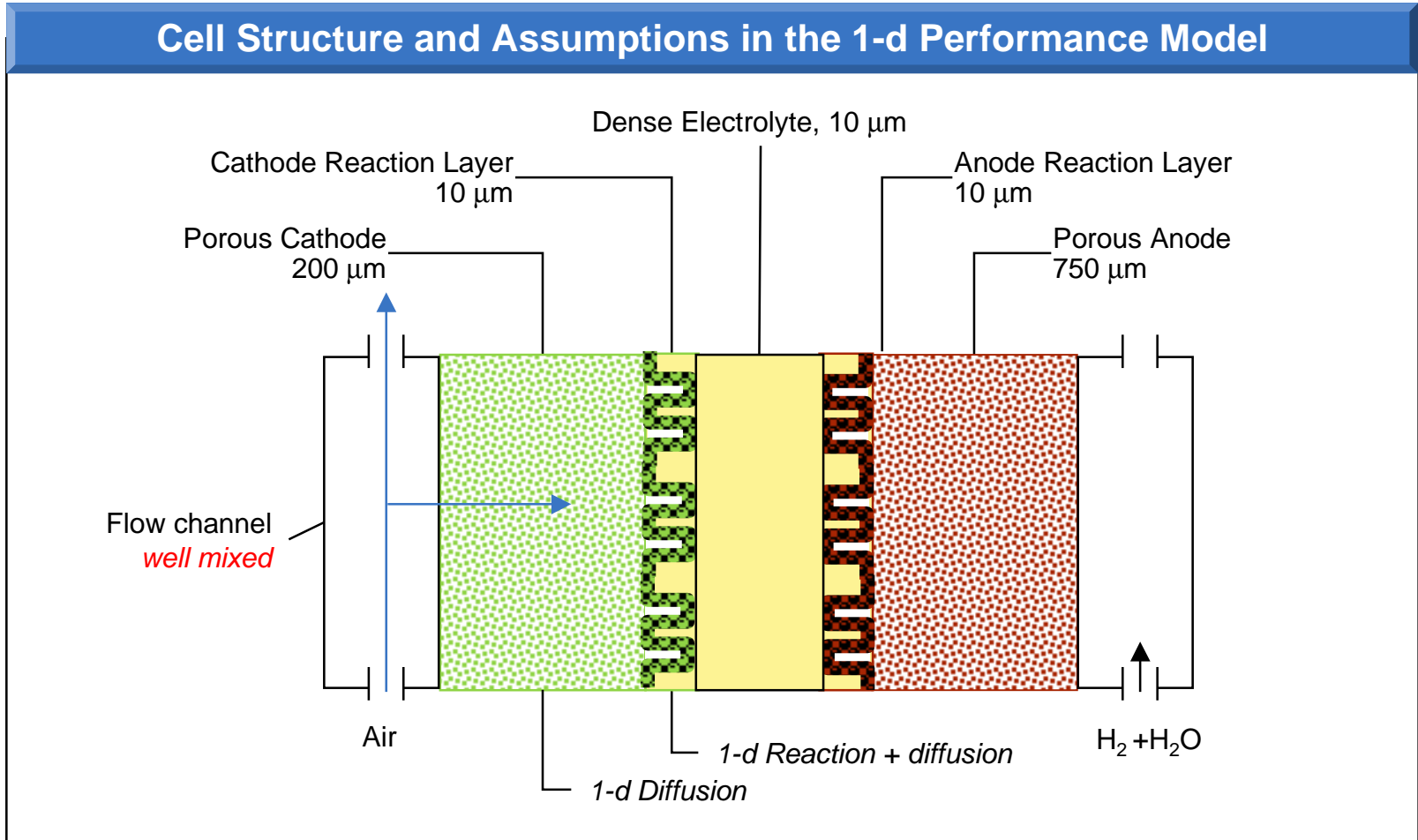


*Parameters describing the microstructure:*

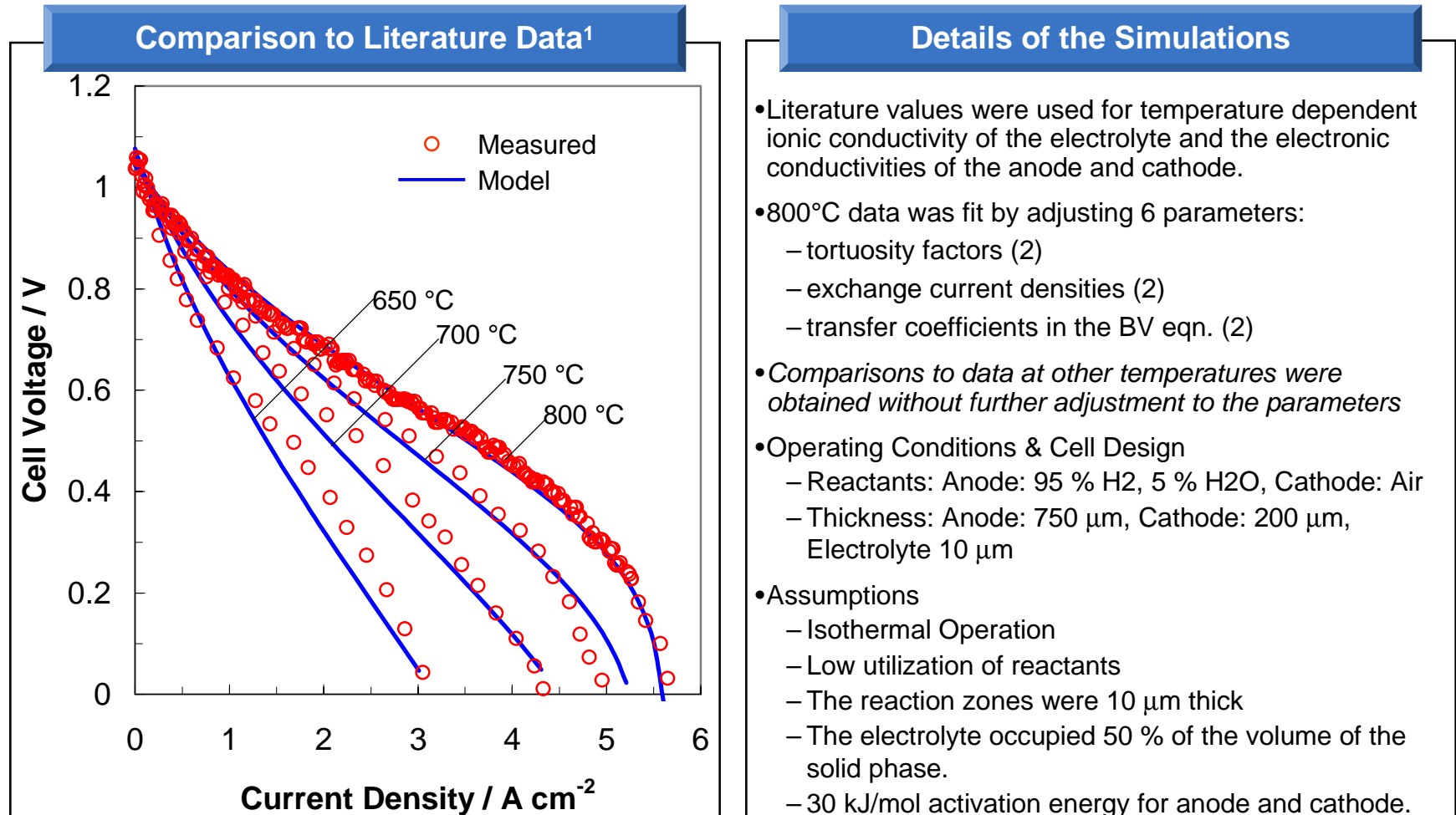
- h*: thickness of the reaction zone
- d*: pore radius
- w*: width of the electrocatalyst + electrolyte grains
- $\epsilon$ :  $d/(w+d)$ , porosity of the reaction zone
- $\phi$ : fraction of the solid material that is the electrolyte

<sup>a</sup> J-W Kim, A. Virkar, K-Z Fung, K. Mehta, S. Singhal, *J. Electrochem. Soc.*, 146 (1999) 69-78,  
<sup>b</sup> Model based on the description in ref. a but modified to account for the effect of species concentrations on electrode kinetics, species diffusion resistance in the electrode layer, and ionic conductivity of the electrolyte in the electrode layers.

The 1-d performance model contains sufficient detail to capture the anode supported SOFC performance at low utilization.



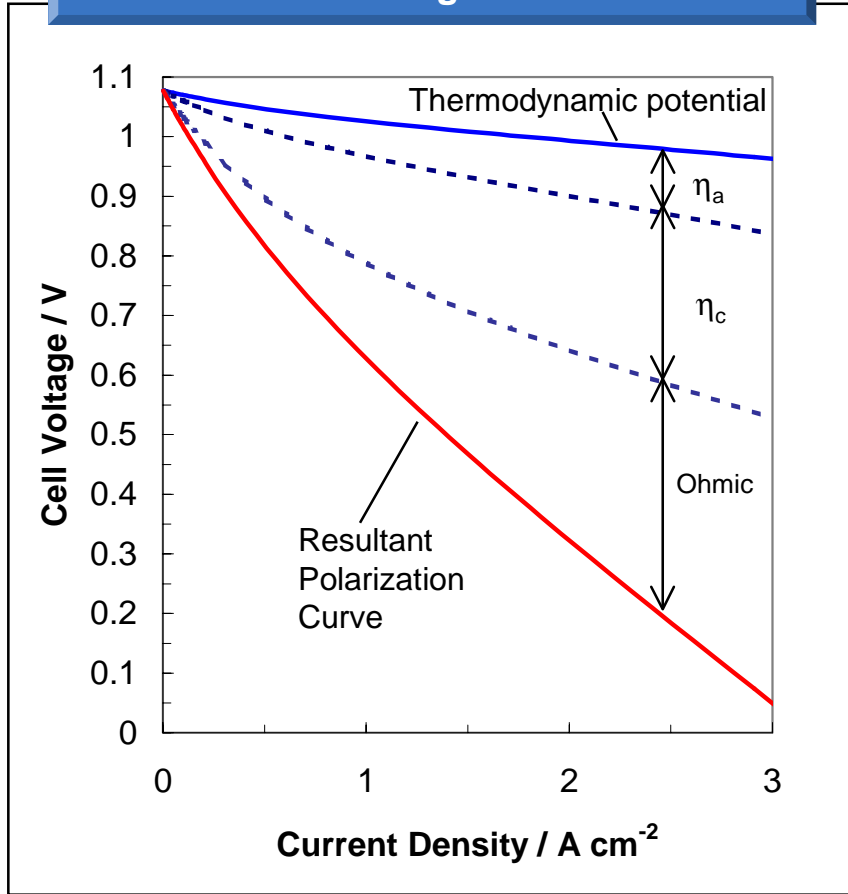
The parameters in the 1-d model were first fitted, and then validated by comparing with temperature-dependent experimental measurements.



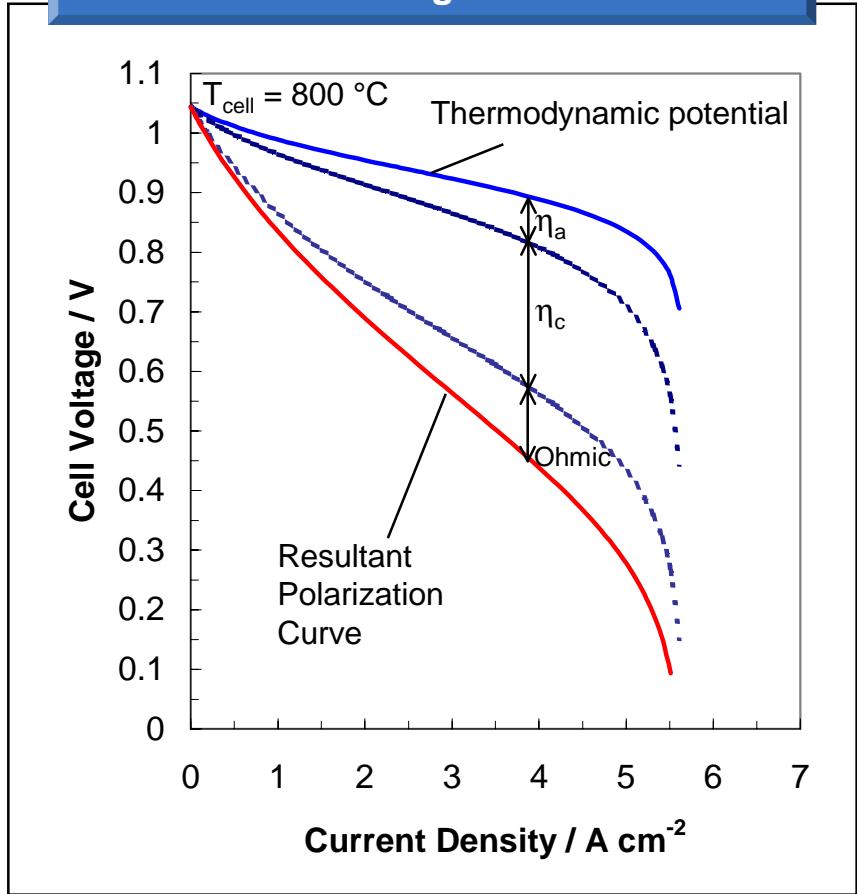
<sup>1</sup> J-W Kim, A. Virkar, K-Z Fung, K. Mehta, S. Singhal, *J. Electrochem. Soc.*, 146 (1999) 69-78.

**Both cathode overpotential and electrolyte ohmic loss are important at low temperatures, but cathode overpotential dominates at higher temperatures.**

Breakdown of Voltage Losses at 650°C



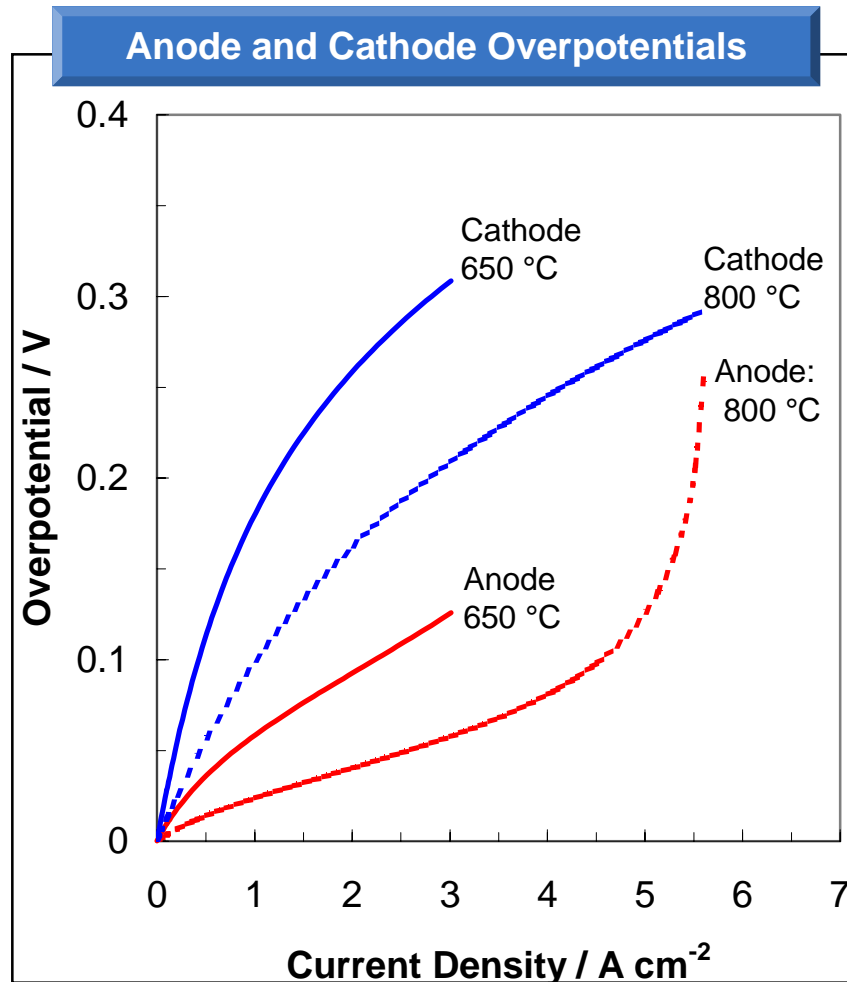
Breakdown of Voltage Losses at 800 °C



$\eta_a$  = Anode Overpotential,  $\eta_c$  = Cathode Overpotential, the ohmic loss represents the voltage drop across the electrolyte due to ionic current only. Although not considered here, any voltage drop due to contact resistances can be easily incorporated.



In general, both improved kinetics and reduced ionic resistance of the electrode result in lower overpotentials at higher temperatures.

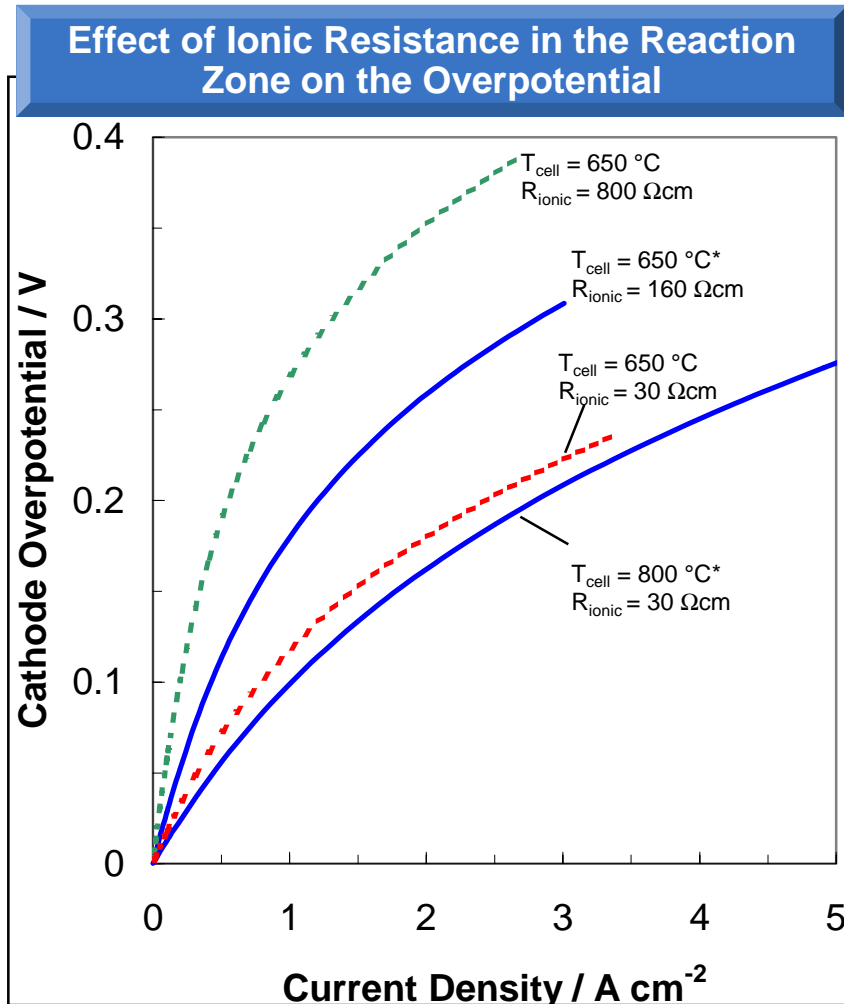


### Notes

- The overpotentials decrease with an increase in temperature because:
  - The electrochemical reactions have a finite activation energy, which increases the reaction rates at the lower temperature;
  - Ionic resistance in the electrode layer decreases, which results in a reduced voltage drop to the ‘ionic inner potential’ in the reaction zone;
  - Overpotential equals the difference in the ‘inner potentials’ of the ionic and electronic phases in the reaction layer. For a given current, the ionic inner potential decreases with an increase in the ionic resistance.



However, model results show that the ionic resistance of the electrode has a stronger influence on the overpotential than the intrinsic kinetics.



**Notes**

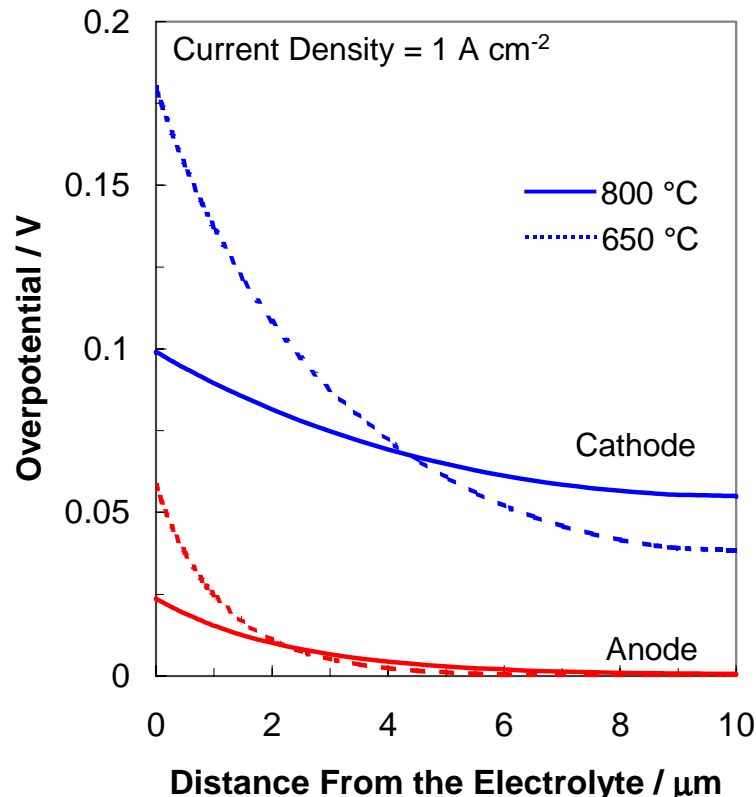
- The results presented here separate the effect on the overpotential of inherent kinetics and ionic resistance in the electrode:
  - Model results show that kinetics improvement alone reduces the overpotential by 20 mV at 1 Am cm<sup>-2</sup> (R<sub>ionic</sub> is constant at 30 Ω cm in going from 650 to 800 C).
  - Whereas, improvement in the ionic resistance alone reduces the overpotential by 80 mV at 1 A cm<sup>-2</sup> (R<sub>ionic</sub> decreases from 160 Ωcm to 30 Ωcm at 650 °C).



\* - base case parameters, R<sub>ionic</sub> = Ionic resistivity of the electrolyte in the cathode reaction zone,

The significance is that incorporation of a high ion conducting compound in the reaction layer alone can reduce the overpotential of LSM cathodes...

### Penetration Depth of the Reaction

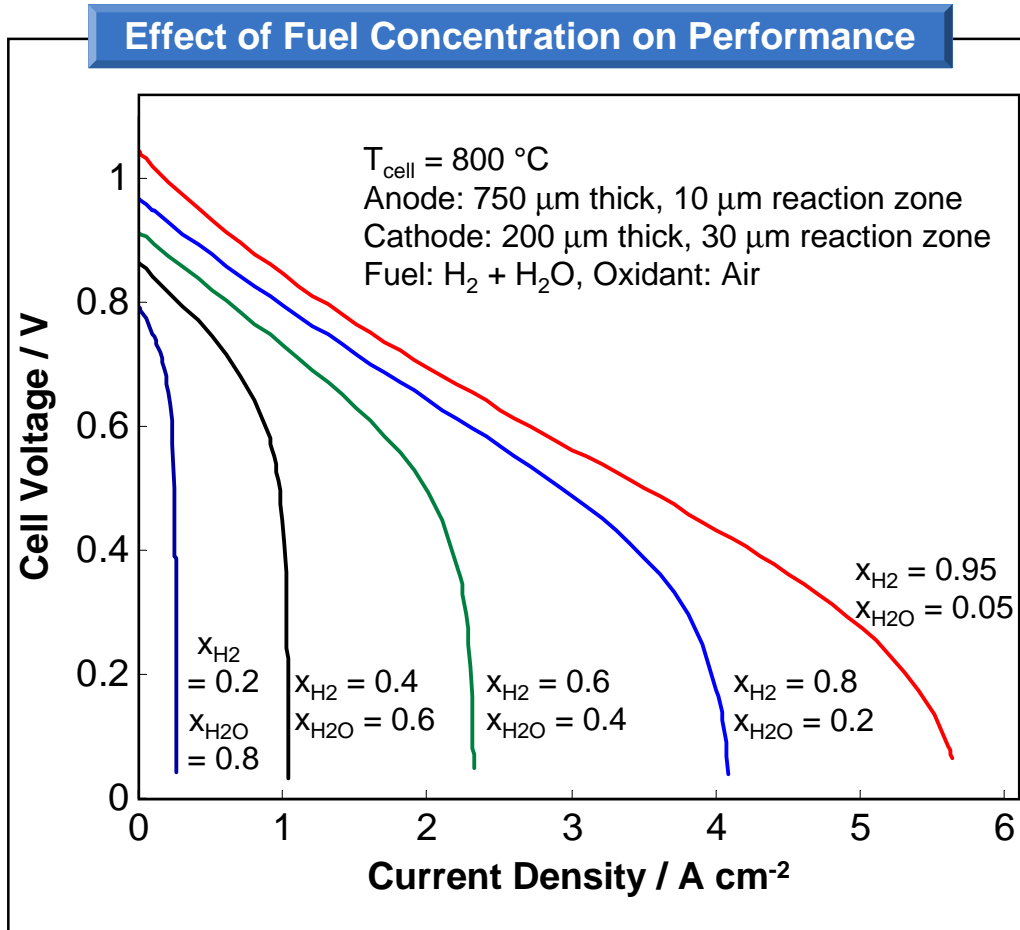


### Details of the Simulations

- Distance = 0 corresponds to the electrolyte/electrode interface. Note that the overpotential typically reported in the literature is measured at distance = 0.
- The extent the reaction penetrates into the electrode depends on the rate of reaction: the slower the reaction the greater the penetration (e.g., see cathode vs. anode)
- Because the reaction rates depend on the local conditions, the penetration depth changes with temperature, species concentrations, length of three phase boundary, porosity, tortuosity, etc.

... The important consequence is that such a modification will not alter the cathode CTE, which is essential to ensure MEA integrity in the SOFC.

The 1-d model also helps probe the effect of ‘what-if’ scenarios, e.g., going from a feed of 95% H<sub>2</sub> to 40% H<sub>2</sub> leads to 50% lower current density at 0.7 V.

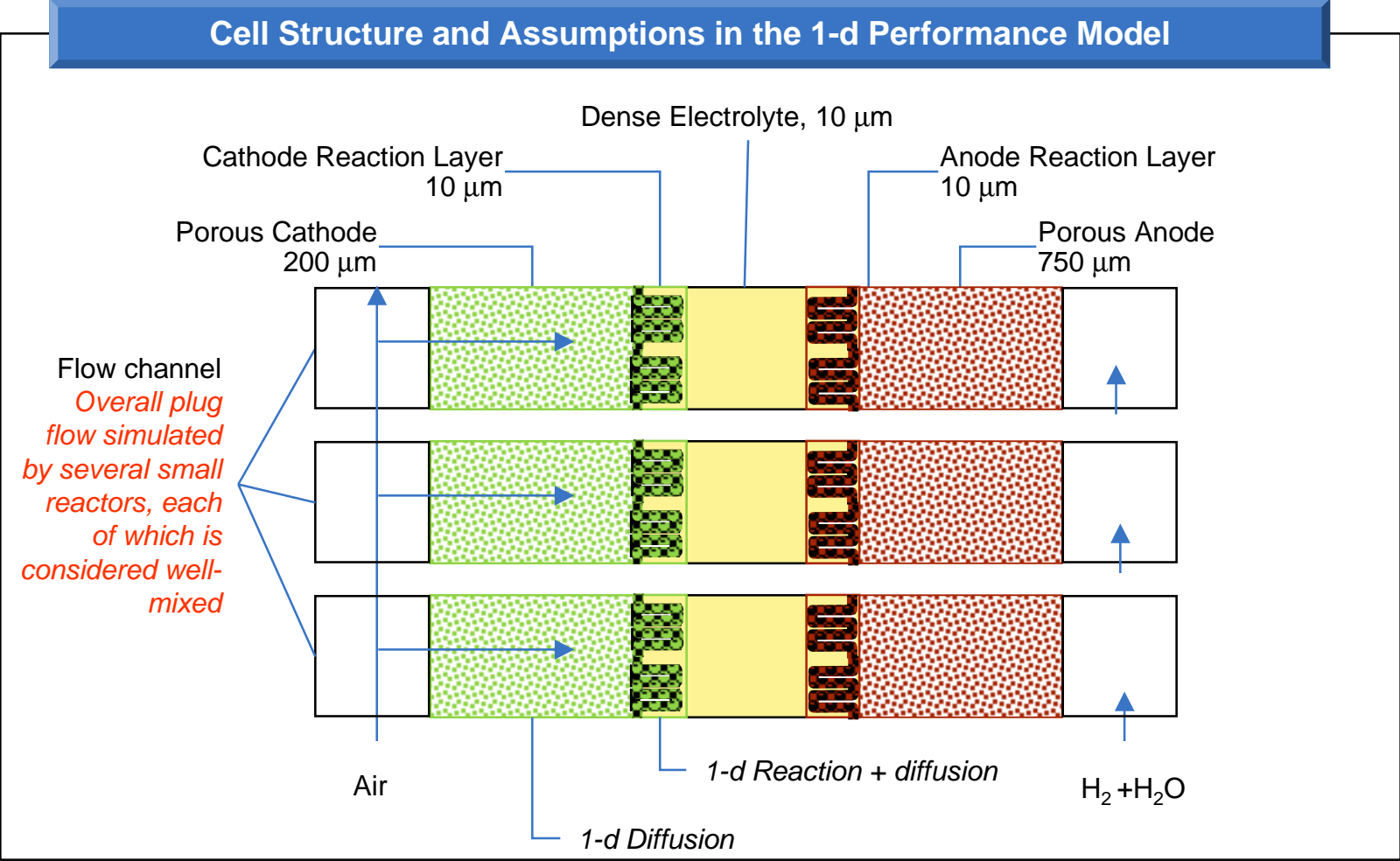


**Notes**

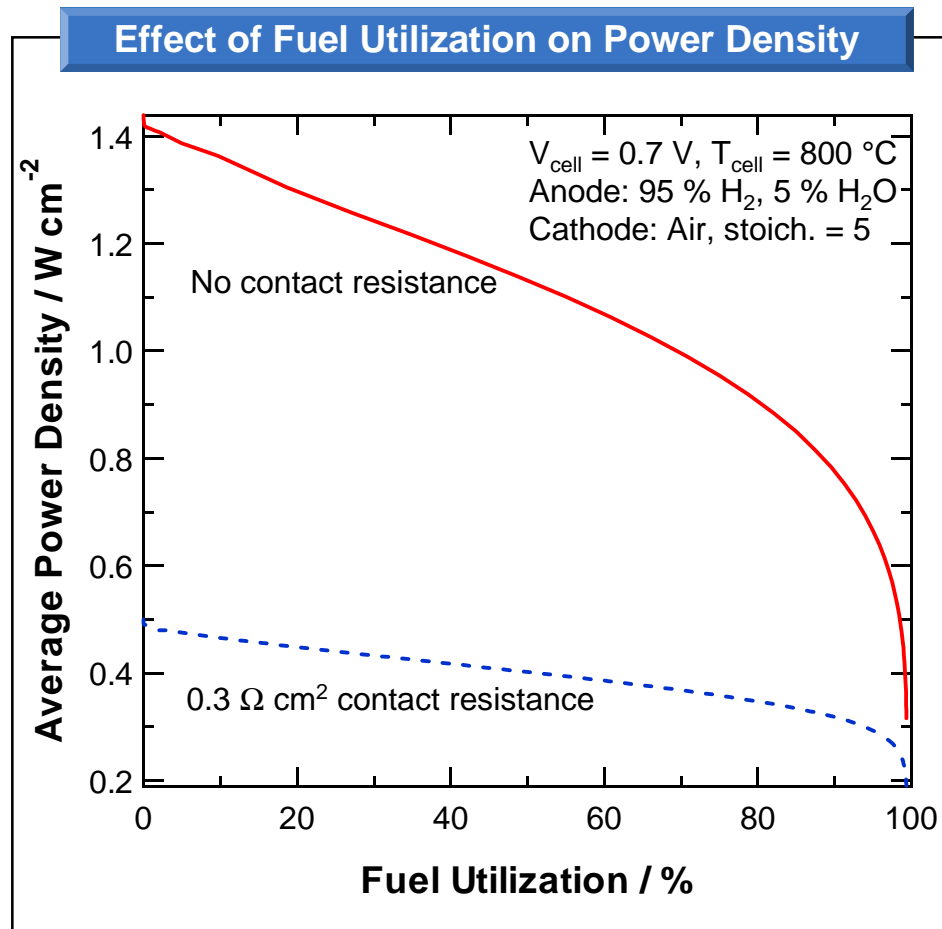
- The results for  $x_{\text{H}_2} = 0.95$  correspond to the best-fit to Virkar’s data.
- The simulations were for negligible utilization of the reactants.
- The results for other concentrations were obtained by changing only the inlet hydrogen and water concentrations.
- The reason for the drastic decrease in current density is due to the decrease in the open circuit voltage at the lower hydrogen concentration (higher water concentration).



The 2-d performance model contains sufficient detail to simulate cell performance under conditions of high fuel utilization.



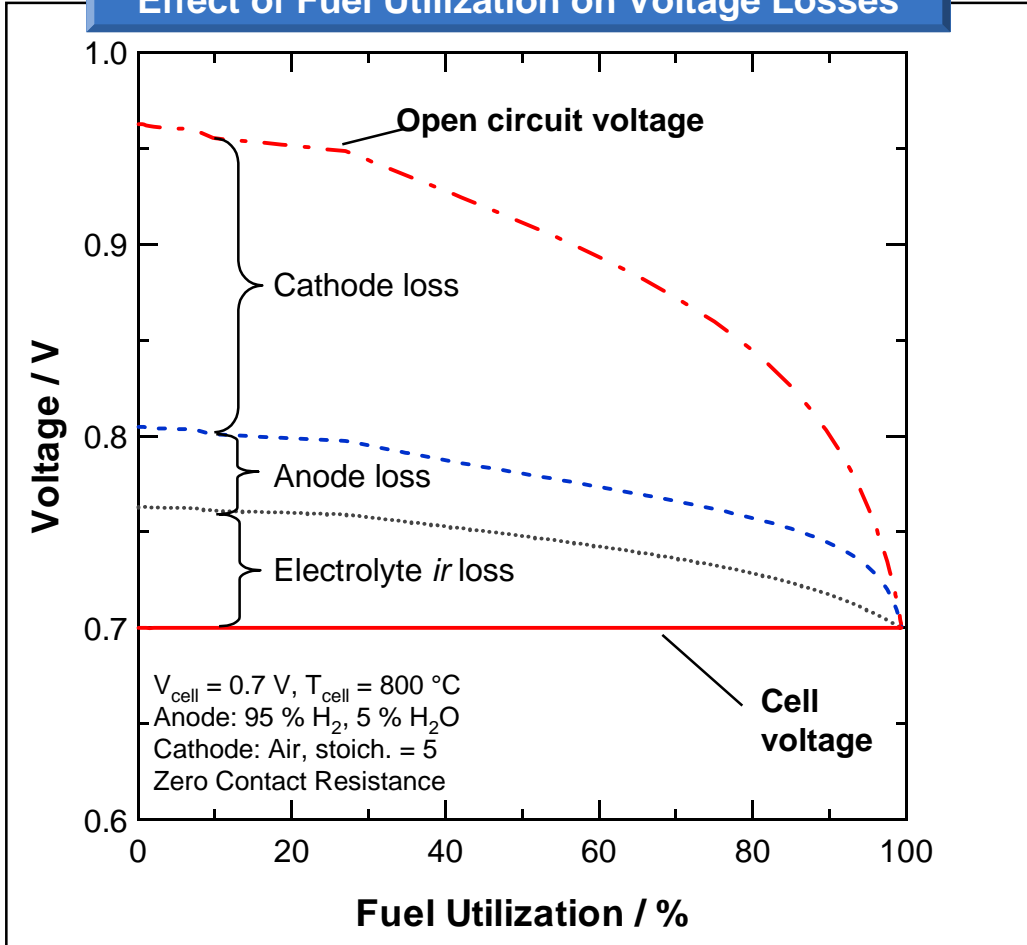
The power density decreases with increasing fuel utilization; the decrease, is less pronounced when the internal resistance of the cell is high.

**Notes**

- This simulation corresponds to the case where the inlet fuel flow is held constant and the cell area is increased in order to increase the fuel utilization.
- In this simulation, the fuel concentration decreased along the length of the flow channel, but there was no significant change in the oxygen concentration.
- The cell dimensions used were:
  - Anode:  $750 \text{ } \mu\text{m}$
  - Cathode:  $200 \text{ } \mu\text{m}$
  - Electrolyte:  $10 \text{ } \mu\text{m}$

**This decrease is primarily due to reduction in the hydrogen concentration (and water accumulation), which reduces the driving force for the reaction.**

**Effect of Fuel Utilization on Voltage Losses**



**Notes**

- The decrease in the open circuit voltage is due to decrease in the hydrogen concentration and increase in the water concentration in the anode side.
- The cathode overpotential and  $ir$  loss in the electrolyte decrease with increasing utilization because of decrease in the current
- The anode overpotential appears approximately constant because even though the current is decreasing (which will lower the overpotentials), the hydrogen concentration is also decreasing (which will raise the overpotentials).
- The cathode overpotential dominate the voltage loss over the entire range of hydrogen utilization.



**In addition to facilitating in the construction of the structural model, the simple performance models provide critical insight into SOFC operation.**

- We have developed 1-d and 2-d, isothermal performance models for planar, anode supported SOFCs, that account for the details of the microstructures of the electrodes.
- The 1-d model calculates cell performance under conditions of low fuel utilization, whereas the 2-d model calculates the performance under high fuel utilization.
- The main results from using these models are:
  - The 1-d model was able to predict the temperature dependence of the performance of an anode-supported SOFC.
  - The cathode overpotential dominated the anode overpotential for operation between 650 - 800 °C, both at low and high fuel utilizations.
  - The higher cathode overpotential at the lower temperatures is a result as much of the poor ionic conductivity of the electrode as of the reduced kinetics.
  - Fuel utilization has a major impact on the power density of the cell mainly due to accumulation of water, which lowers the thermodynamic driving force and the hydrogen mole fraction.

# Outline of Final Report

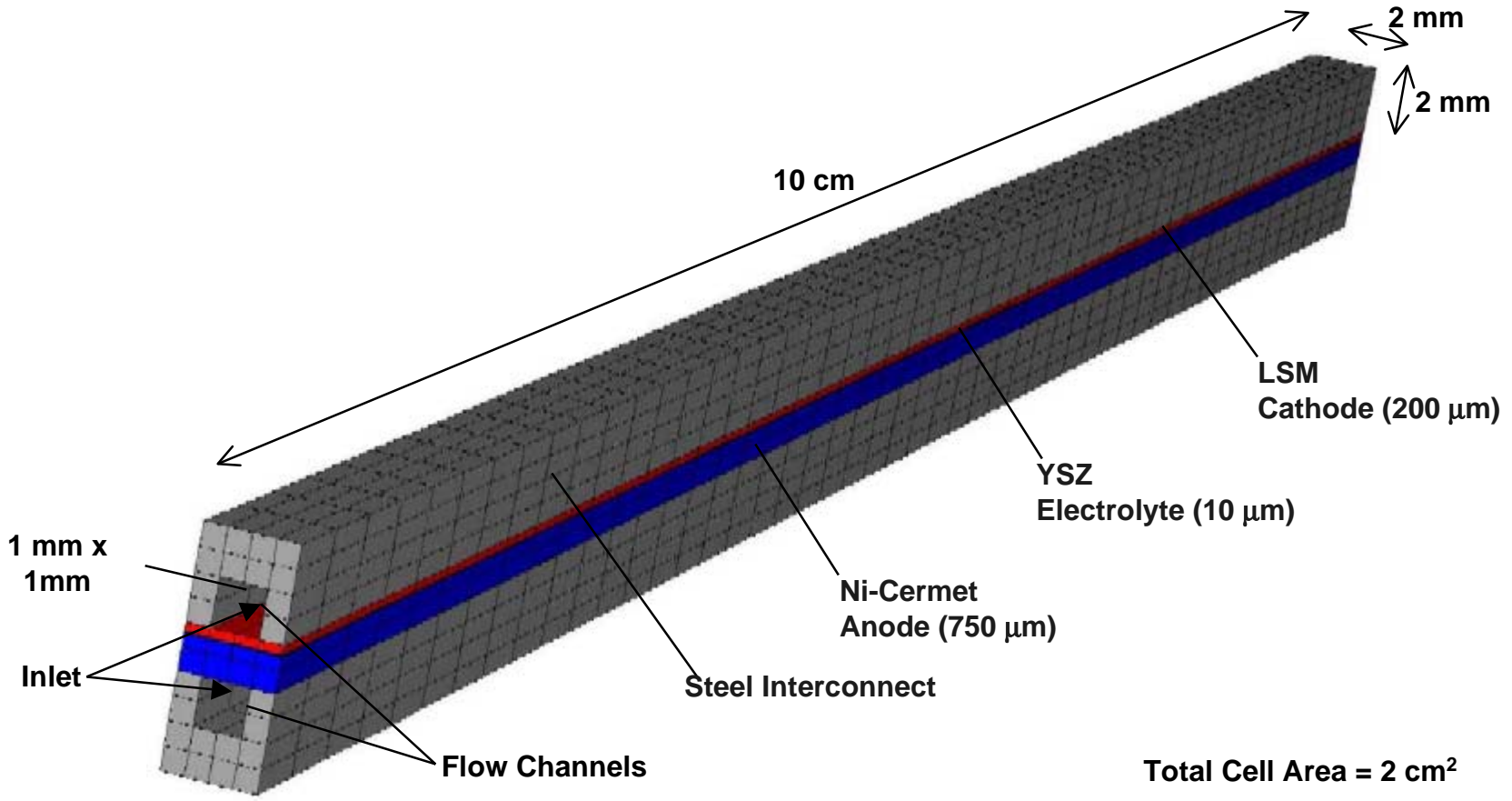
---

0	Executive Summary
1	Background & Objectives
2	Approach & Scope
3	Model Development
4	Single Channel SOFC Results
5	Multi Channel SOFC Results
6	Limitations for Cell Size
7	Summary
A	Appendix





We constructed the SOFC model in ABAQUS and used a simple geometry to verify the successful implementation of the different model elements.



## The single channel geometry was used to verify model performance.

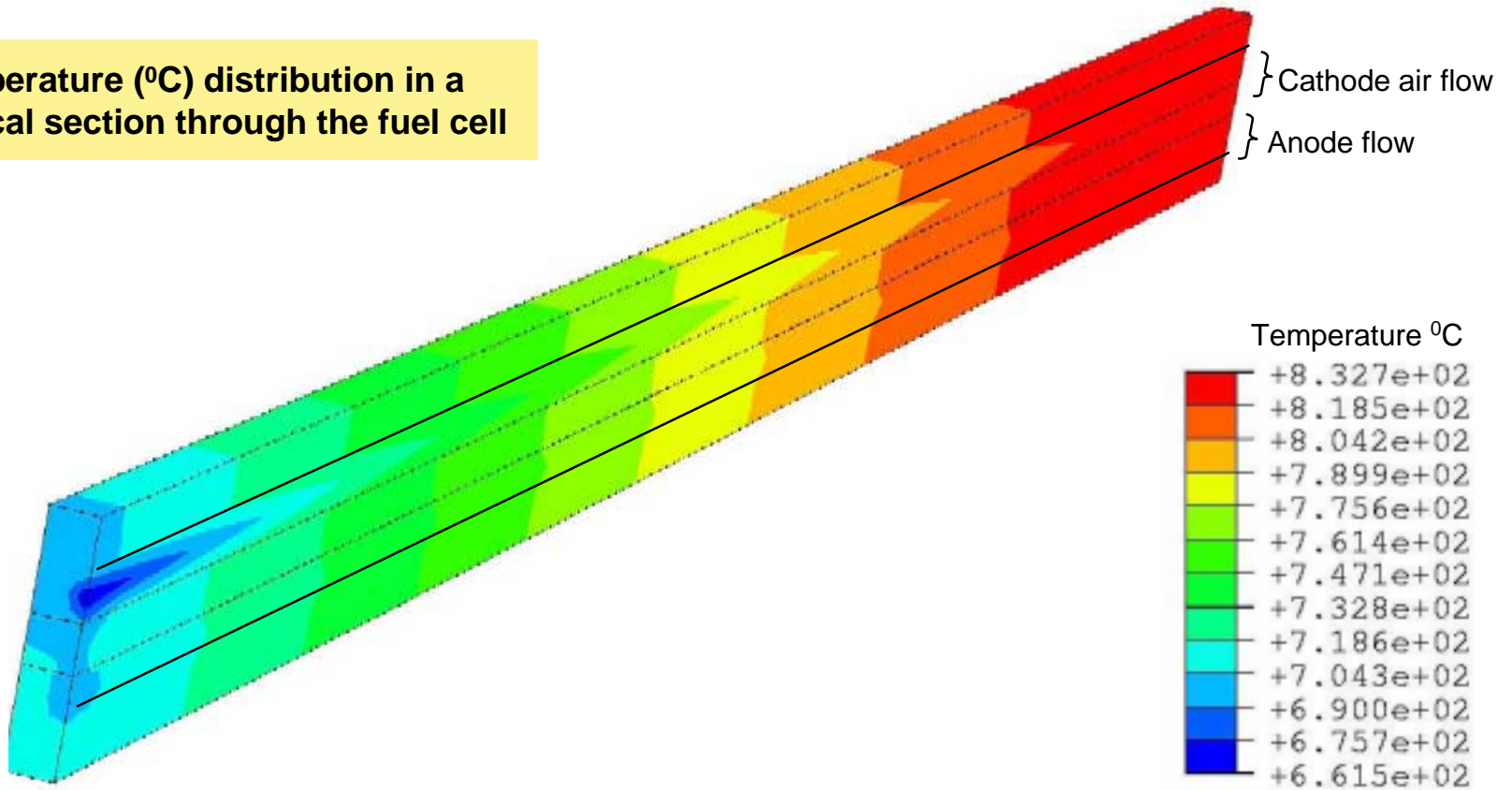
- Verify that the modules key to calculating the fuel cell performance worked without error:
  - Module for calculating the local current density accounting for species concentration, temperature, and electrolyte resistance.
  - Module for calculating the heat released due to electrochemical reaction accounting for the cell voltage and current density.
  - Module for calculating the diffusion of species through the porous electrodes
- Verify the conservation of mass, energy, and charge both on a local basis and an overall basis
- Develop procedures for estimating the stress distribution in the cell components during operation
- Verify the robustness of the numerical solution through a sensitivity analysis

**We selected typical operating conditions for the base case test simulations, consistent with assumptions in previous TIAx studies.**

Parameter	Value
<ul style="list-style-type: none"><li>• Cell voltage</li></ul>	<ul style="list-style-type: none"><li>• 0.7 V</li></ul>
<ul style="list-style-type: none"><li>• Composition of the reactant streams</li></ul>	<ul style="list-style-type: none"><li>• Anode: 97 % H<sub>2</sub>, 3 % H<sub>2</sub>O, Cathode: air</li></ul>
<ul style="list-style-type: none"><li>• Gas inlet temperatures</li></ul>	<ul style="list-style-type: none"><li>• 650 C at the Anode and Cathode</li></ul>
<ul style="list-style-type: none"><li>• Fuel utilization</li></ul>	<ul style="list-style-type: none"><li>• ~ 65 %</li></ul>
<ul style="list-style-type: none"><li>• Cathode stoichiometry</li></ul>	<ul style="list-style-type: none"><li>• ~4, the cathode flow rate was adjusted such that the temperature at the cell outlet was nominally 800 C.</li></ul>

An air stichiometry of four is required to ensure that at 0.7 V, the cell outlet temperature is nominally 800 C.

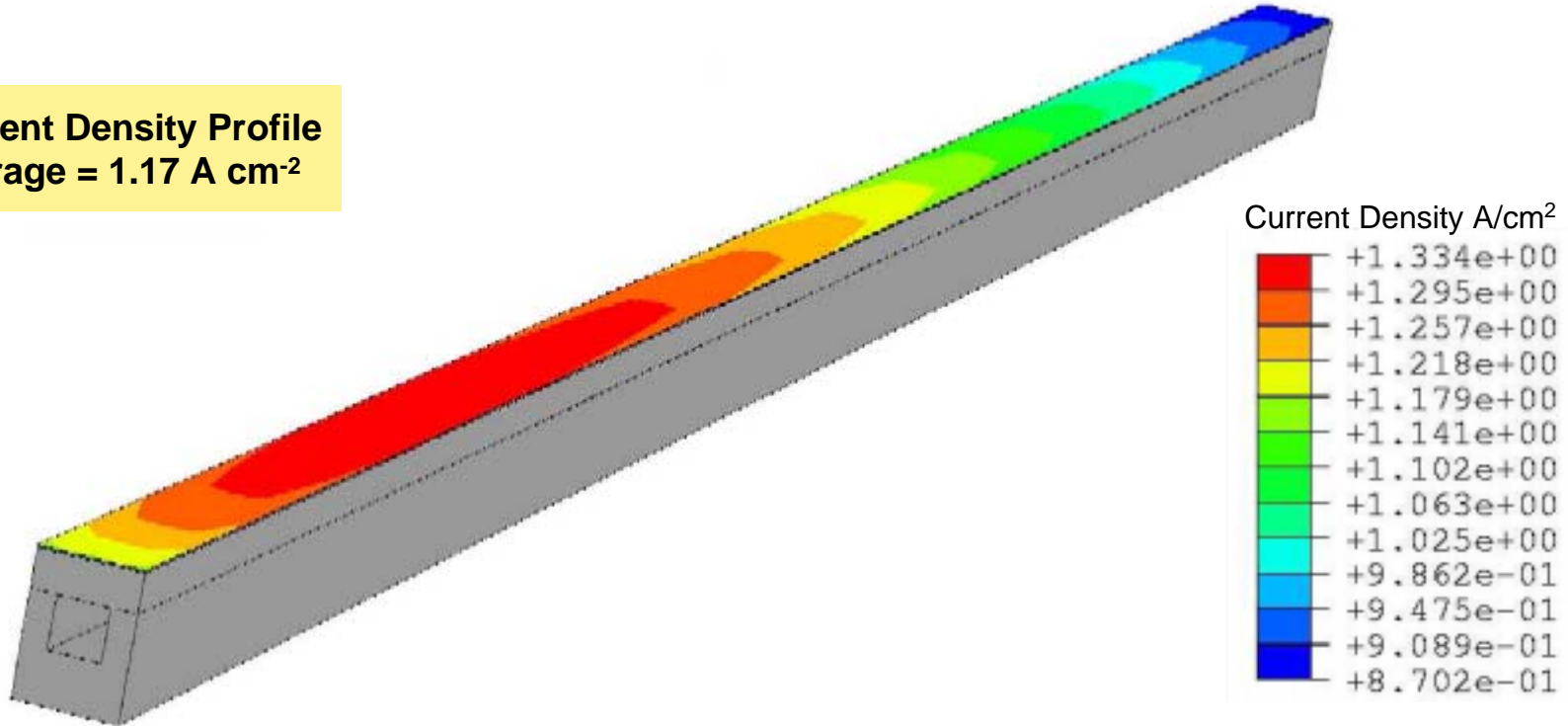
Temperature (°C) distribution in a vertical section through the fuel cell



Due to exothermic reaction in the cell and an adiabatic boundary condition on the cell, the gas temperatures increase along the flow channel.

**Predicted average current density is consistent with measured performance\* of anode supported SOFCs at 0.7 V and 800 C.**

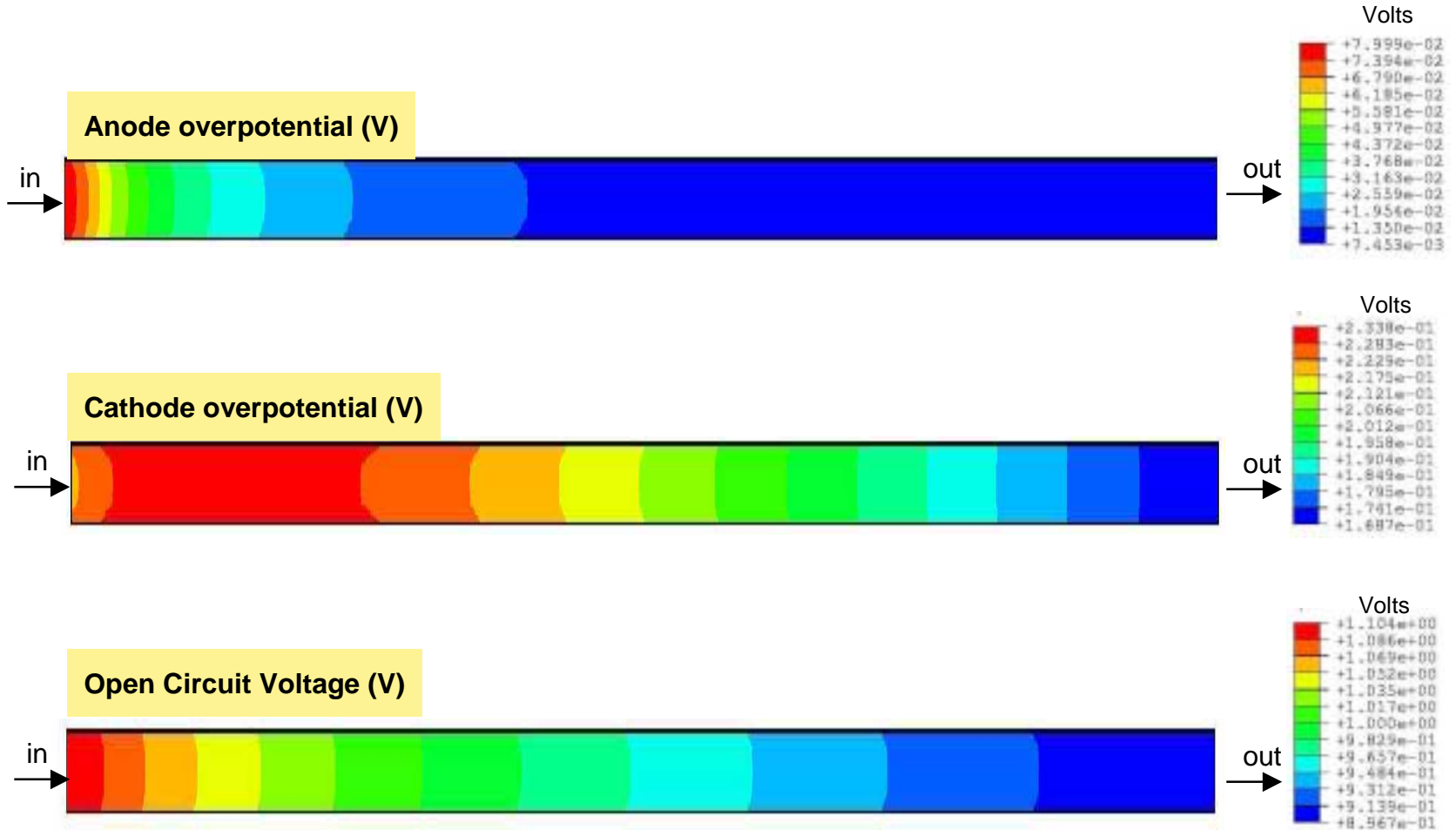
**Current Density Profile**  
Average = 1.17 A cm<sup>-2</sup>



- The current initially rises along the channel because of the rising temperature but falls subsequently because of water accumulation in the anode channel, which lowers the thermodynamic driving force.
- The current density in the region immediately underneath the flow channel is higher than that underneath the channel ridge.

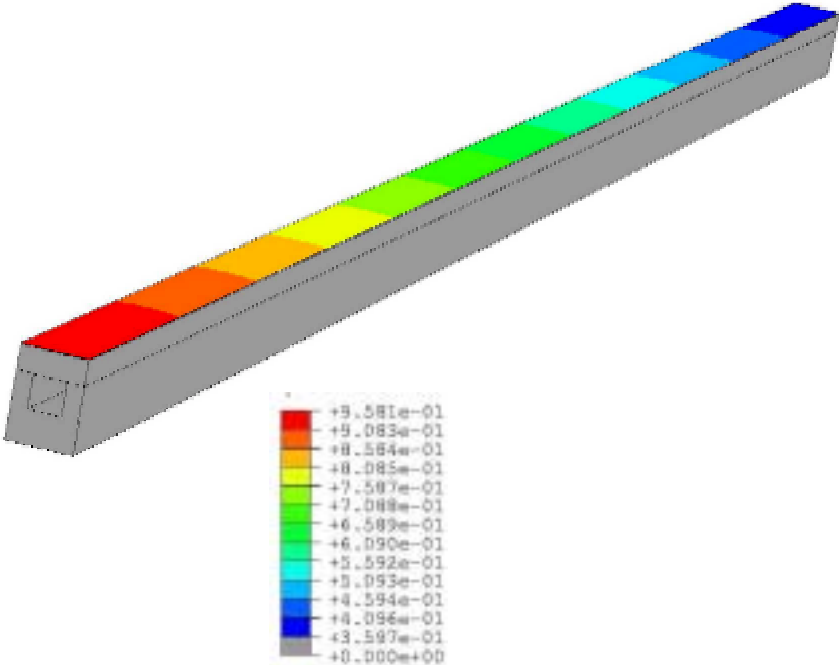
\*J-W Kim, A. Virkar, K-Z Fung, K. Mehta, S. Singhal, *J. Electrochem. Soc.*, 146 (1999) 69-78.

As expected, the cathode overpotential dominates the losses throughout the cell for this configuration and operating conditions.

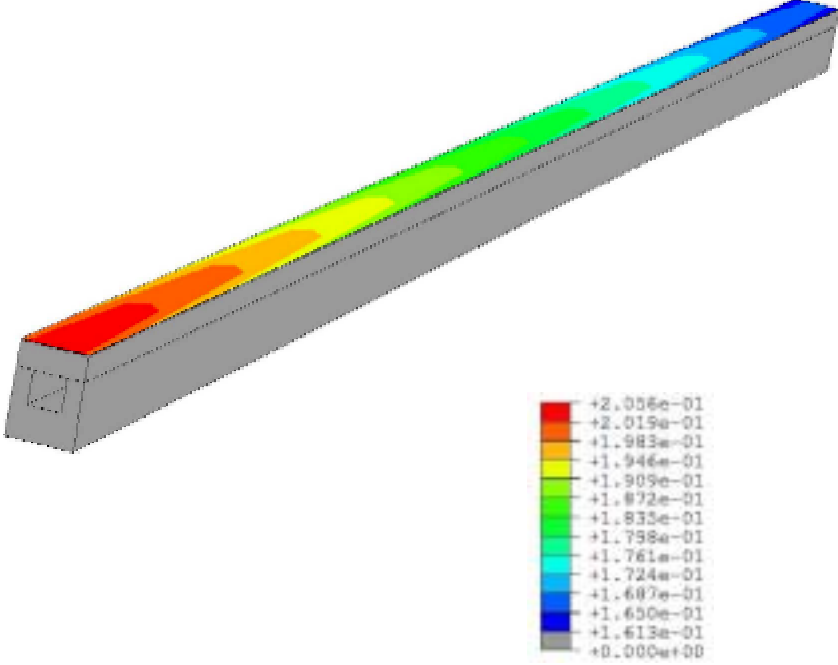


As expected, the thick anode does not limit H<sub>2</sub> diffusion as evidenced by the laterally uniform H<sub>2</sub> distribution in the anode reaction zone.

Hydrogen mole fraction in the anode reaction zone



Oxygen mole fraction in the cathode reaction zone



In contrast, the slower diffusion of O<sub>2</sub> leads to depletion in the region immediately under the channel ridge.



**To characterize the stress-state of SOFC components during operation, manufacturing procedures must be taken into account.**

**Procedure for residual stress calculations**

**Step 0: Sintering Ceramics**

- Assume that all the ceramic layers in the MEA are stress-free at the co-sintering temperature of 1400 C.
- The component layers in the ceramic MEA are assumed to be fused together.
- Assume interconnects are stress free at room temperature

**Step 1: Cool Down to Room Temperature**

- Calculate the stresses in the ceramic layers when the MEA is cooled down to room temperature (residual stresses).

**Step 2: Flatten Ceramics**

- Apply appropriate confining pressure to flatten the MEA (this is needed to ensure sealing and electric contact).
- Assemble flat MEA between interconnects

**Step 3: Heat Up to Operating Temperature**

- Assume no-slip condition between interconnect and ceramics
- Calculate stress distribution by applying the steady temperature gradients calculated for cell operation

\* Assumption of no-slip appears justified for the metallic interconnects that are non bonded to the ceramic electrodes.





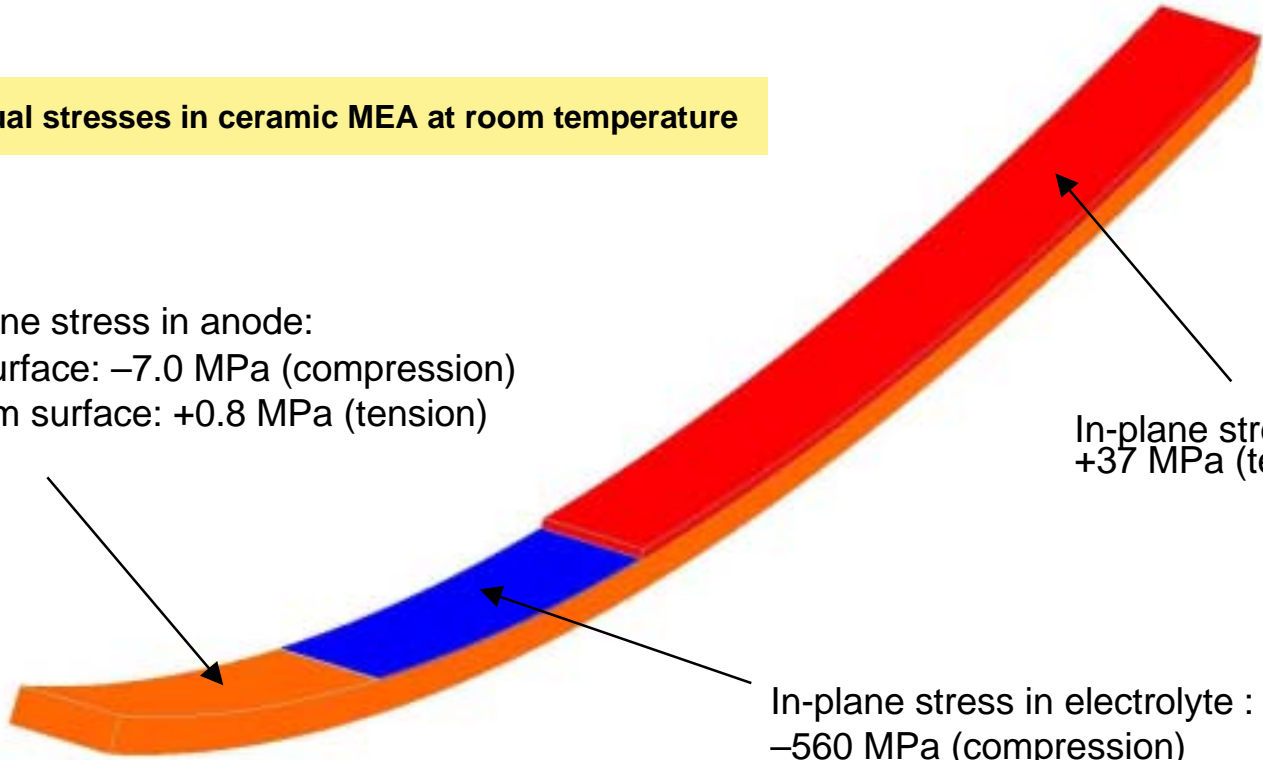
In Step 1, bending stresses that arise to balance the moments created by anode/cathode TCE mismatch cause bowing of the ceramic MEA layers.

Residual stresses in ceramic MEA at room temperature

In-plane stress in anode:  
top surface:  $-7.0$  MPa (compression)  
bottom surface:  $+0.8$  MPa (tension)

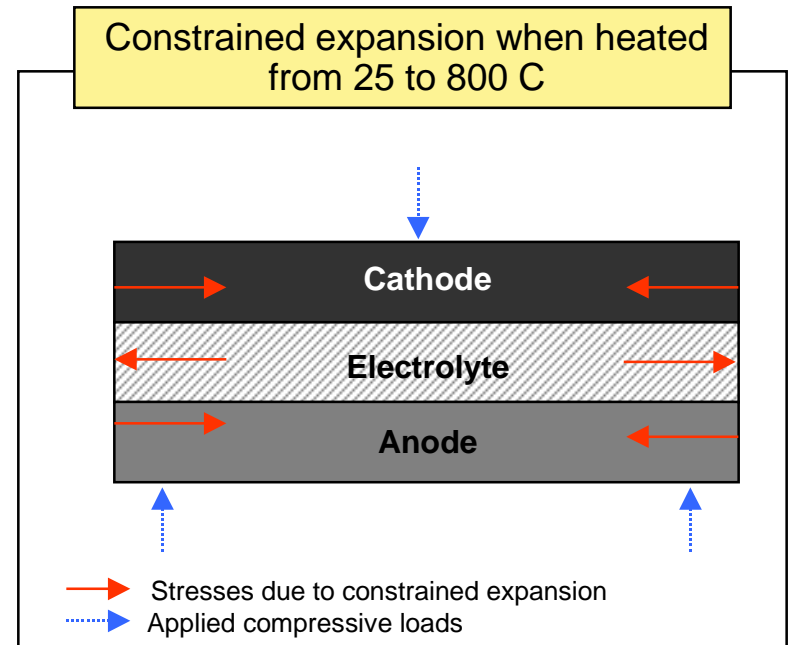
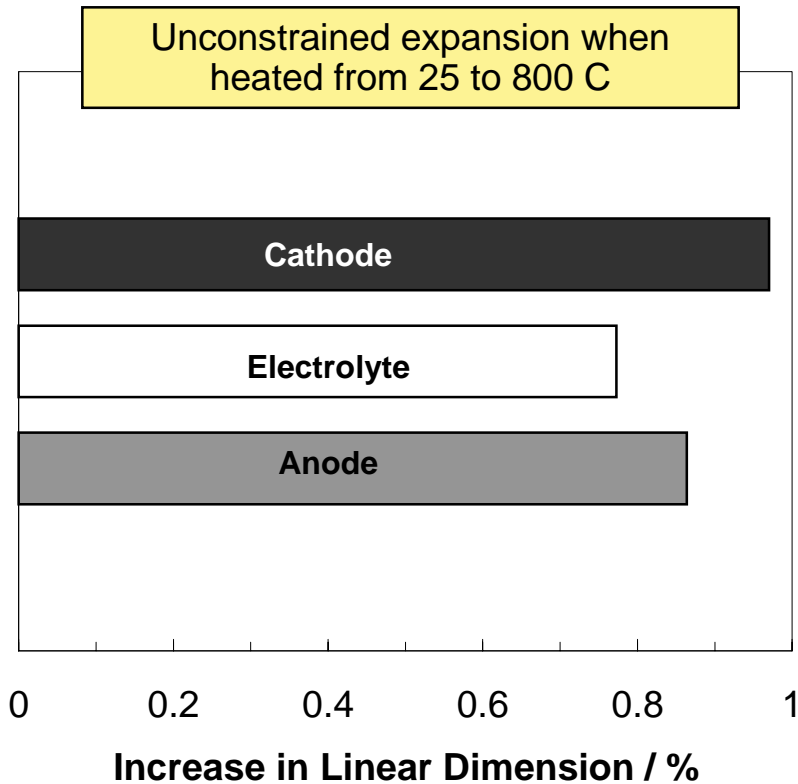
In-plane stress in cathode:  
 $+37$  MPa (tension)

In-plane stress in electrolyte :  
 $-560$  MPa (compression)



Note: displacements magnified 25 times. Total bowing of the cell layers in direction perpendicular to plane =  $0.07$  mm.

**Mismatch in the thermal expansion coefficients can give rise to relatively large strains, or bending moments in constrained expansion.**



**The mechanical behavior in Step 1 is driven by the anode layer, which is thickest and stiffest component of the ceramic MEA.**

- Thermal strain in each layer arises according to the formula:

$$\varepsilon_{th} = \alpha(T)[T-T_0] - \alpha(T_i)[T_i-T_0]$$

where  $\alpha$  is the CTE,  $T_i$  is the initial temperature and  $T_0$  is the reference temperature (room temperature).

- This implies that the strain at room temperature is controlled by the value of  $\alpha$  at 1400 C.
- Assuming that the 3 layers 'fuse' at 1400 C, a negative thermal strain arises in each layer which is a function of  $\alpha$  at 1400 C.
- Since  $\alpha$  at 1400 C is larger for the cathode layer (data in the Appendix), it wants to shrink more, but is constrained by the anode layer. A tensile stress therefore arises in the cathode layer.
- A smaller compressive stress arises in the anode layer to balance the tensile forces in the cathode layer.
- A bending stress arises in both layers to balance moments. It is more pronounced in the thicker anode layer. This stress results in warping of the MEA layers.
- The thin electrolyte effectively 'goes along for the ride'. Since  $\alpha$  at 1400 C is much smaller for the electrolyte layer, a large compressive stress arises in it.

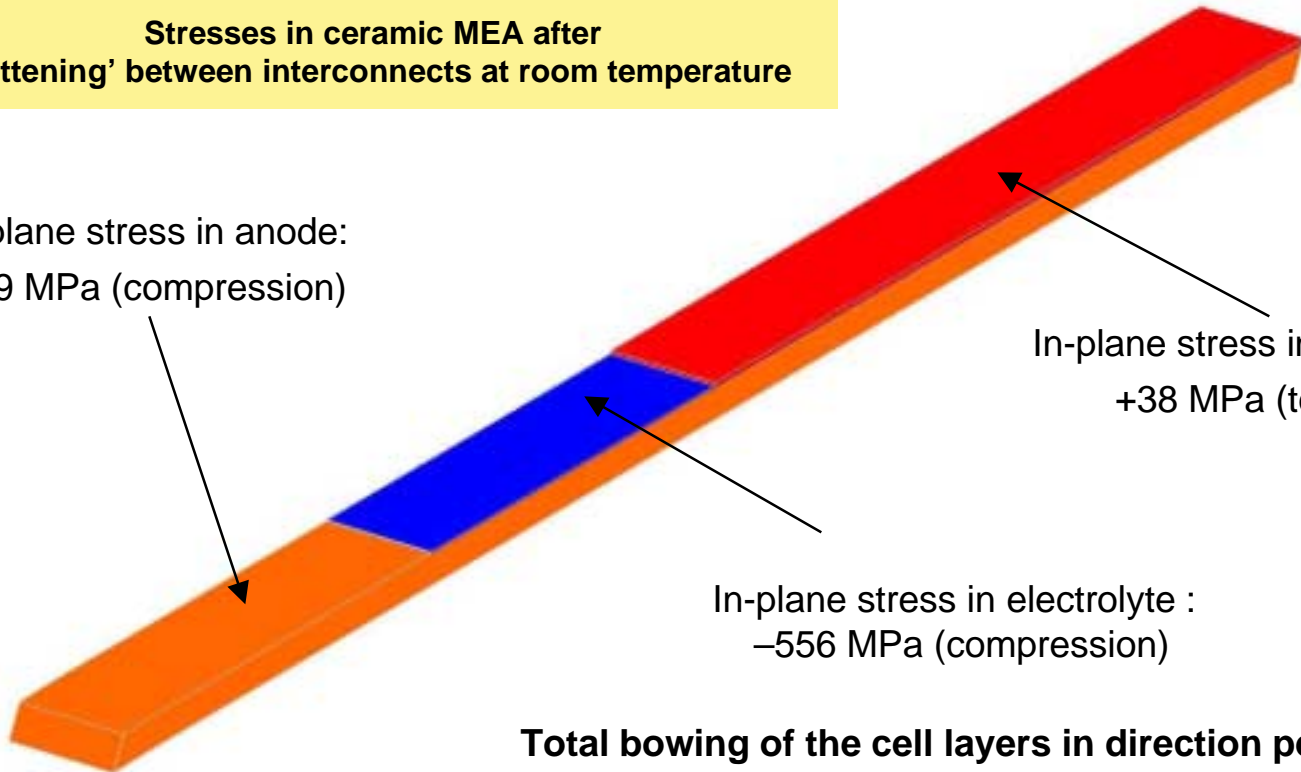
In step 2, a confining pressure (0.4 MPa) flattens the warped MEA, but does not significantly affect the stress in the cathode or electrolyte layers.

Stresses in ceramic MEA after 'flattening' between interconnects at room temperature

In-plane stress in anode:  
-2.9 MPa (compression)

In-plane stress in cathode:  
+38 MPa (tension)

In-plane stress in electrolyte :  
-556 MPa (compression)



Total bowing of the cell layers in direction perpendicular to plane reduced to less than 0.0006 mm

However, the bending stress in the anode layer is eliminated.

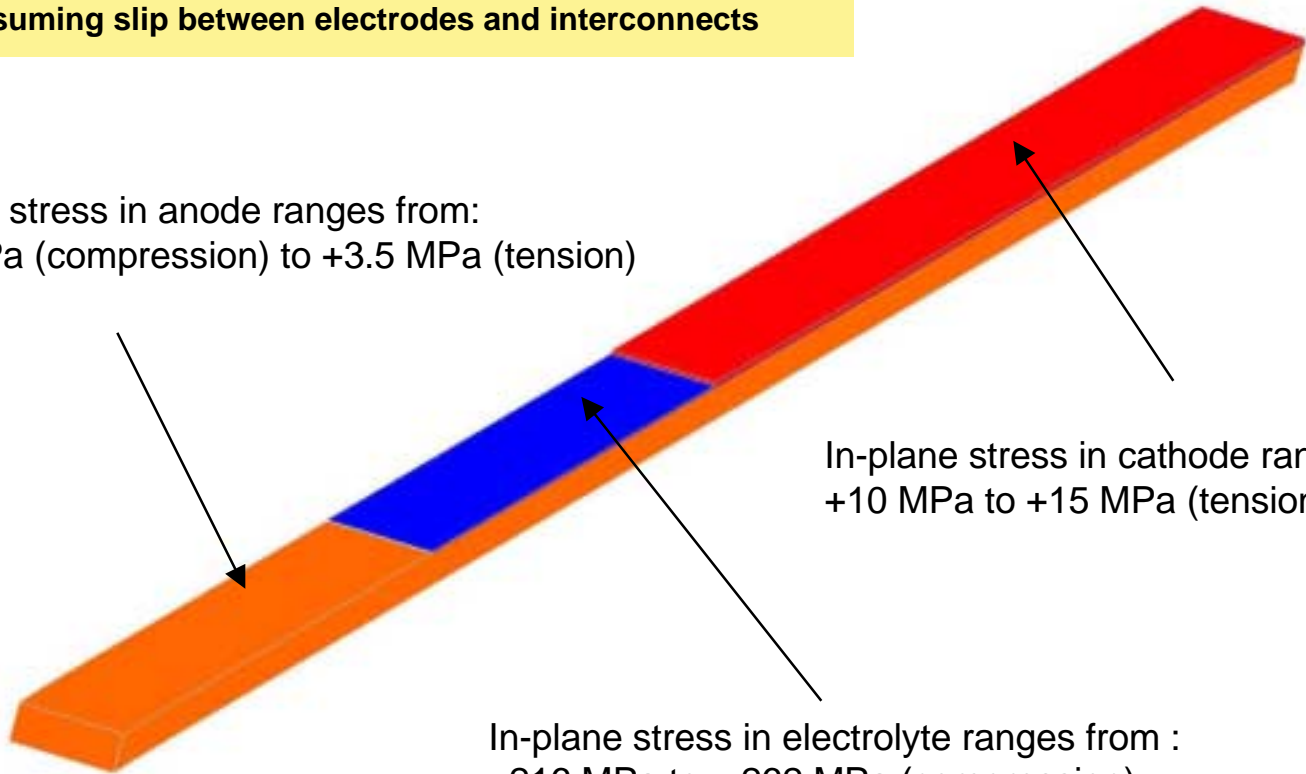
## Imposition of the steady-state operating temperature profile results in significantly reduced stresses from those at room temperature.

Stresses in ceramic MEA under steady state operation at 0.7 V assuming slip between electrodes and interconnects

In-plane stress in anode ranges from:  
-2.7 MPa (compression) to +3.5 MPa (tension)

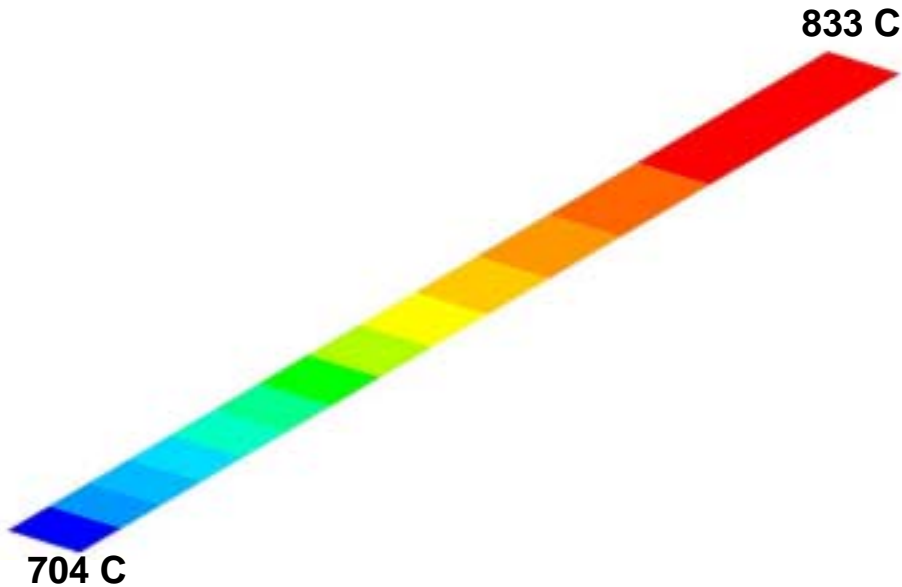
In-plane stress in cathode ranges from:  
+10 MPa to +15 MPa (tension)

In-plane stress in electrolyte ranges from :  
-216 MPa to -262 MPa (compression)

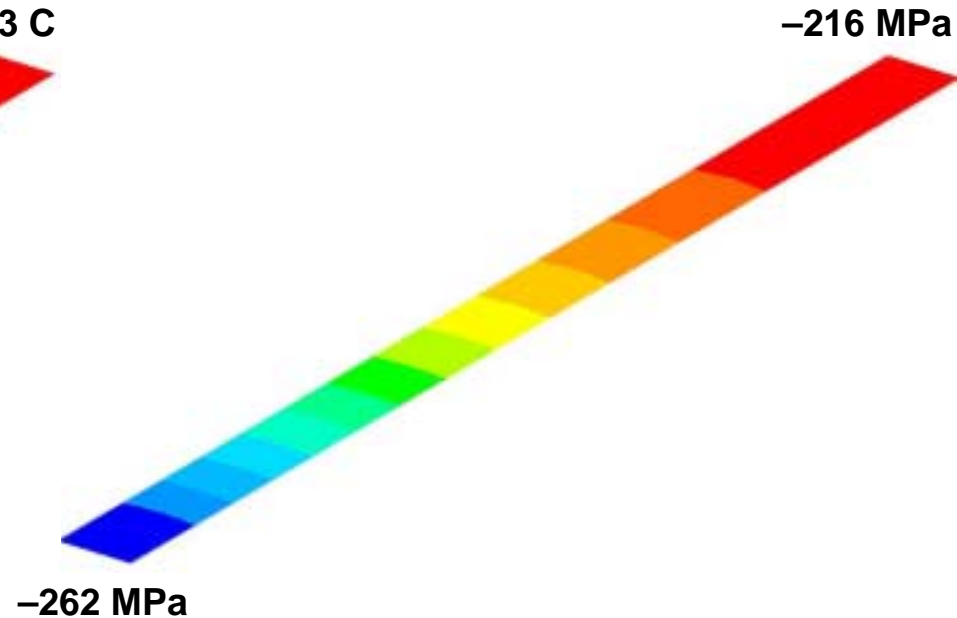


**Although the magnitude of the stresses is lower during steady state cell operation, the in-plane stress profile follows the temperature gradient.**

Temperature gradient in the electrolyte at 0.7 V



In-plane stress distribution in the electrolyte at 0.7 V

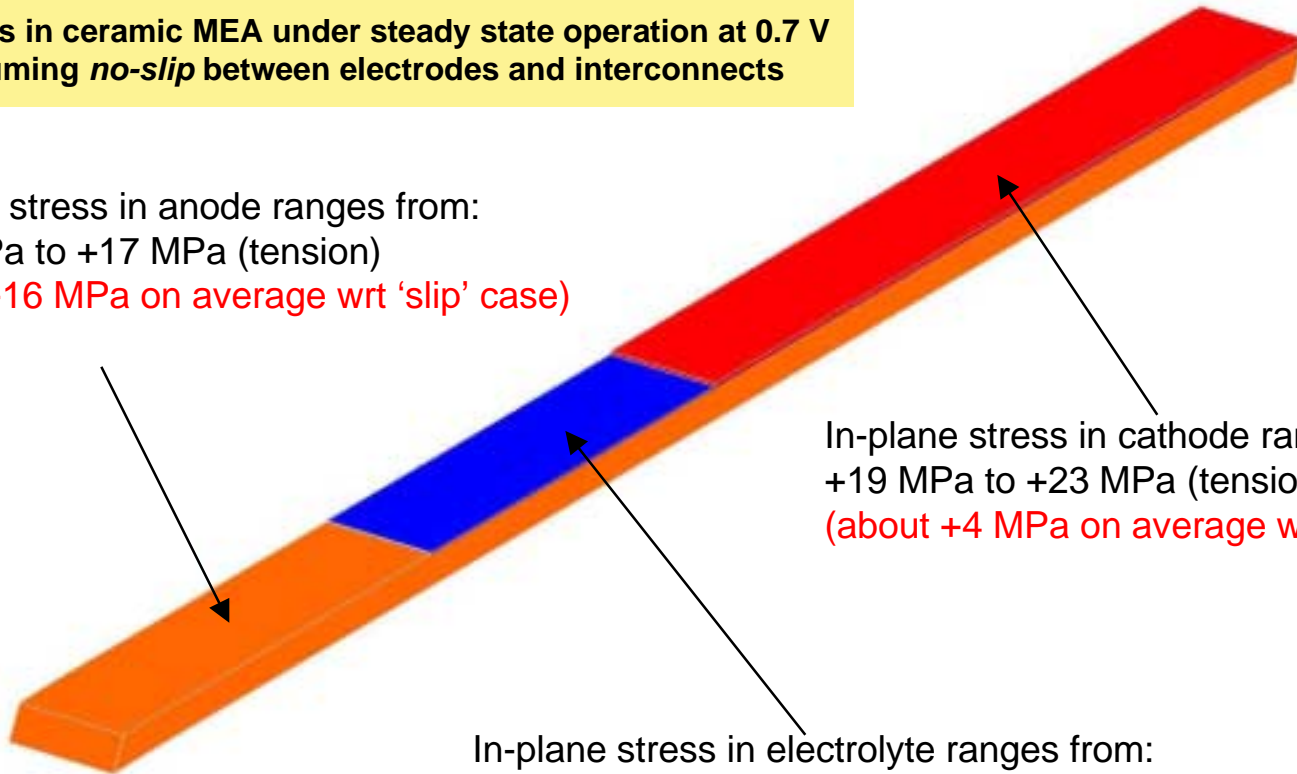


**Essentially, the stress distribution under operating conditions is dominated by the stress-state of the components at room temperature.**

With the no-slip assumption, a compressive stress of  $-4.6$  MPa arises in the metal, which is balanced by tensile stresses in the ceramic layers.

Stresses in ceramic MEA under steady state operation at  $0.7$  V assuming *no-slip* between electrodes and interconnects

In-plane stress in anode ranges from:  
 $+0.1$  MPa to  $+17$  MPa (tension)  
(about  $+16$  MPa on average wrt 'slip' case)

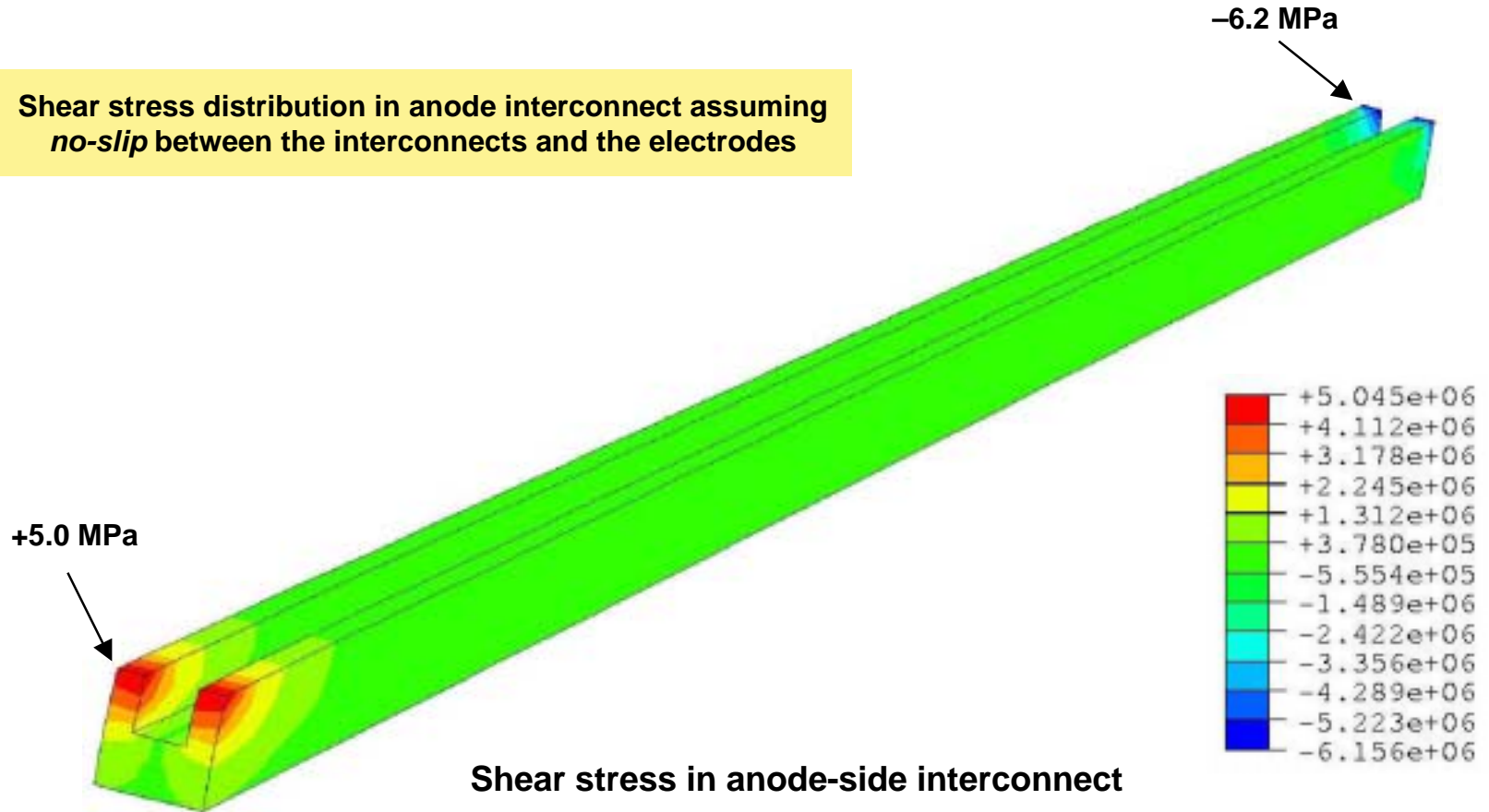


In-plane stress in cathode ranges from:  
 $+19$  MPa to  $+23$  MPa (tension)  
(about  $+4$  MPa on average wrt 'slip' case)

In-plane stress in electrolyte ranges from:  
 $-206$  MPa to  $-273$  MPa (compression)  
(about  $+11$  MPa on average wrt 'slip' case)

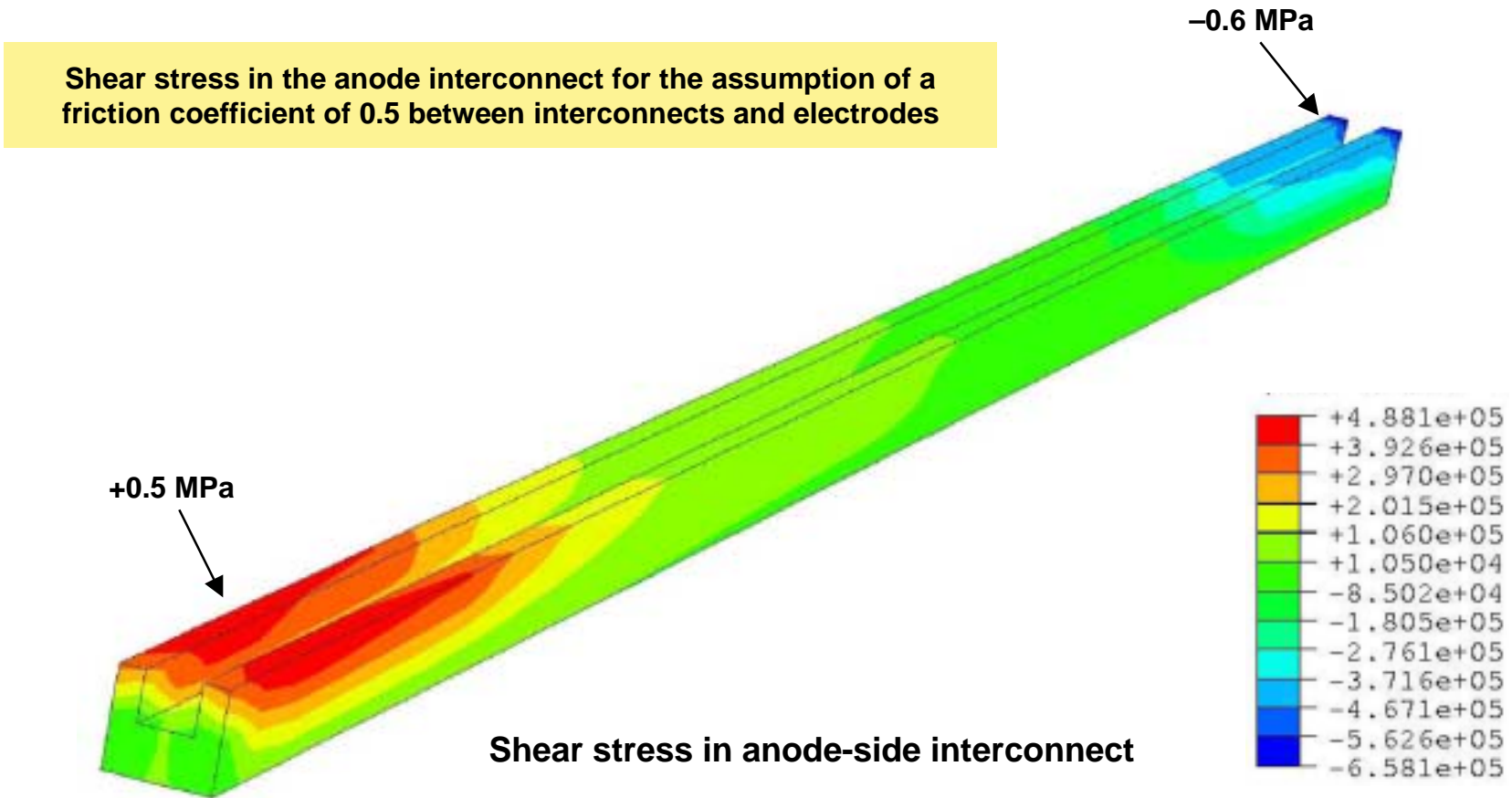
The no-slip condition results in significant shear stresses (near the ends of the cell) that can be sustained only with interfacial bonding.

Shear stress distribution in anode interconnect assuming *no-slip* between the interconnects and the electrodes





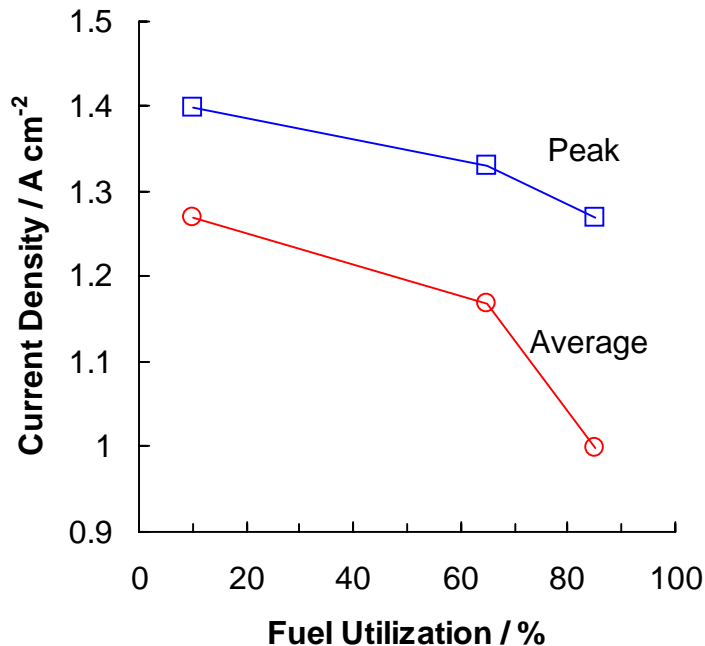
Considerably lower shear stresses result when a friction coefficient of 0.5 is assumed for the MEA/interconnect interface.



**We selected the parameters for the sensitivity analysis so as to test the robustness of the model under extreme conditions.**

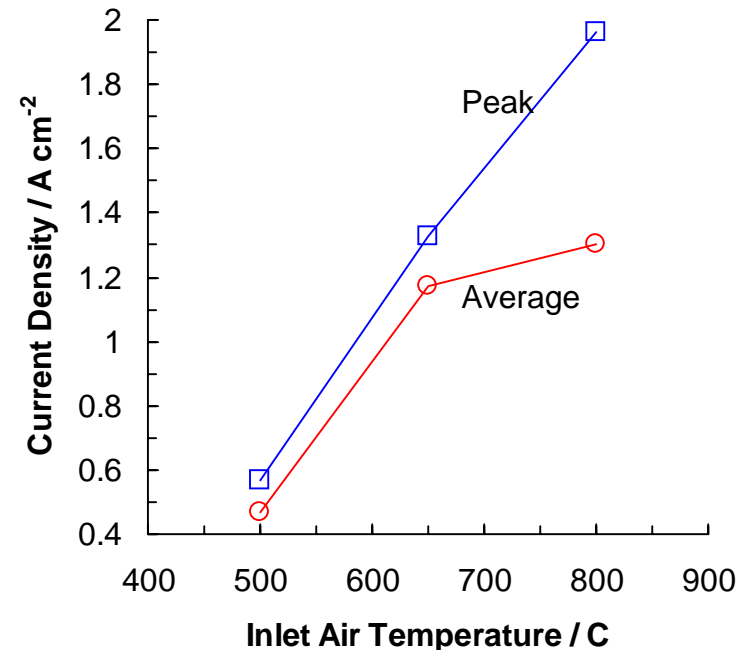
Parameter	Value
• Cell voltage (V)	• 0.6, <u>0.7</u> , 0.8
• Fuel Utilization (%)	• 10, <u>65</u> , 85
• Inlet air temperatures (C)	• 500, <u>650</u> , 800
• Inlet air stoichiometry	• 2, <u>4</u> , 8
	• Base case values are underlined

## Increasing the fuel utilization or decreasing the inlet air temperature reduces the average current from the fuel cell.

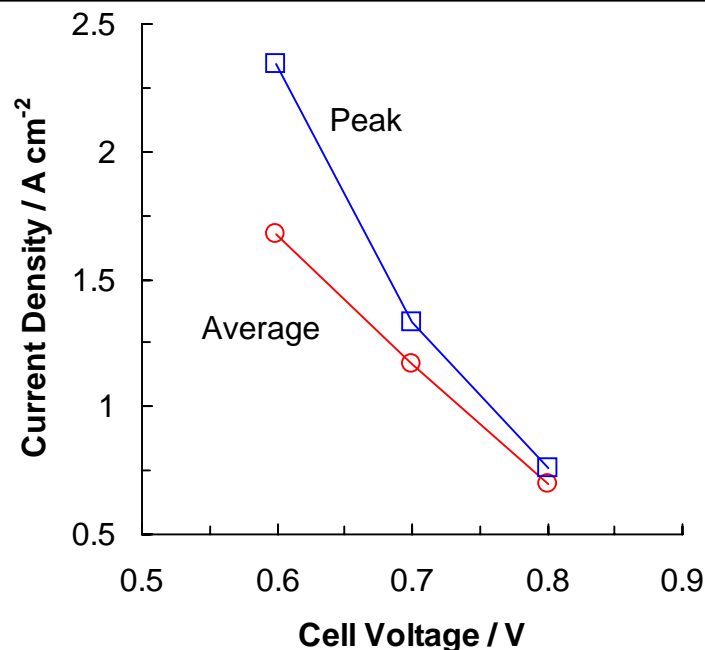


- The average current drops by ~ 30 % in going from 10 % to 85 % fuel utilization because the thermodynamic driving force decreases with increasing water content in the anode gas. A similar effect was also observed with the 2-d performance models discussed earlier.
- Experimental data\* also shows that the current density drops by 20 % in going from 10 % to 85 % fuel utilization.
- The peak current does not change much because the peak current occurs close to the anode inlet, where the local fuel utilization is not very high.

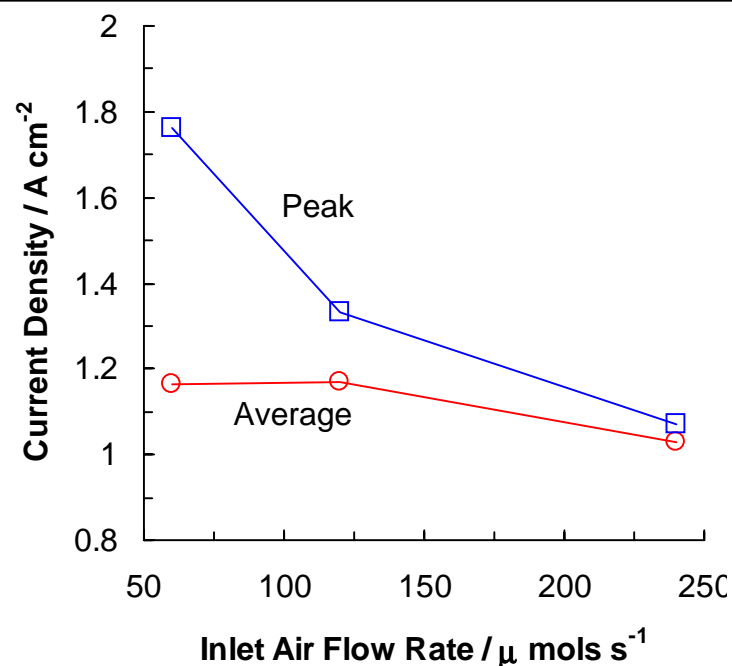
\* I. Yasuda, T. Ogiwara, H. Yakabe, Y. Matsuzaki, in *Solid Oxide Fuel Cells VII (SOFC-VII)* (S. C. Singhal, H. Yokogawa, eds.), Tsukuba, Japan, 2001, p. 131.



- At low inlet air temperatures, the reaction kinetics are quite slow so that the cell temperature does not rise sufficiently and hence the peak and average currents are low.
- At high inlet air temperatures, the average cell temperature is high, which leads to the high peak current. But, the fuel utilization is also higher which results in the large difference between the peak and average currents.

**Low cell voltage and low air flow rate lead to low average currents.**

- At the high cell voltage, the electrode overpotentials are low resulting in a low currents. Also, efficient operation means that the heat release is low leading to more or less isothermal operation. This causes the peak current and average current to be almost equal.
- At the low cell voltage, the higher overpotentials cause higher currents. Also, inefficient operation means more heat is released leading to large temperature gradients and hence the peak current is much higher than the average current.



- High flow rates of air cause the cell temperature to become more uniform (closer to the air inlet temperature) resulting in the equality of the peak and average currents. Also, the low average temperature leads to low currents.
- Low air flow rates leads to a higher average cell temperature, which results in the large difference between the peak and average currents. Also, very low air flow rates may lead to the cell becoming starved for oxygen, which would lead to severe polarization of the cathode and result in low currents.

**We verified the successful implementation and debugging of the SOFC performance model in ABAQUS using a single-channel fuel cell geometry.**

- We constructed the SOFC model in ABAQUS and used a simple geometry to verify the successful implementation of the different model elements.
- The model successfully calculated the profiles of temperature, current density, overpotentials, species concentrations, and stress for steady state operation under typical operating conditions.
- We probed the robustness of the model through a sensitivity analysis. The operating conditions were chosen so as to tax the numerical solution scheme:
  - high fuel utilization (85 %);
  - low cell voltage (0.6 V) ;
  - low air inlet temperature (500 C);
  - low flow of air (< 2 x stoichiometry).
- In all of these simulations, the model successfully converged and the resulting profiles of temperature, current density, species concentrations, and overpotentials were consistent with each other.
- In all of these simulations, the error in the mass balance was less than 1 % and error in the energy balance was less than 6 %.

**The protocols for calculating the stress distribution during operation were also successfully implemented in ABAQUS.**

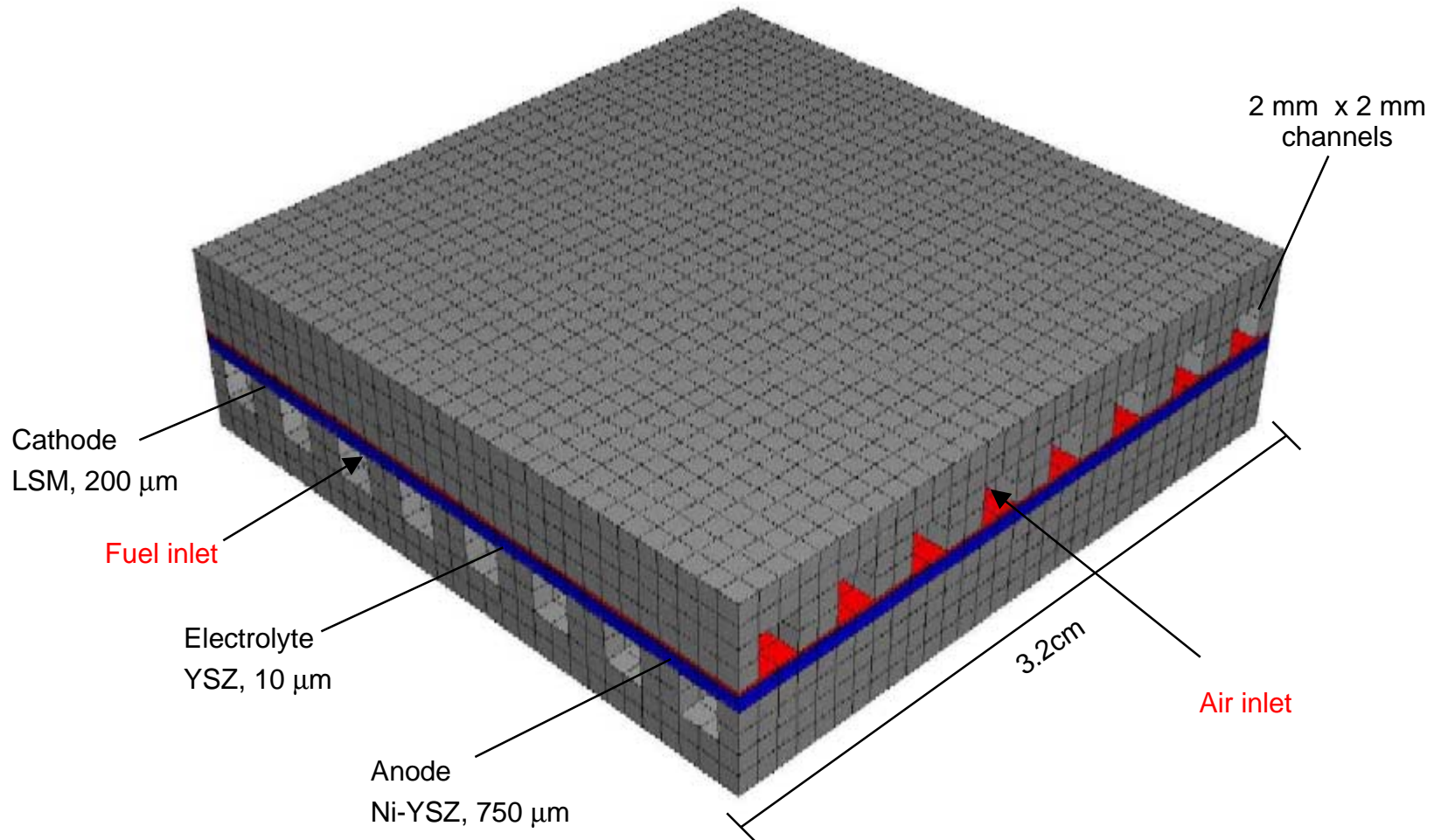
- The highest levels of stress occur following cool-down from the sintering temperature of 1400 C to room temperature.
  - The thick anode controls the deformation and experiences an in-plane stress of  $-3$  MPa (compression).
  - The compressive stress in the anode is balanced by tensile stress of 38 MPa in the thinner, more compliant cathode.
  - Because of its high coefficient of thermal expansion, the thin electrolyte develops a  $-556$  MPa compressive stress.
- Because the operating temperature is closer to the stress-free sintering temperature, the operating conditions actually relieve the stresses generated during the initial cooling step to room temperature.
- Imposition of ‘no-slip’ conditions along the MEA-interconnect interface increases the tensile stresses in the ceramic by 4 to 16 MPa and produces a shear stress of 5 to 6 MPa at the ends of the cell.
- It is unlikely that such high shear stresses could be sustained without interfacial bonding; simulation of interfacial friction reduces the shear stresses to less than 1 MPa.

## Outline of Final Report

---

0	Executive Summary
1	Background & Objectives
2	Approach & Scope
3	Model Development
4	Single Channel SOFC Results
5	<b>Multi Channel SOFC Results</b>
6	Limitations for Cell Size
7	Summary
A	Appendix

The SOFC structural model was extended to simulate a more realistic cross-flow, multi-channel geometry for an anode supported SOFC.





**For the base case, we selected operating conditions consistent with previous TIAx studies.**

Parameter	Value
<ul style="list-style-type: none"><li>• Cell voltage</li><li>• Composition of the reactant streams</li><li>• Gas inlet temperatures</li><li>• Fuel utilization</li><li>• Cathode stoichiometry</li></ul>	<ul style="list-style-type: none"><li>• 0.7 V</li><li>• Anode: 97 % H<sub>2</sub>, 3 % H<sub>2</sub>O, Cathode: air</li><li>• 650 °C at the Anode and Cathode</li><li>• ~ 50 %</li><li>• ~ 5, the cathode flow rate was adjusted such that the temperature at the cell outlet was nominally 800 °C.</li></ul>

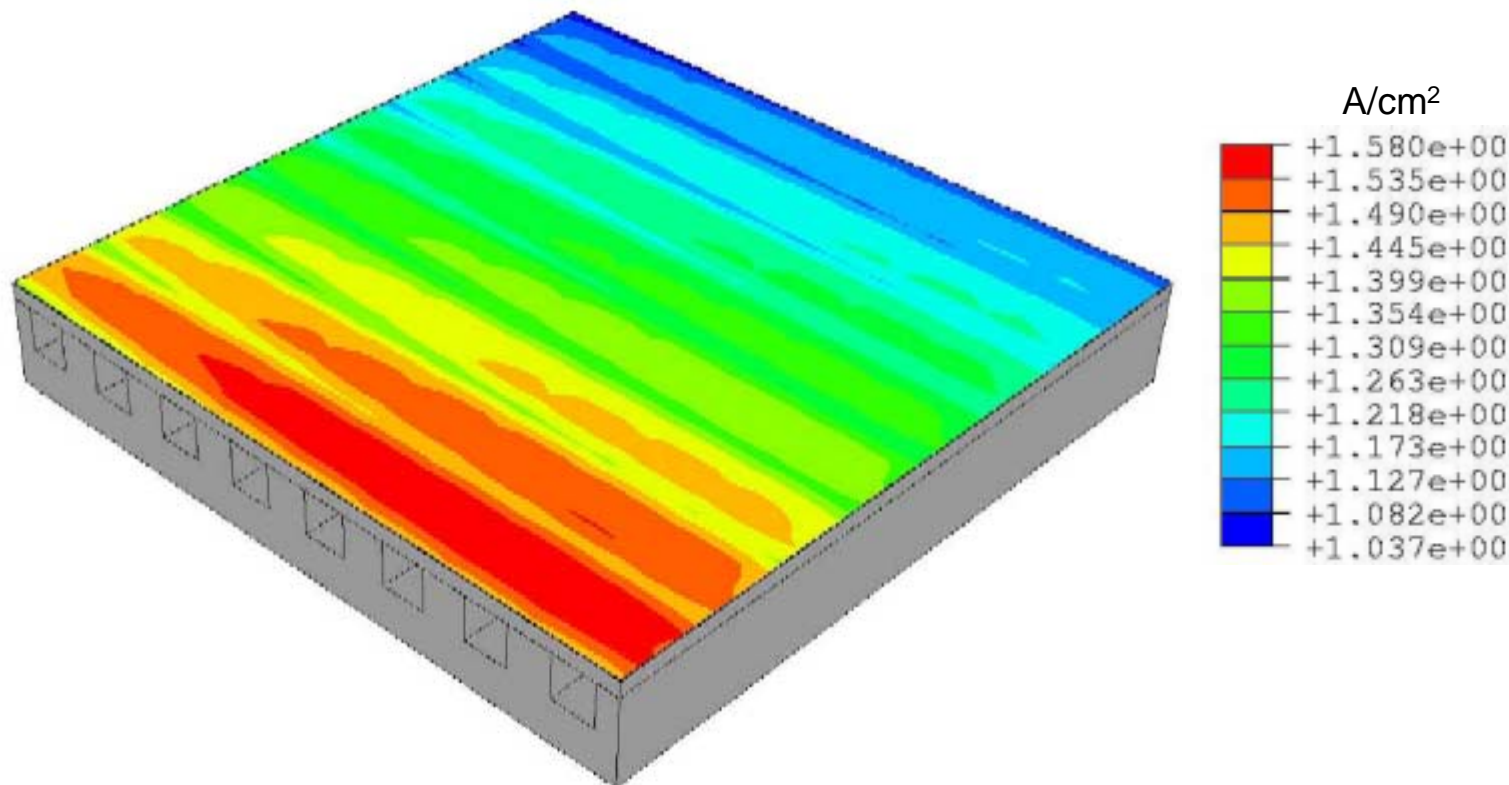
**The fuel utilization was chosen to represent a realistic situation, but at the same time not stress the solution scheme.**

**In addition, the following assumptions were made to facilitate calculations:**

- Adiabatic thermal boundary conditions
- Stress-free state for the ceramics is at the sintering temperature of 1400 °C
- The ceramic MEA layers are bonded
- The ceramic layers and the MEA are defect-free at all temperatures
- The interconnects are not bonded to the electrodes

The calculated current density for the cross-flow cell is close to that measured in anode supported stacks\*.

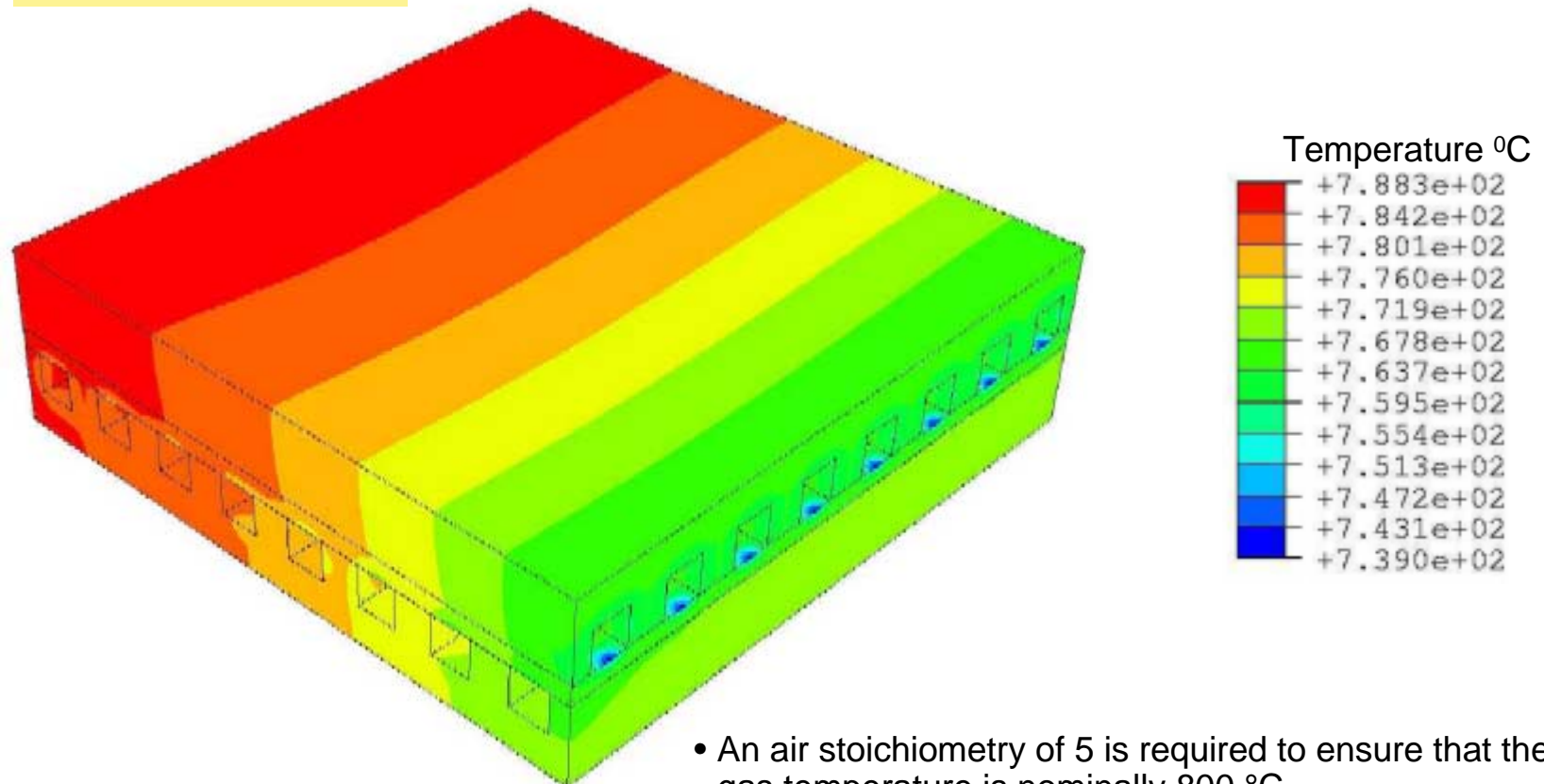
Current density distribution, average = 1.3 A/cm<sup>2</sup>



- Typically, single cell measurements are performed in isothermal ovens and hence are not relevant for comparison to the adiabatic simulations reported here. Ideally the comparison should be with the measured performance of thermally self-sustaining stacks.
- \*D. Ghosh, M. Perry, D. Prediger, M. Pastula, and R. Boersma, in Electrochemical Society Proceedings, Vol. 2001-16, 2001, p. 100.

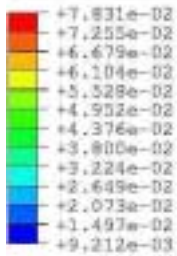
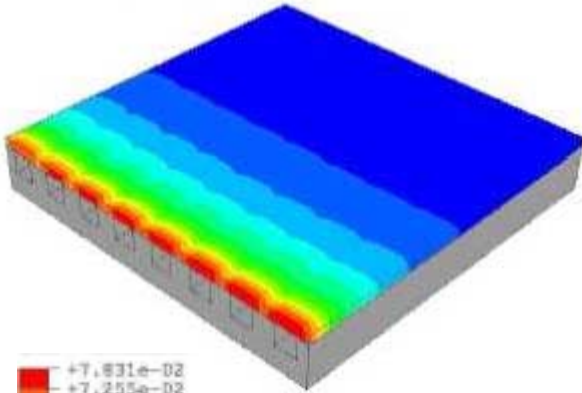
**Only modest temperature gradients occur even with the inlet gases at 650 C because of the high thermal conductivity of the metallic interconnects.**

### Temperature distribution

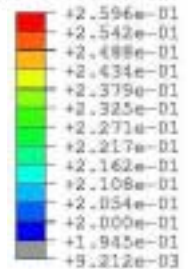
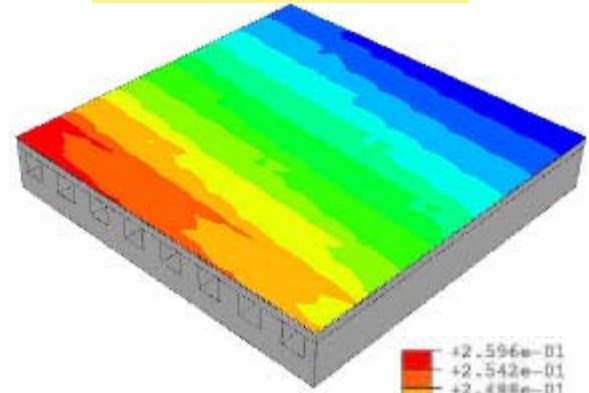


As expected, the cathode overpotential dominates the losses throughout the cell for this configuration and operating conditions.

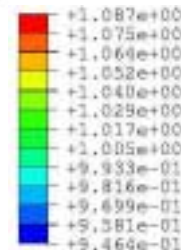
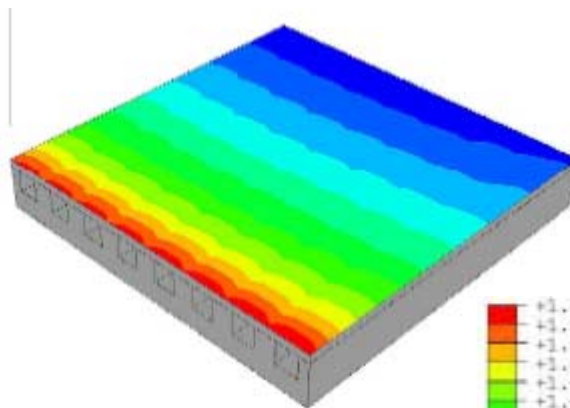
Anode overpotential



Cathode overpotential

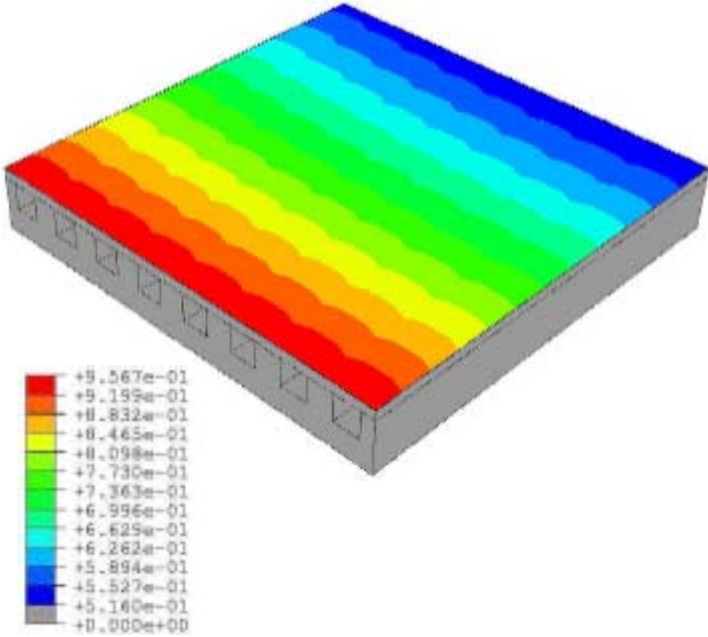


Open circuit voltage

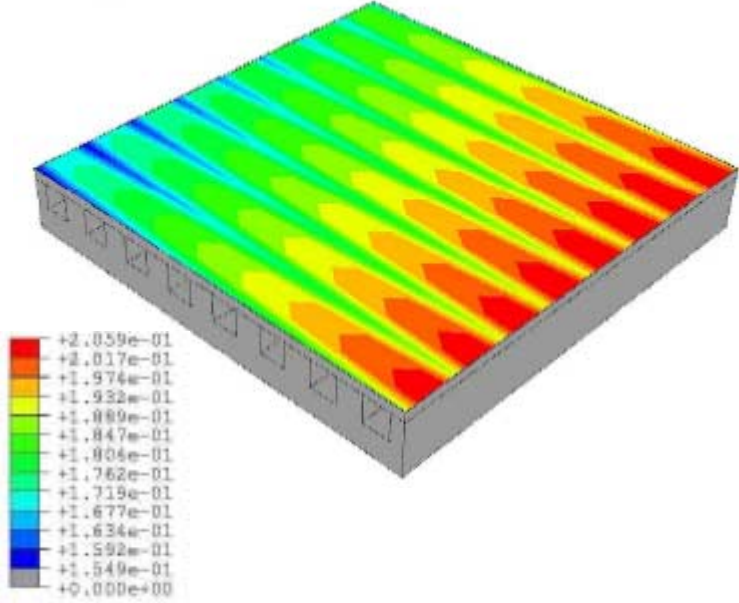


As expected, the thick anode does not limit H<sub>2</sub> diffusion as evidenced by the laterally uniform H<sub>2</sub> distribution in the anode reaction zone.

Hydrogen mole fraction in the anode reaction zone



Oxygen mole fraction in the cathode reaction zone



In contrast, the slower diffusion of O<sub>2</sub> leads to depletion in the region immediately under the channel ridge.



## The stress calculation followed the same procedure used for the single channel models:

### Procedure for residual stress calculations

#### Step 0: Sintering Ceramics

- Assume that all the ceramic layers in the MEA are stress-free at the co-sintering temperature of 1400 °C.
- The component layers in the ceramic MEA are assumed to be fused together.
- Assume interconnects are stress free at room temperature

#### Step 1: Cool Down to Room Temperature

- Calculate the stresses in the ceramic layers when the MEA is cooled down to room temperature (residual stresses).

#### Step 2: Flatten Ceramics

- Apply appropriate confining pressure to flatten the MEA (this is needed to ensure sealing and electric contact).
- Assemble flat MEA between interconnects

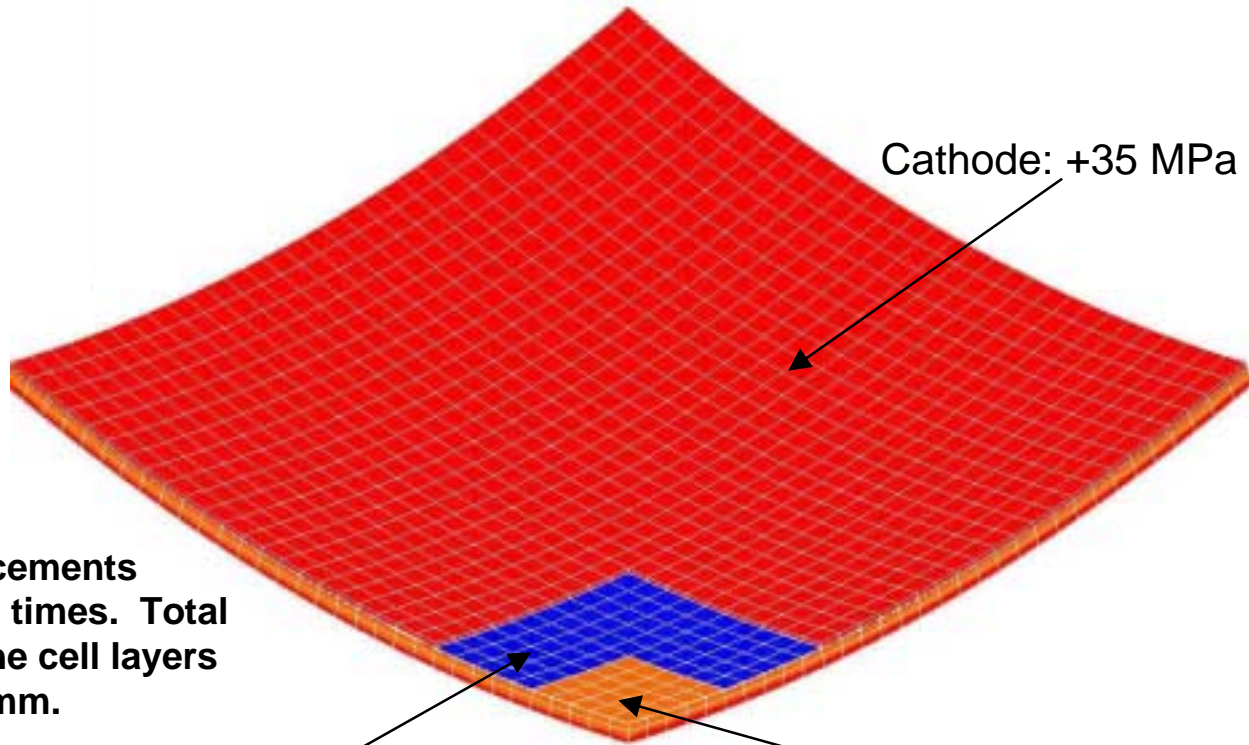
#### Step 3: Heat Up to Operating Temperature

- Assume no-slip condition between interconnect and ceramics
- Calculate stress distribution by applying the steady temperature gradients calculated for cell operation

**In the ensuing calculations, we assume that the ceramic MEA is defect free.**

In Step 1, bending stresses that arise to balance the moments created by anode/cathode TCE mismatch, cause warping of the ceramic MEA layers.

Residual stresses and warping in the ceramic layers at room temperature



Cathode: +35 MPa

Note: displacements magnified 40 times. Total warping of the cell layers equals 0.03 mm.

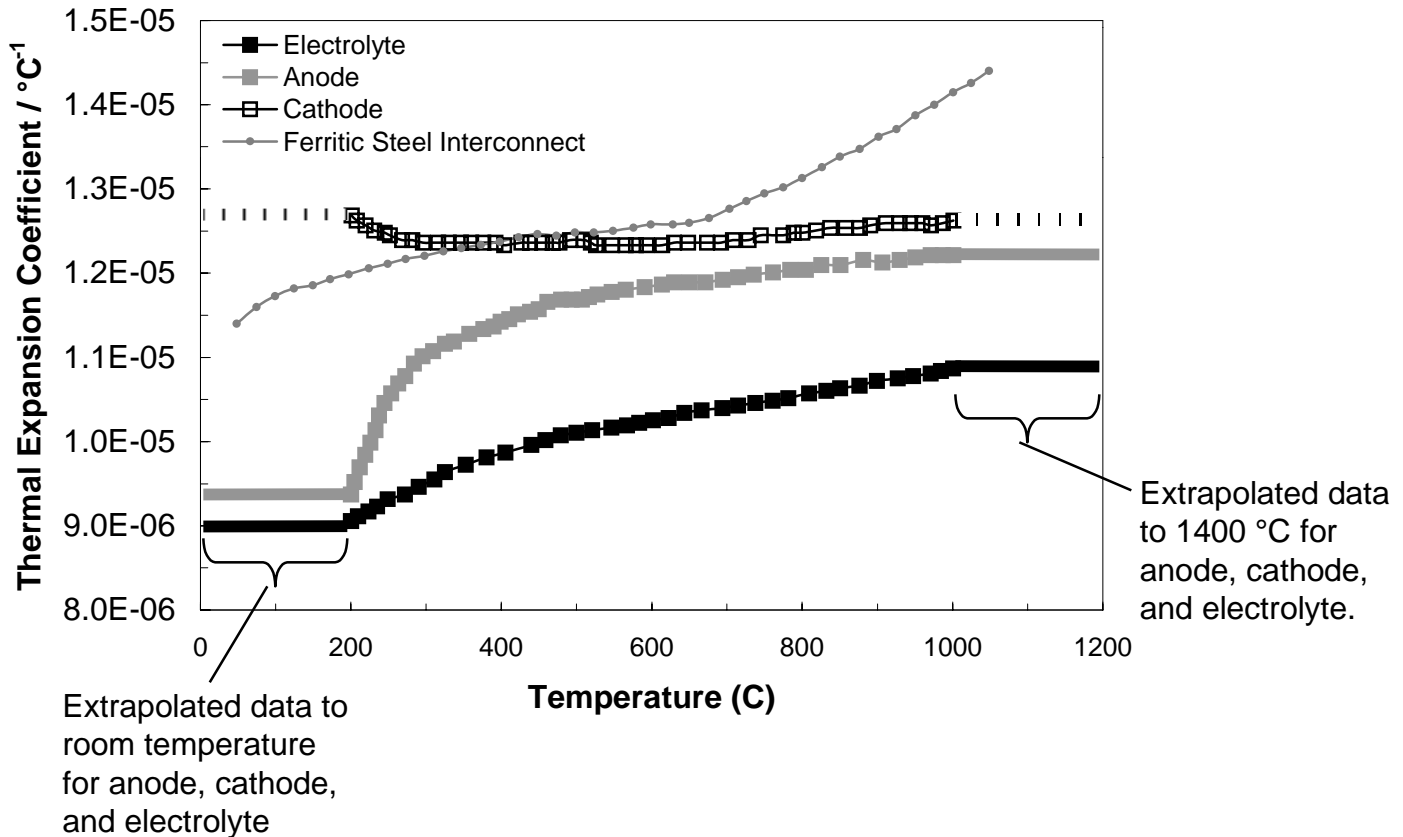
Electrolyte: -563 MPa

Anode: -11 MPa (top) to +3 MPa (bottom)





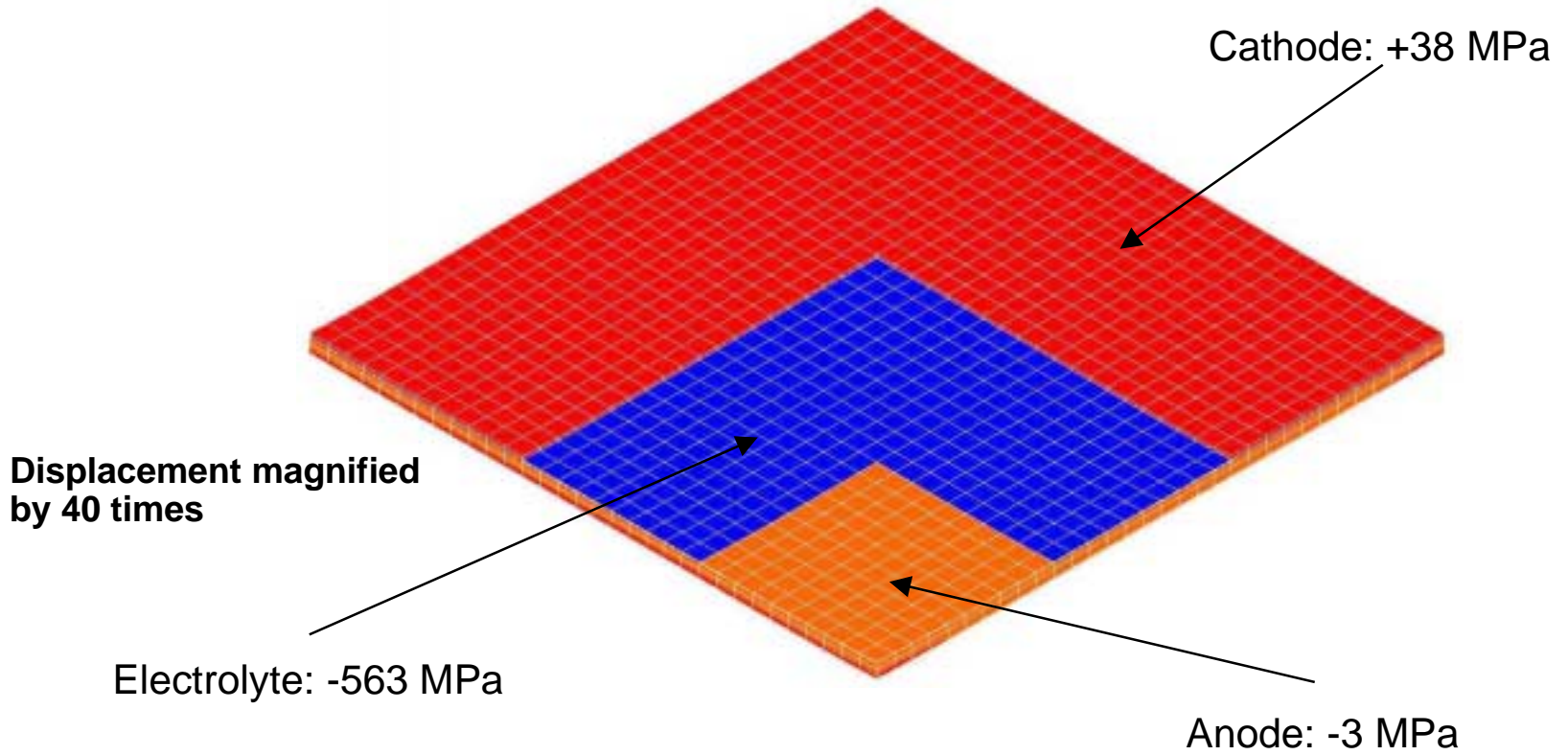
The residual stresses and the extent of warping are very sensitive to the assumed values for the thermal expansion coefficients.



\* Data from J. P. Abellan, F. Tietz, L. Singheiser, W. J. Quadackers, A. Gil, in Proceedings of SOFC-V, S. Singhal, U. Stimming, H. Tagawa, W. Lehnert, Eds., Published by The Electrochemical Society (1997) 652.

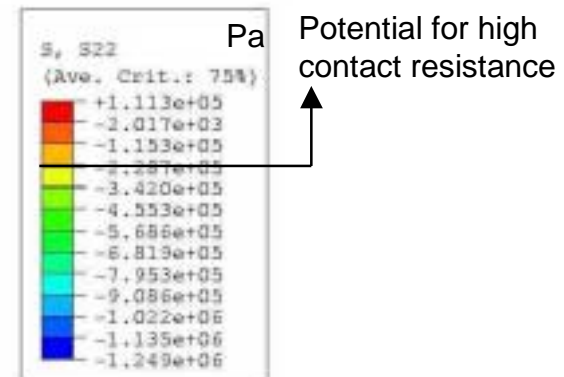
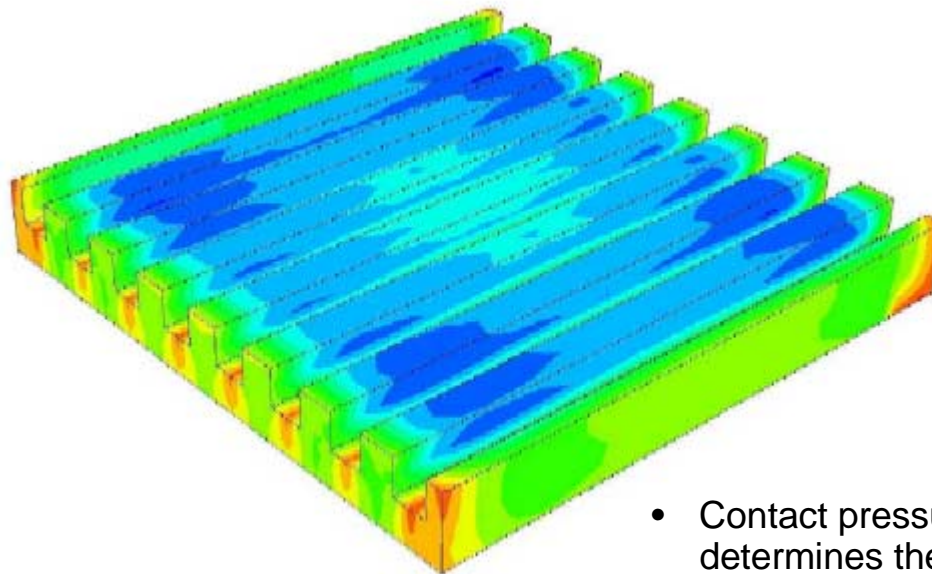
In step 2 a confining pressure (0.4 MPa ) flattens the MEA and removes the anode bending stress but does not alter the cathode or electrolyte stresses.

Stress in the ceramic MEA layers after 'flattening' between interconnects at room temperature



The resulting compressive stresses may lead to high contact resistance, along the edges, between the interconnect and electrodes.

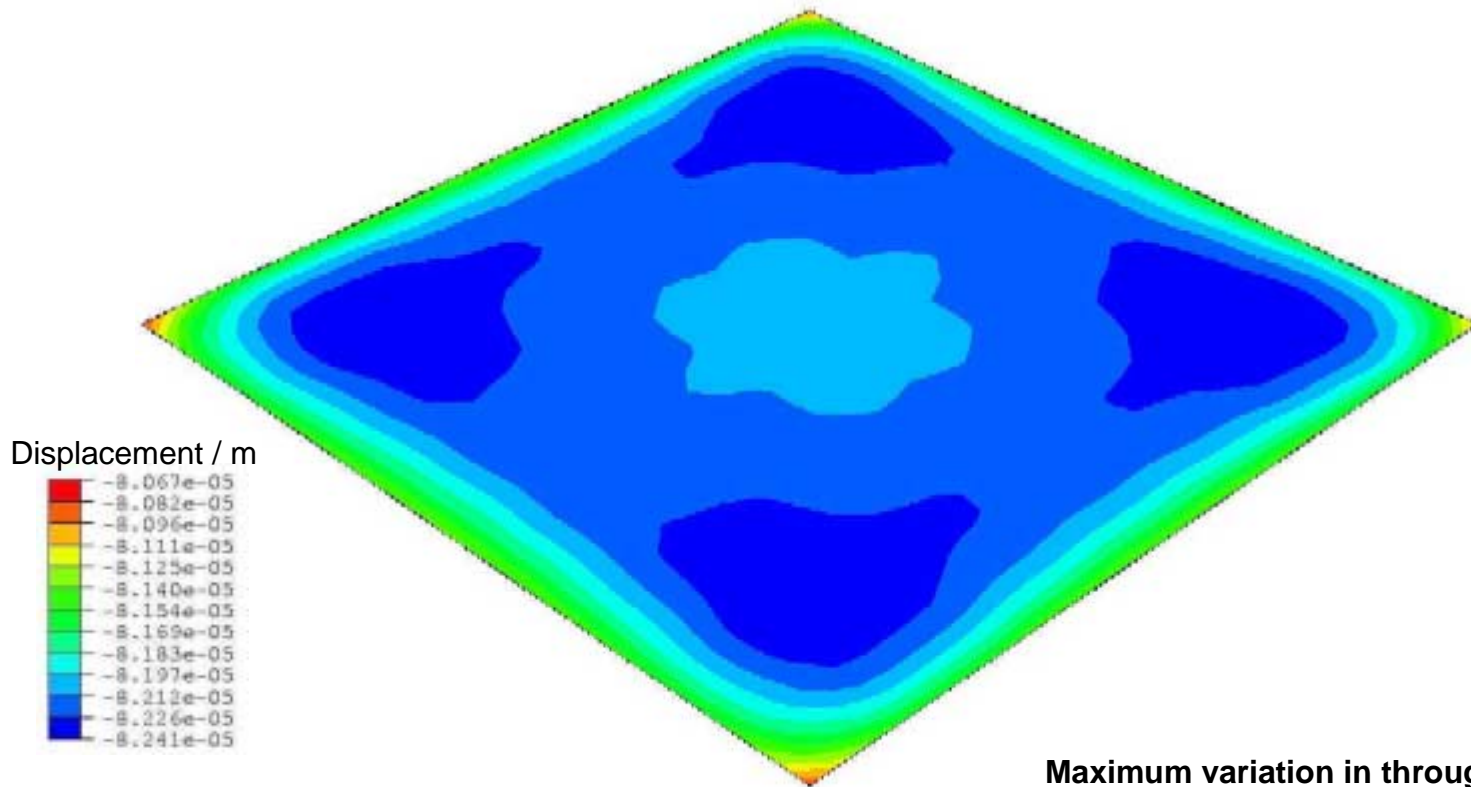
Through thickness stress in the metallic interconnect at room temperature



- Contact pressure between the interconnect and electrodes determines the interfacial resistance
- A rule of thumb states that contact pressure greater than  $1.4 \times 10^5$  Pa (20 psi) leads to negligible contact resistance

The variation in through-thickness displacement of the electrolyte also highlights the degree to which the ceramic layers exhibit 'out of flatness'.

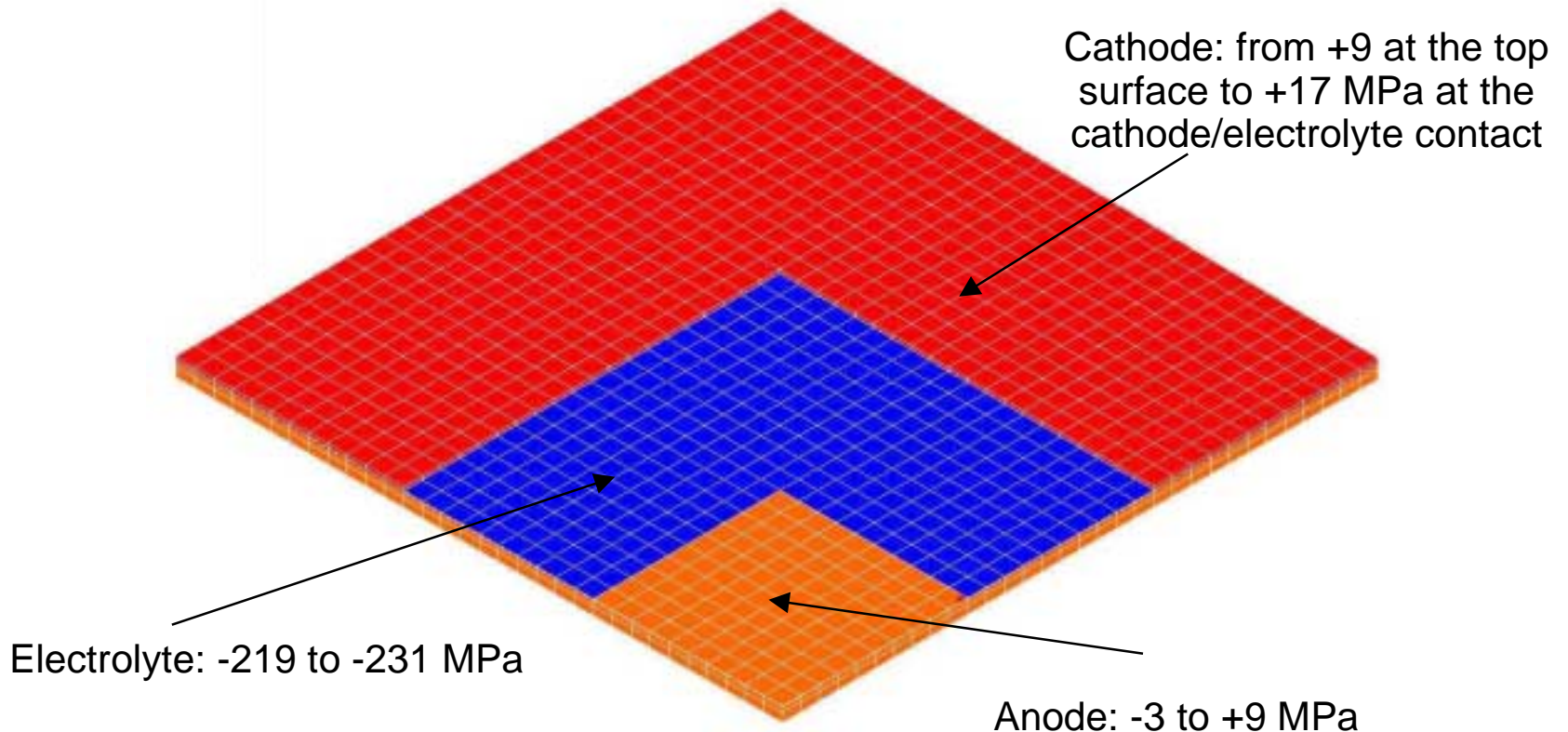
Through thickness displacement of electrolyte at room temperature



Maximum variation in through-thickness displacement: 1.7 microns

In step 3, imposing the steady-state temperature field results in significantly lower MEA stresses compared to room temperature.

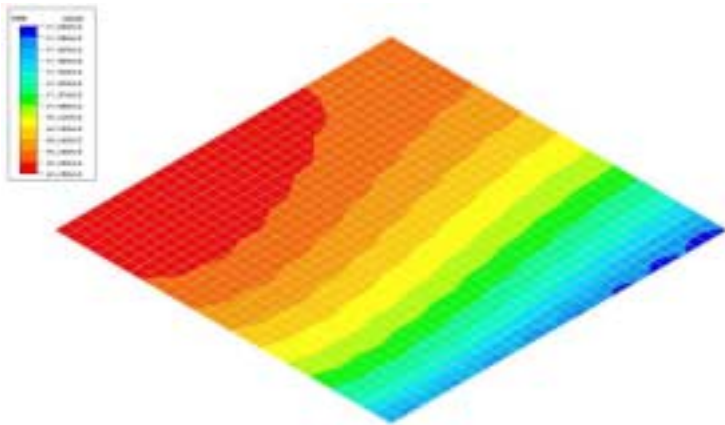
Stress in the ceramic MEA for steady state operation at 0.7 V for the assumption of slip between the electrodes and the interconnect



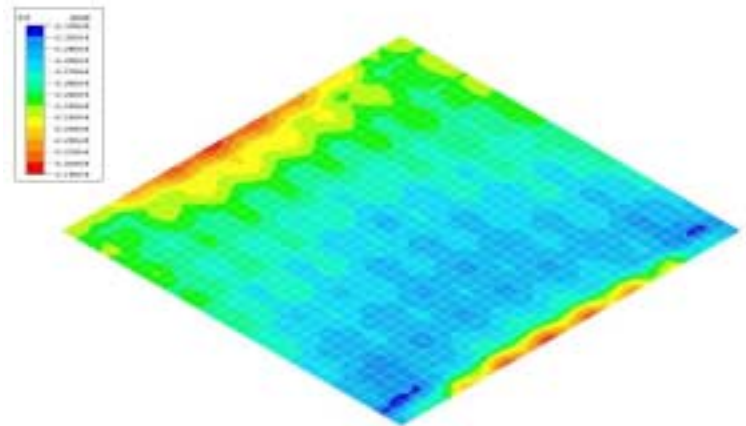


**In step 3, the modest temperature gradient during cell operation causes a relatively minor in-plane stress gradient.**

Electrolyte temperature varies from 786 C (blue) to 810 °C (red)



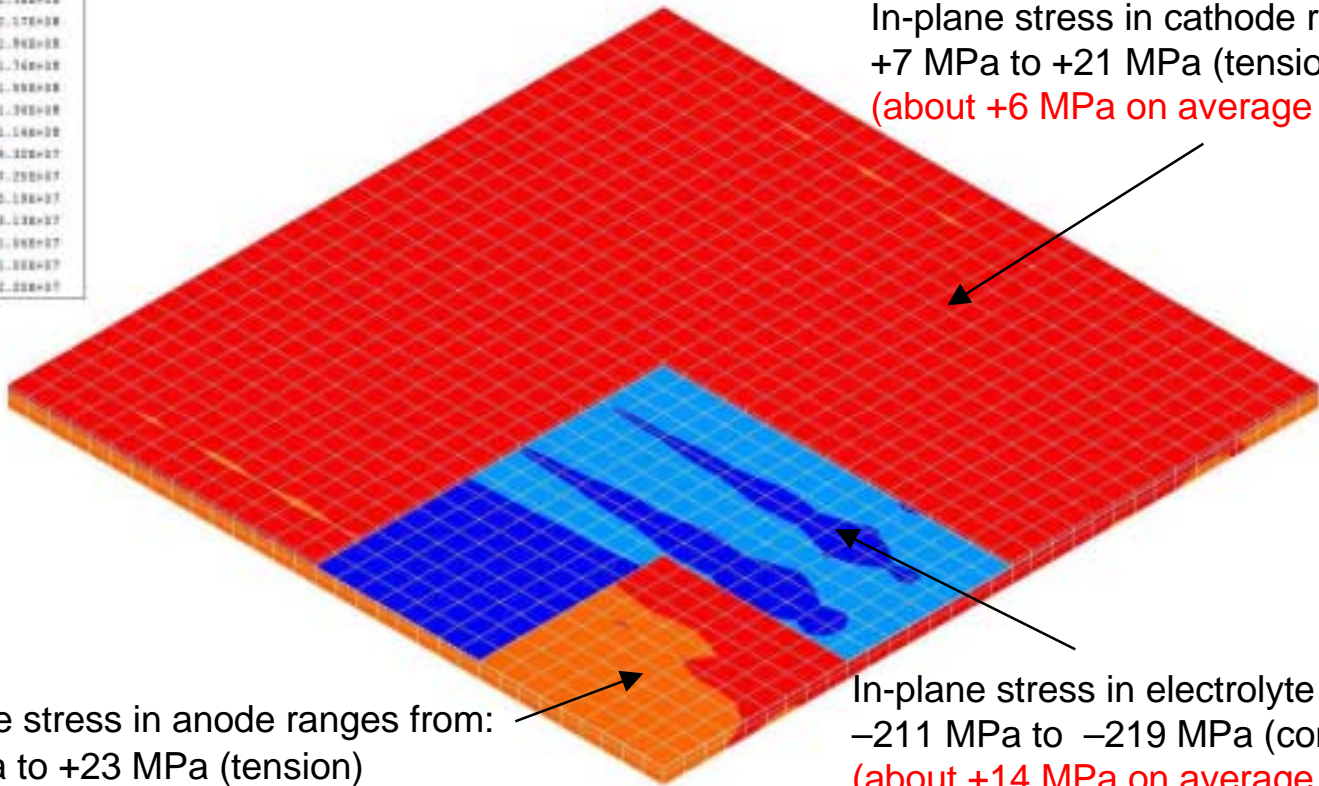
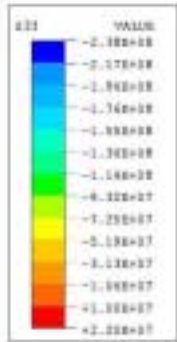
Electrolyte stress varies from -231 MPa (blue) to -219 MPa (red) for the slip assumption



**The modest temperature gradients are because of the high conductivity of the metal interconnects.**

The shear stresses that arise for the for the no-slip assumption cannot be sustained without bonding of the interconnect to the electrodes.

Stress in the ceramic MEA for steady state operation at 0.7 V for the assumption of slip between the electrodes and the interconnect



In-plane stress in cathode ranges from: +7 MPa to +21 MPa (tension) (about +6 MPa on average wrt 'slip' case)

In-plane stress in anode ranges from: -2 MPa to +23 MPa (tension) (about +17 MPa on average wrt 'slip' case)

In-plane stress in electrolyte ranges from: -211 MPa to -219 MPa (compression) (about +14 MPa on average wrt 'slip' case)

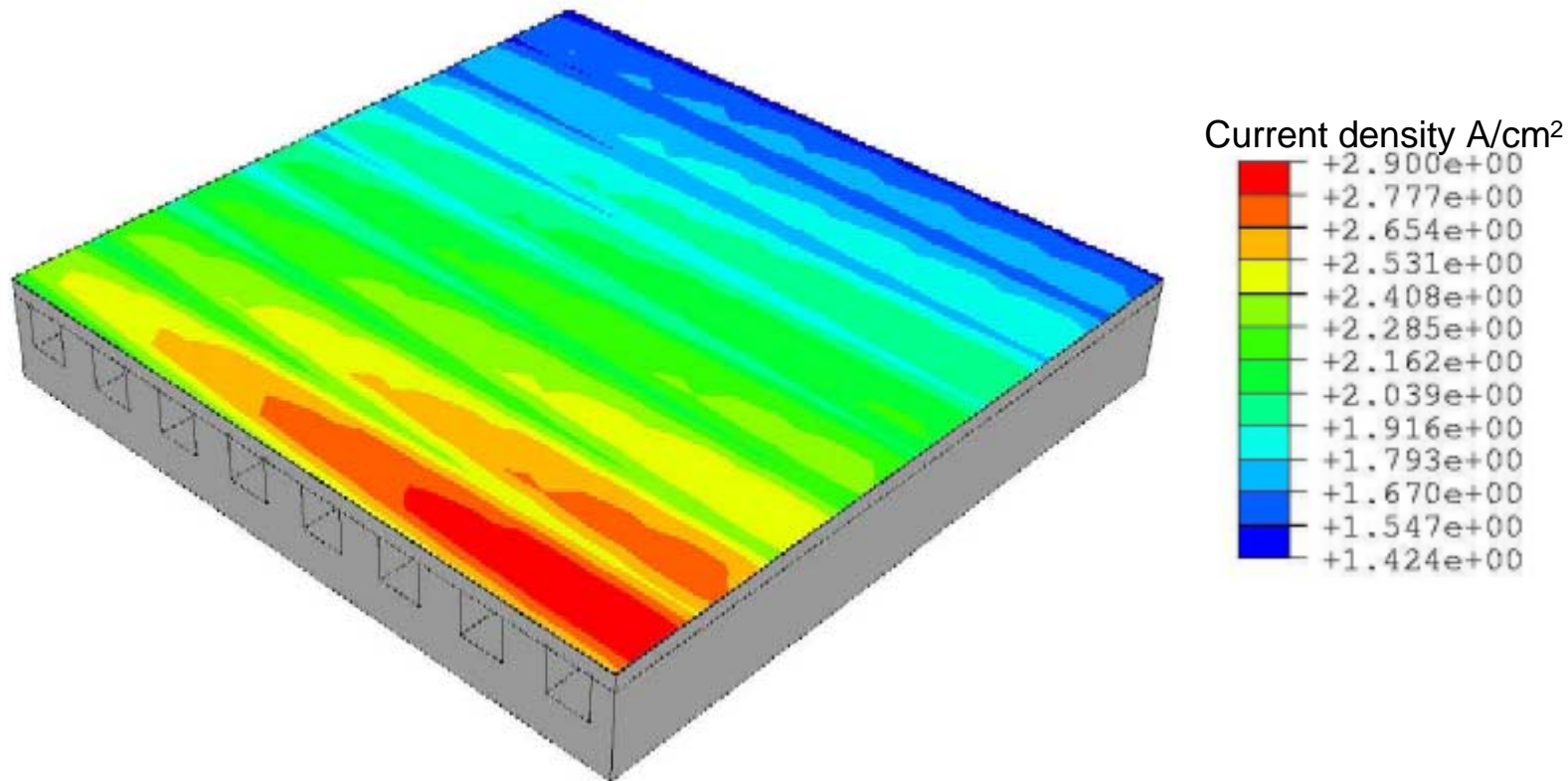
**We selected the parameters for the sensitivity analysis that might create strong temperature gradients and hence might create higher stresses.**

Parameter	Value
<ul style="list-style-type: none"><li>• Cell voltage (V)</li><li>• Inlet air stoichiometry</li></ul>	<ul style="list-style-type: none"><li>• 0.6, <u>0.7</u></li><li>• 2.5, <u>5</u></li></ul> <p>(base case values are underlined)</p>



**In agreement with experimental single-cell results\*, operation at 0.6 V almost doubles the current density compared to the base case.**

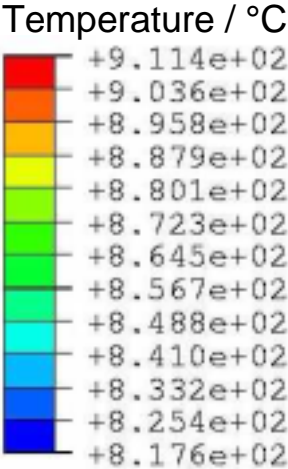
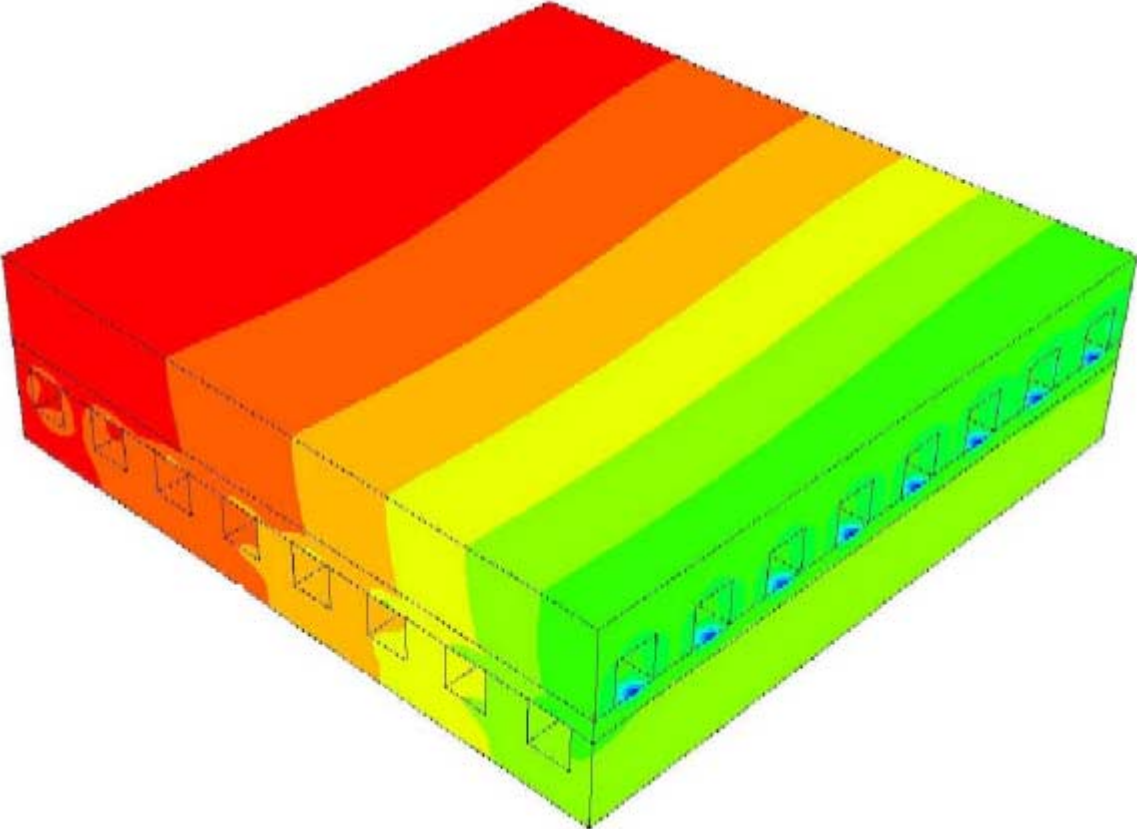
Current density distribution, average = 2.1 A/cm<sup>2</sup>



\* J-W Kim, A. Virkar, K-Z Fung, K. Mehta, S. Singhal, *J. Electrochem. Soc.*, 146 (1999) 69-78.

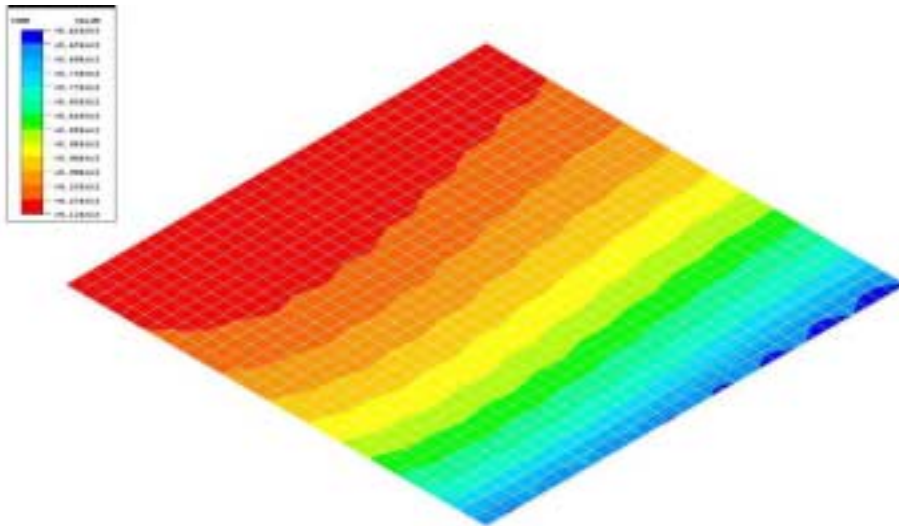
At the lower cell voltage the average temperature is higher than in the base case, but the temperature gradient is still quite modest.

Temperature distribution

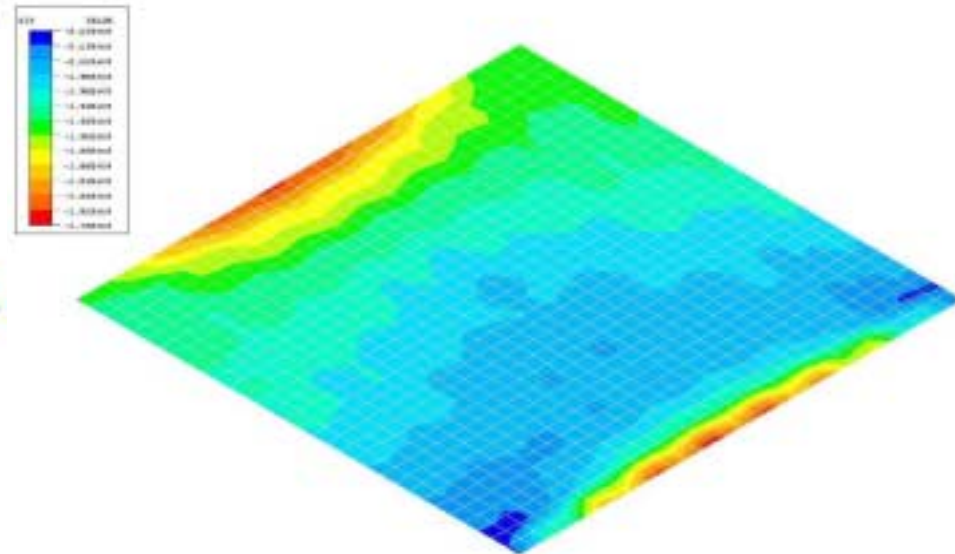


**A larger variation in stress in the electrolyte results at 0.6 V, but the average stress is smaller, because the average temperature is higher.**

Electrolyte temperature varies from 861 °C (blue) to 911 °C (red) at 0.6 V

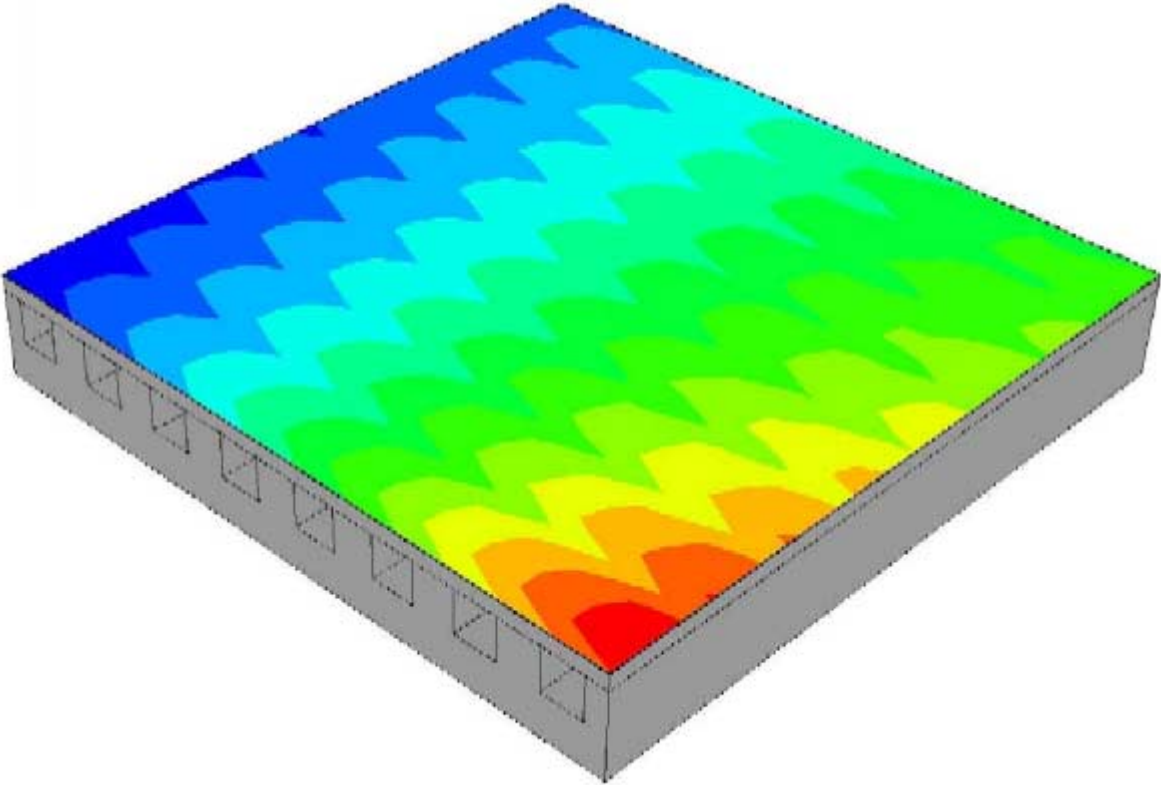


Electrolyte stress varies from -205 MPa (blue) to -178 MPa (red) at 0.6 V

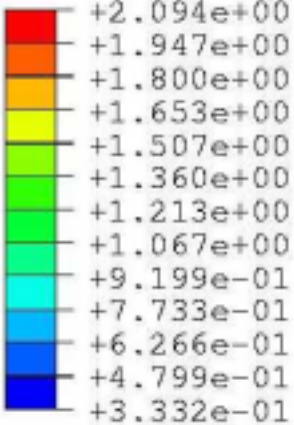


For low air flow, the current density is limited by the availability of oxygen and decreases sharply along the cathode flow channel.

Current density distribution, average = 2.1 A/cm<sup>2</sup>

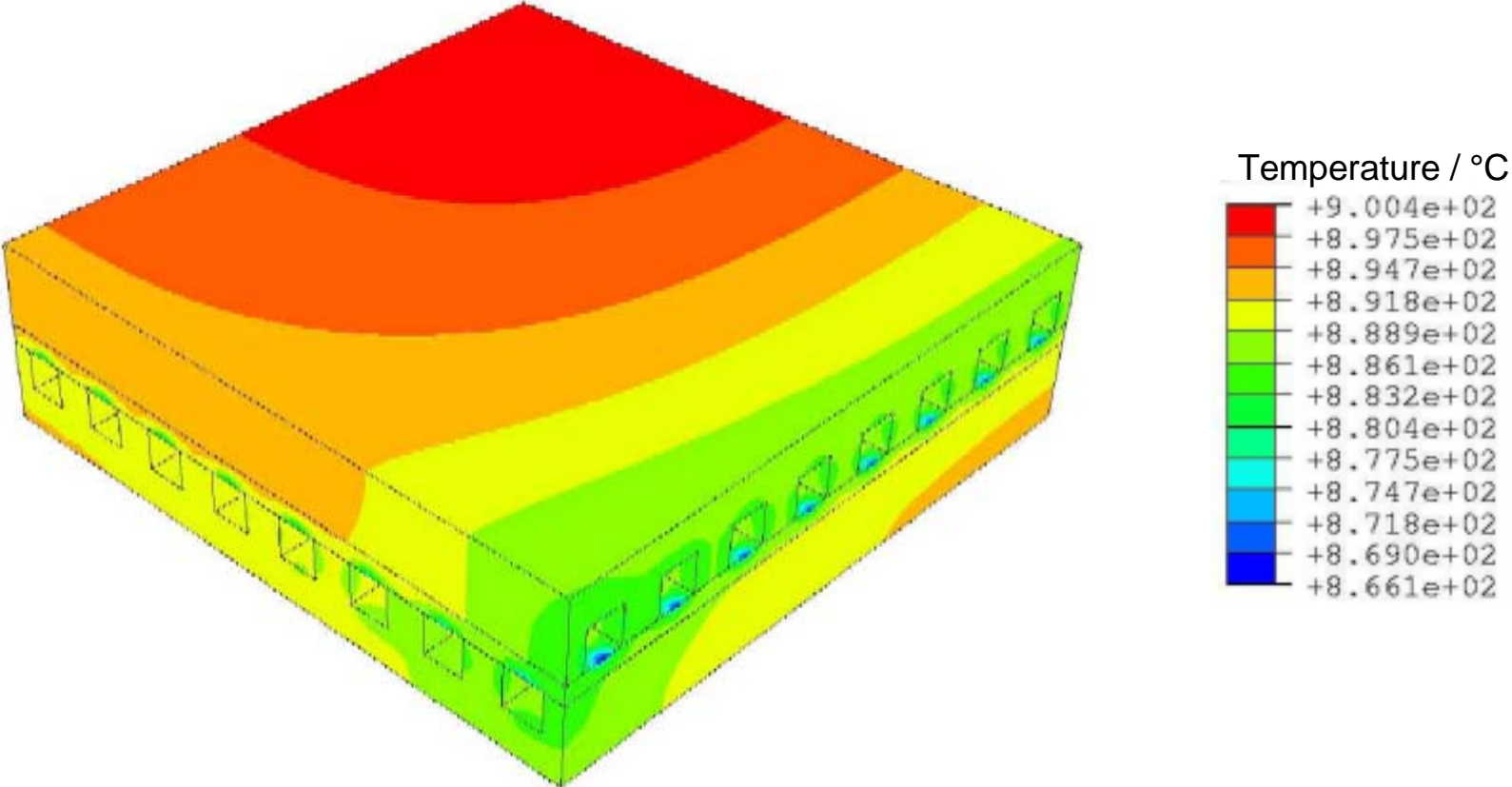


Current density A/cm<sup>2</sup>



Even under these conditions, the temperature gradients within the cell are modest due to the thick interconnects.

Temperature distribution





**We successfully verified the implementation of the model for a three-dimensional anode supported SOFC with cross-flow of reactants.**

- The modules key to calculating the fuel cell performance were verified to worked without error:
  - Module for calculating the local current density accounting for species concentration, temperature, and electrolyte resistance.
  - Module for calculating the heat released due to electrochemical reaction accounting for the cell voltage and current density.
  - Module for calculating the diffusion of species through the porous electrodes
- We Verified the robustness of the numerical solution through a sensitivity analysis
- We verified the conservation of mass and charge to within 0.1 % and energy balance to within 6 % on a local and overall basis.
  - The large discrepancy in the energy balance is a consequence of the solution scheme inherent to ABAQUS: the energy balance equations are written with the assumption that the molar flow rate does not change along the channel length.
  - We have identified potential solutions, which will be incorporated in the next version of the model.



**Stress calculations so far show that, absent defects, the ceramics are unlikely to fail due to temperature gradients during cell operation.**

- For conditions we have simulated so far, the most severe stress state for the ceramics occurs at room temperature and not during cell operation.
- Severe residual stresses were built-up in the ceramic layers of the MEA during cool down from the stress-free sintering temperature.
  - Bending stresses, which arose to balance the moments created by anode/cathode TCE mismatch, caused warping of the ceramic MEA layers.
  - The warped MEA was ‘flattened’ by the application of a small confining pressure.
- At the steady state operating temperatures (650 - 850 °C), the residual stresses were relieved to some extent because the temperatures were closer to the stress-free sintering temperature (1400 °C).
- Under conditions simulated in this study, the temperature gradients during steady state operation did not generate severe stresses
  - The high thermal conductivity of the thick metallic interconnect lead only to modest temperature gradients
  - Also, the temperature gradients through the thickness of the ceramic layers were negligible

# Outline of Final Report

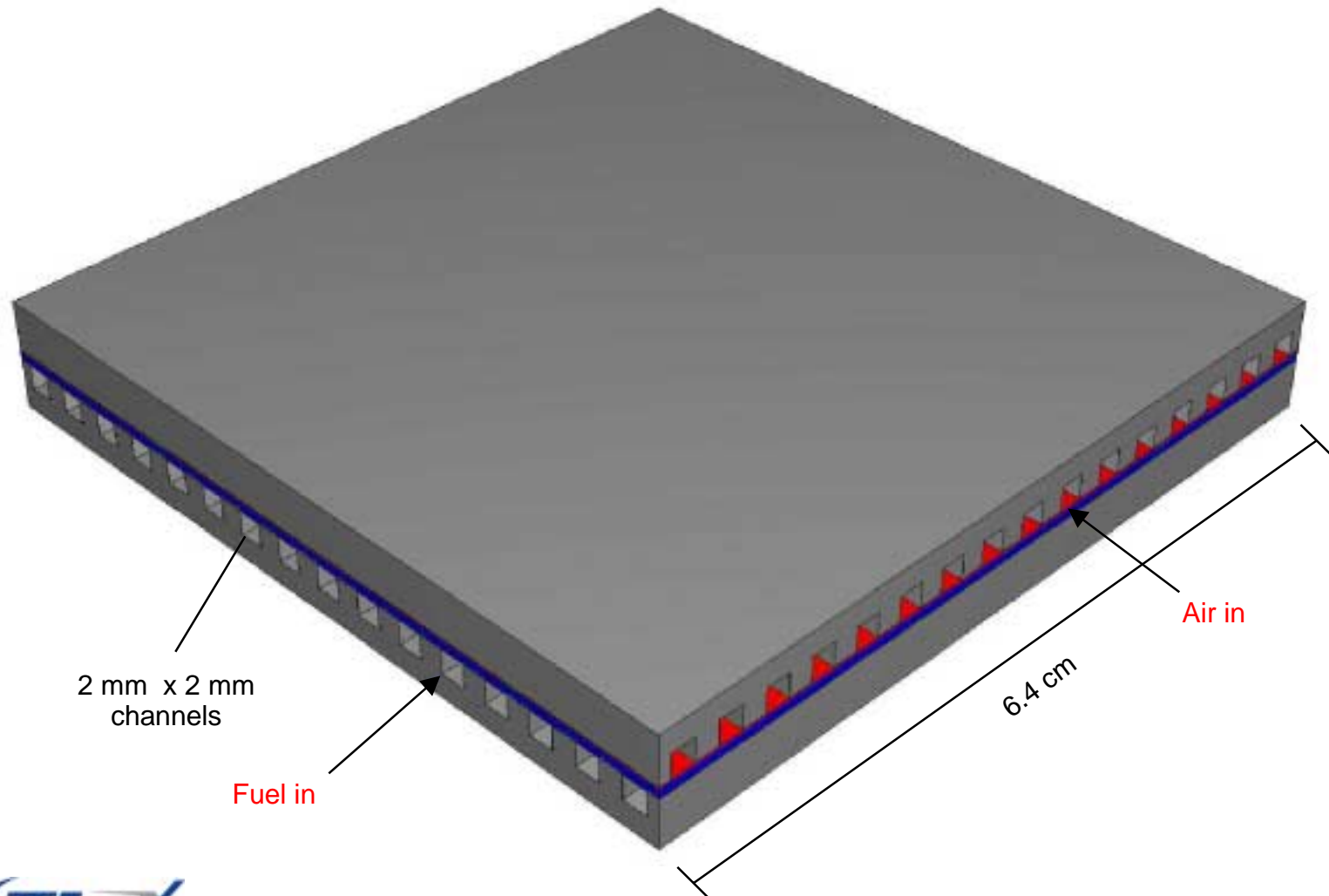
---

0	Executive Summary
1	Background & Objectives
2	Approach & Scope
3	Model Development
4	Single Channel SOFC Results
5	Multi Channel SOFC Results
6	Limitations for Cell Size
7	Summary
A	Appendix





To evaluate the impact of cell size, the model was extended to a 6.4-cm square cell with 16 channels in cross-flow.

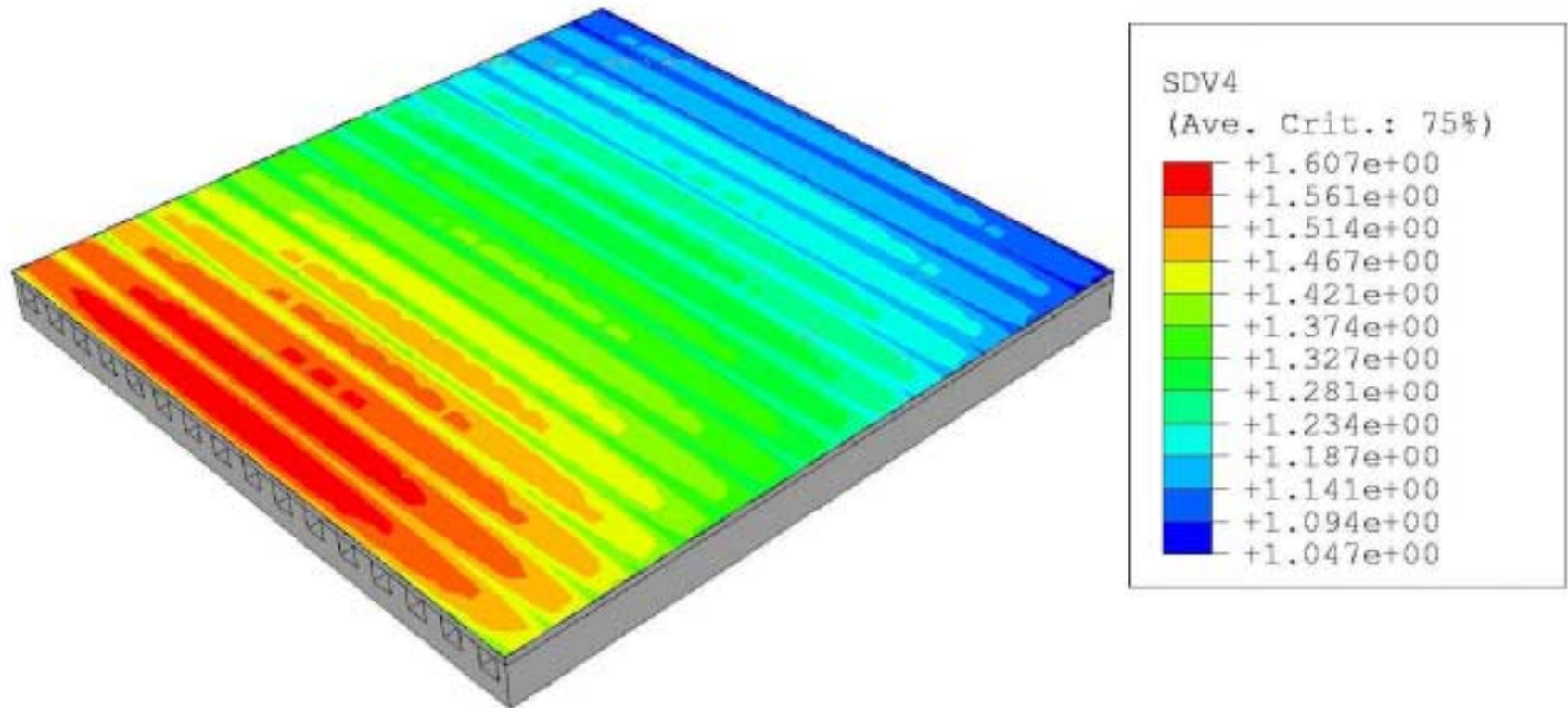


**We selected typical operating conditions consistent with the previous base cases.**

Parameter	Value
<ul style="list-style-type: none"> <li>• Cell voltage</li> <li>• Composition of the reactant streams</li> <li>• Gas inlet temperatures</li> <li>• Fuel utilization</li> <li>• Cathode stoichiometry</li> </ul>	<ul style="list-style-type: none"> <li>• 0.7 V</li> <li>• Anode: 97 % H<sub>2</sub>, 3 % H<sub>2</sub>O, Cathode: air</li> <li>• 650 C at the Anode and Cathode</li> <li>• ~ 50 %</li> <li>• ~ 6, the cathode flow rate was adjusted such that the temperature at the cell outlet was nominally 800 °C.</li> </ul>

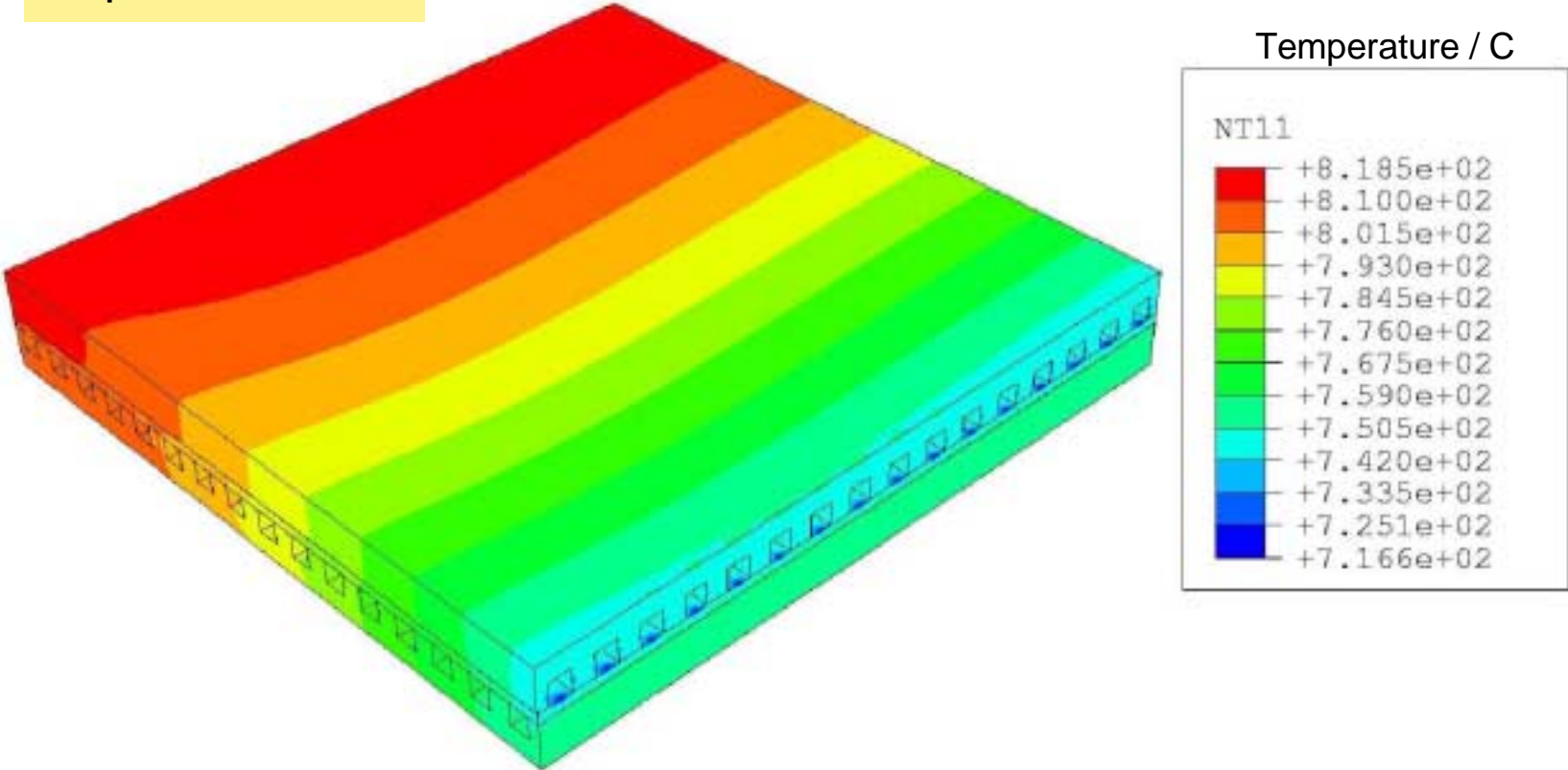
The current density distribution is similar to that obtained using the 3.2-cm cell with the baseline operating conditions.

Current density distribution, average = 1.3 A/cm<sup>2</sup>



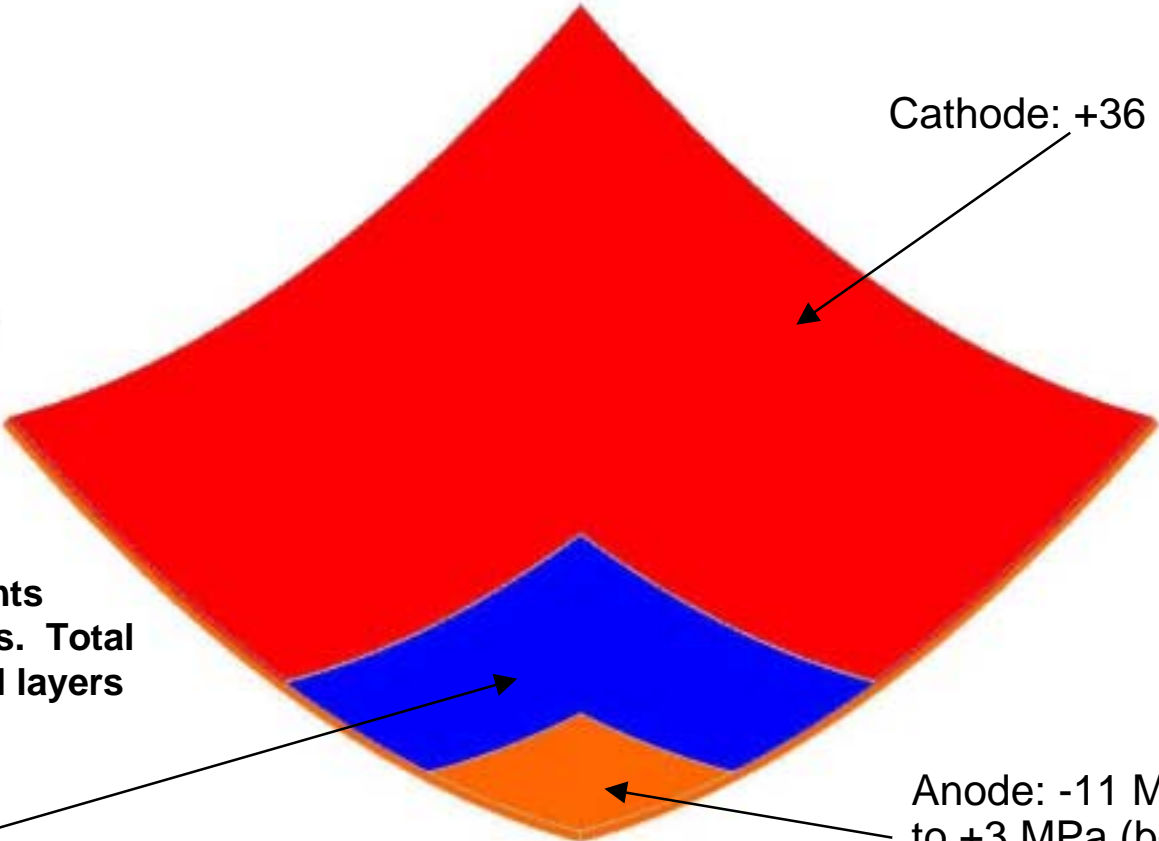
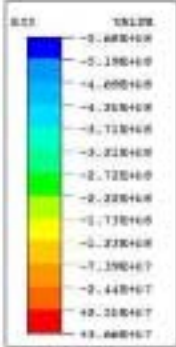
The larger cell dimensions lead to wider temperature distribution, but similar temperature gradients compared to the 3.2-cm cell.

Temperature distribution



In Step 1, the bending stresses are essentially unchanged from those for the 3.2-cm cell. However, the total warping increases linearly with cell area.

Residual stresses and warping in the ceramic layers at room temperature

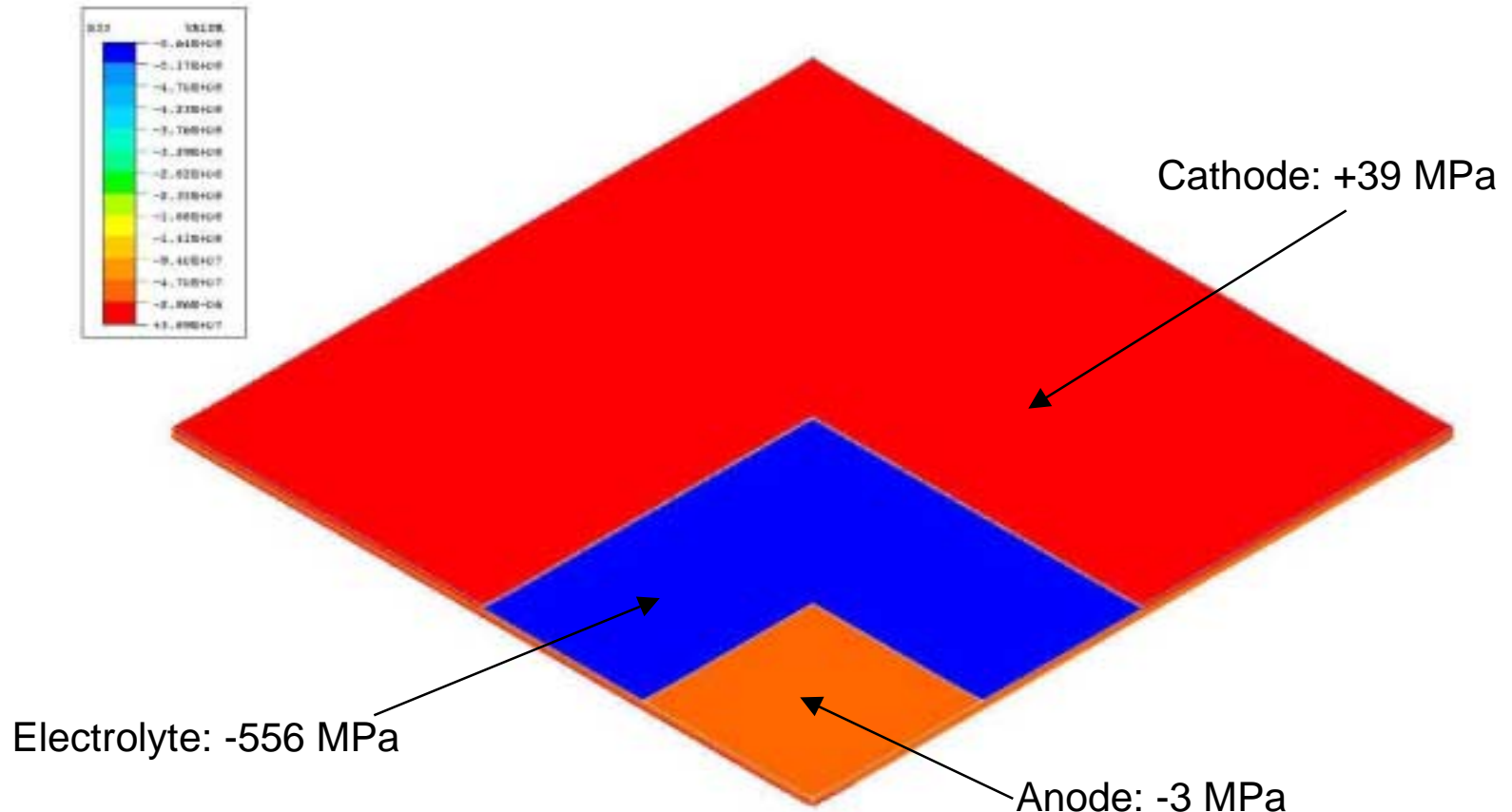


Note: displacements magnified 40 times. Total warping of the cell layers equals 0.12 mm.



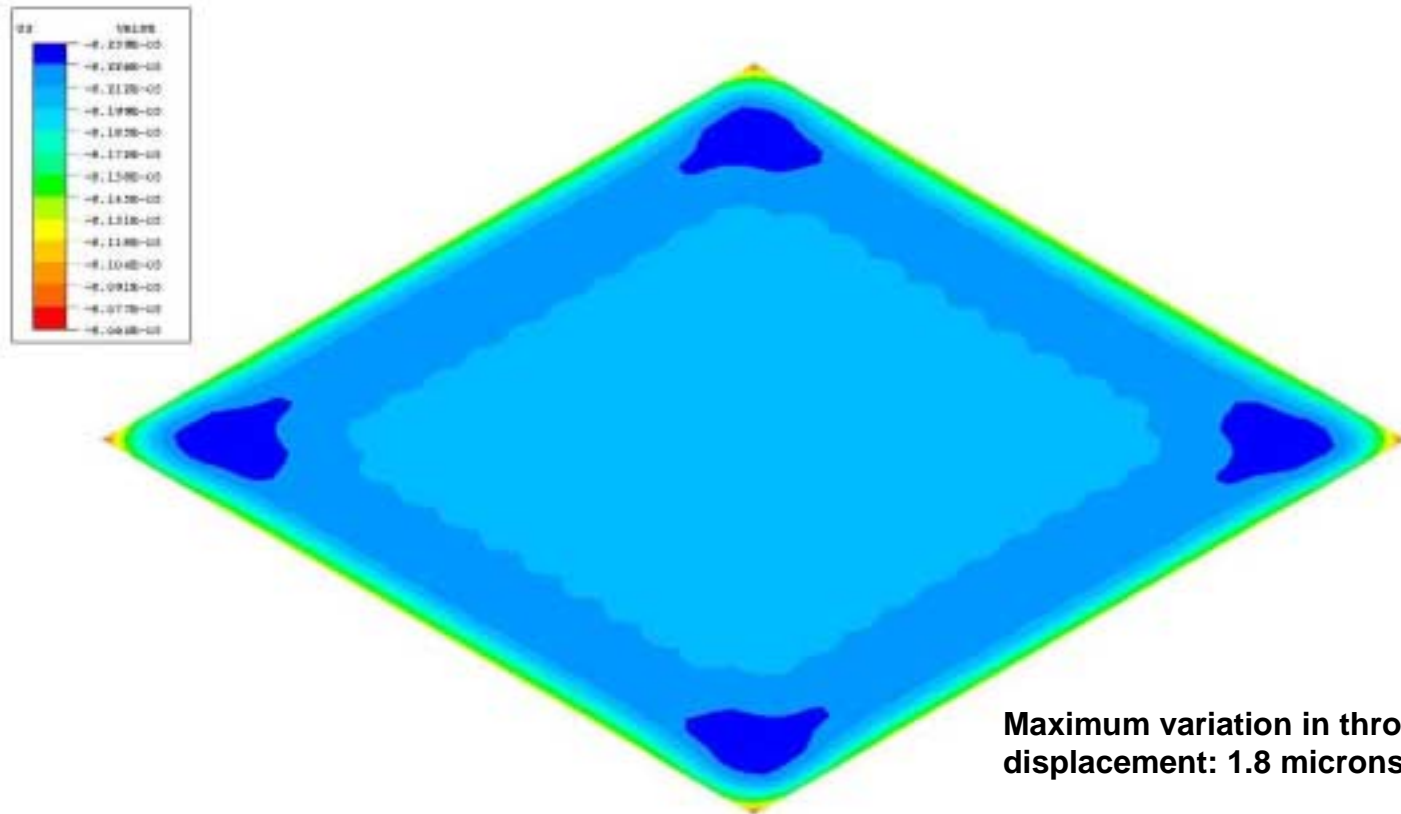
Application of a confining pressure (0.4 MPa) flattens the warped MEA and removes the anode bending stress, but does not alter the cathode or electrolyte stresses.

Stress in the ceramic MEA layers after 'flattening' between interconnects at room temperature



The variation in through-thickness displacement of the electrolyte shows essentially the same level of flatness as observed for the smaller cells.

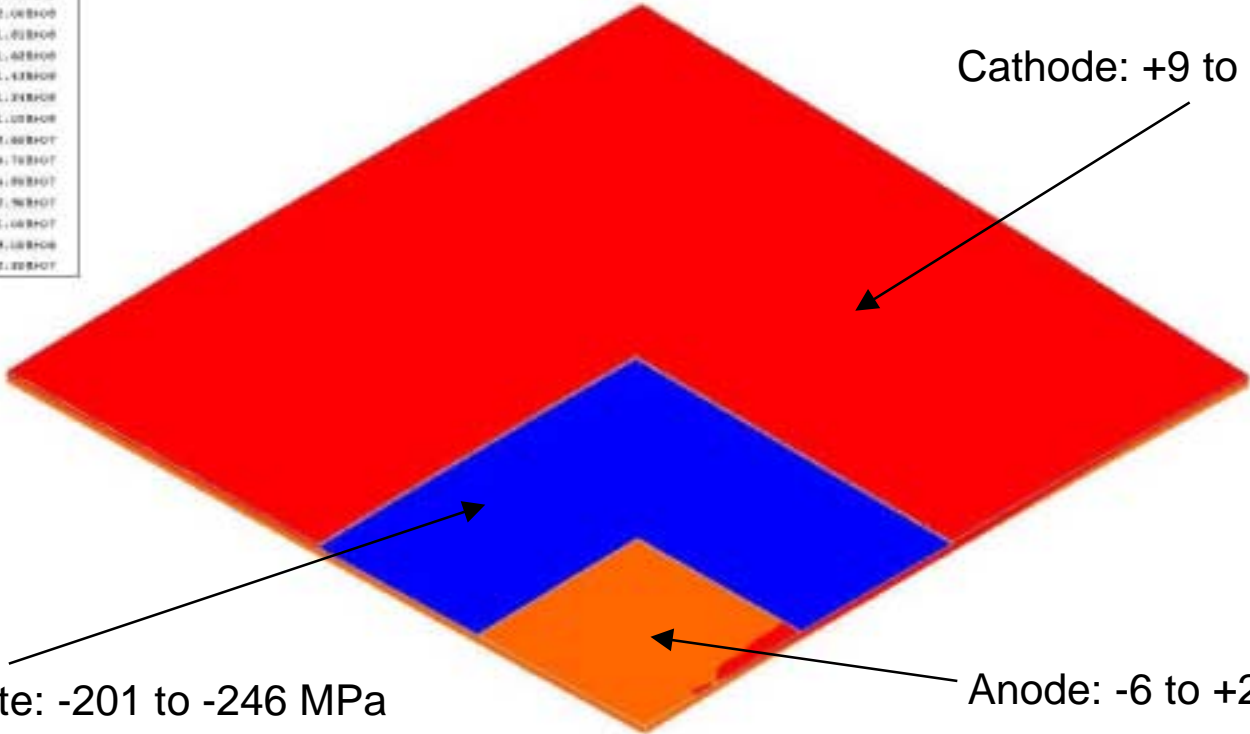
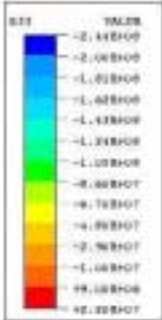
Through thickness displacement of electrolyte at room temperature





At steady-state, the stresses for the 6.4-cm case show a wider variation than those for the 3.2-cm case, though the average stresses are still less severe than the residual stresses.

Stress in the ceramic MEA for steady state operation at 0.7 V for the assumption of slip between the electrodes and the interconnect



Cathode: +9 to +22 MPa

Electrolyte: -201 to -246 MPa

Anode: -6 to +20 MPa

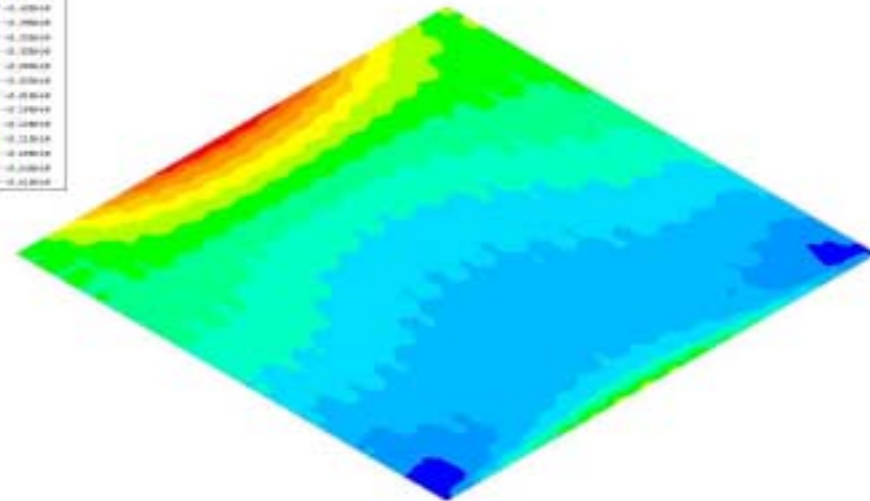
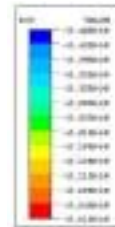
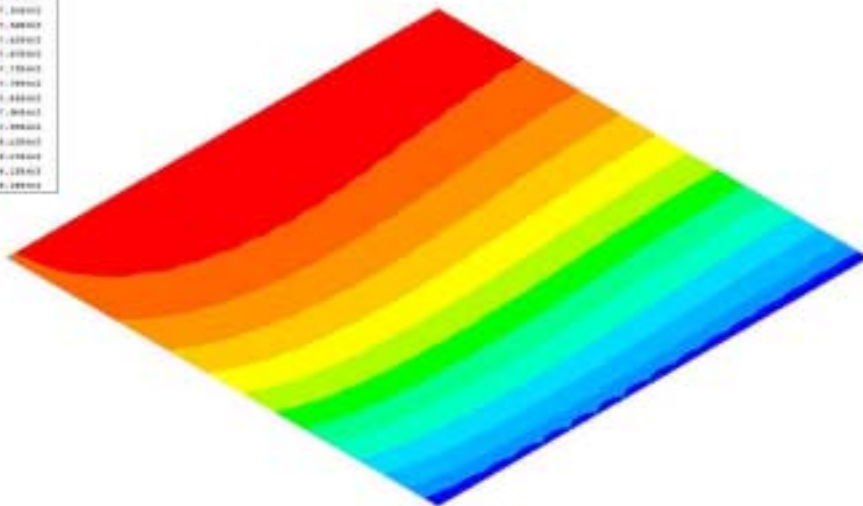
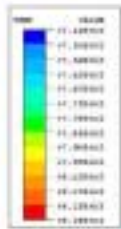




The stress variation in the electrolyte is much wider than it is for the 3.2-cm case ...

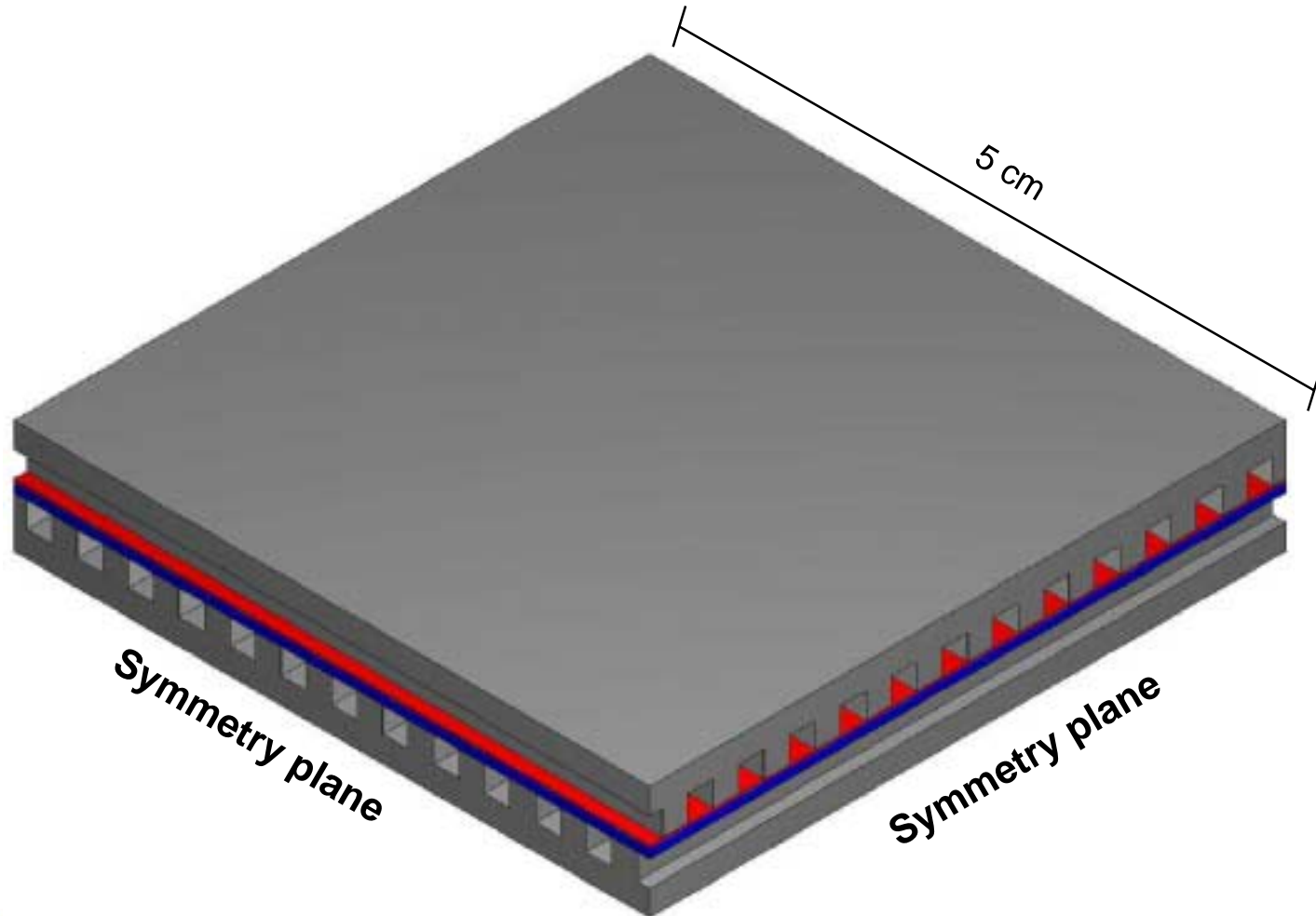
Electrolyte temperature varies from 744 °C (blue) to 818 °C (red) for operation at 0.7 V

Electrolyte stress varies from -246 MPa (blue) to -201 MPa (red) for operation at 0.7 V



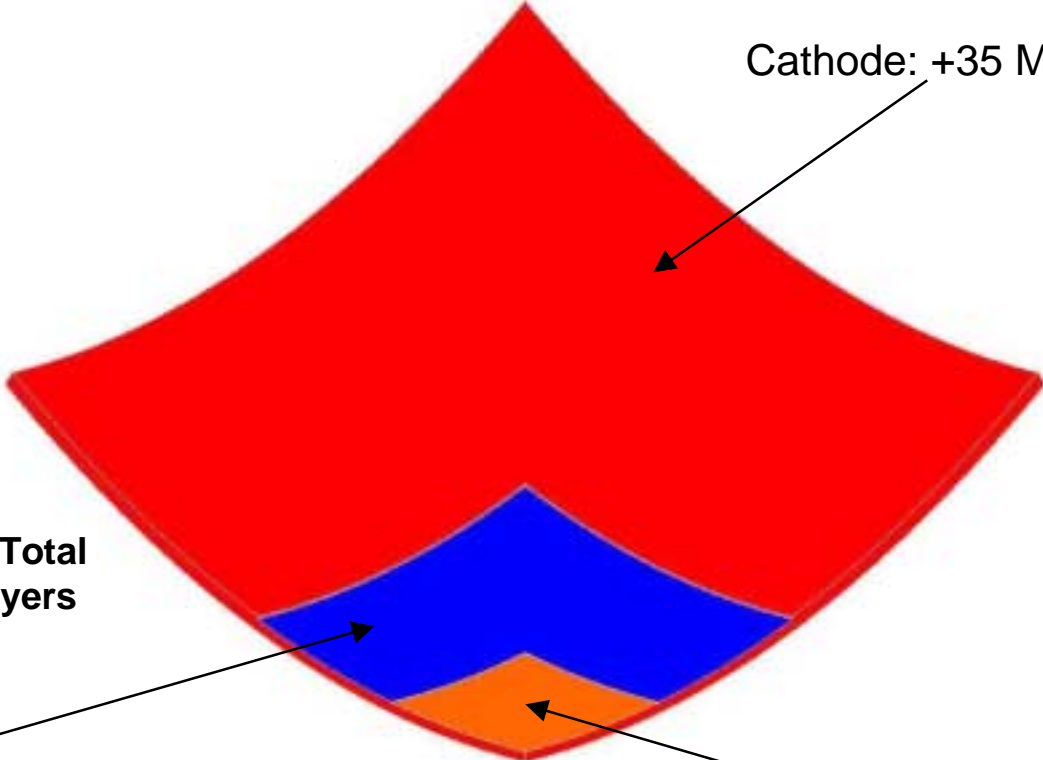
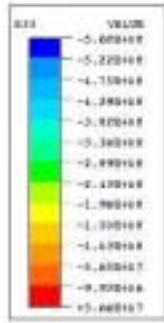
... however, the average stress value is unchanged, and the stress is much less severe than that at room temperature.

To calculate the room temperature stresses and displacements of larger cells we created a quarter model of a 10 x 10 cm cell.



In Step 1, the bending stresses are unchanged from those for the 3.2-cm and 6.4-cm cells. But, the total warping increases linearly with cell size.

Residual stresses and warping in the ceramic layers at room temperature

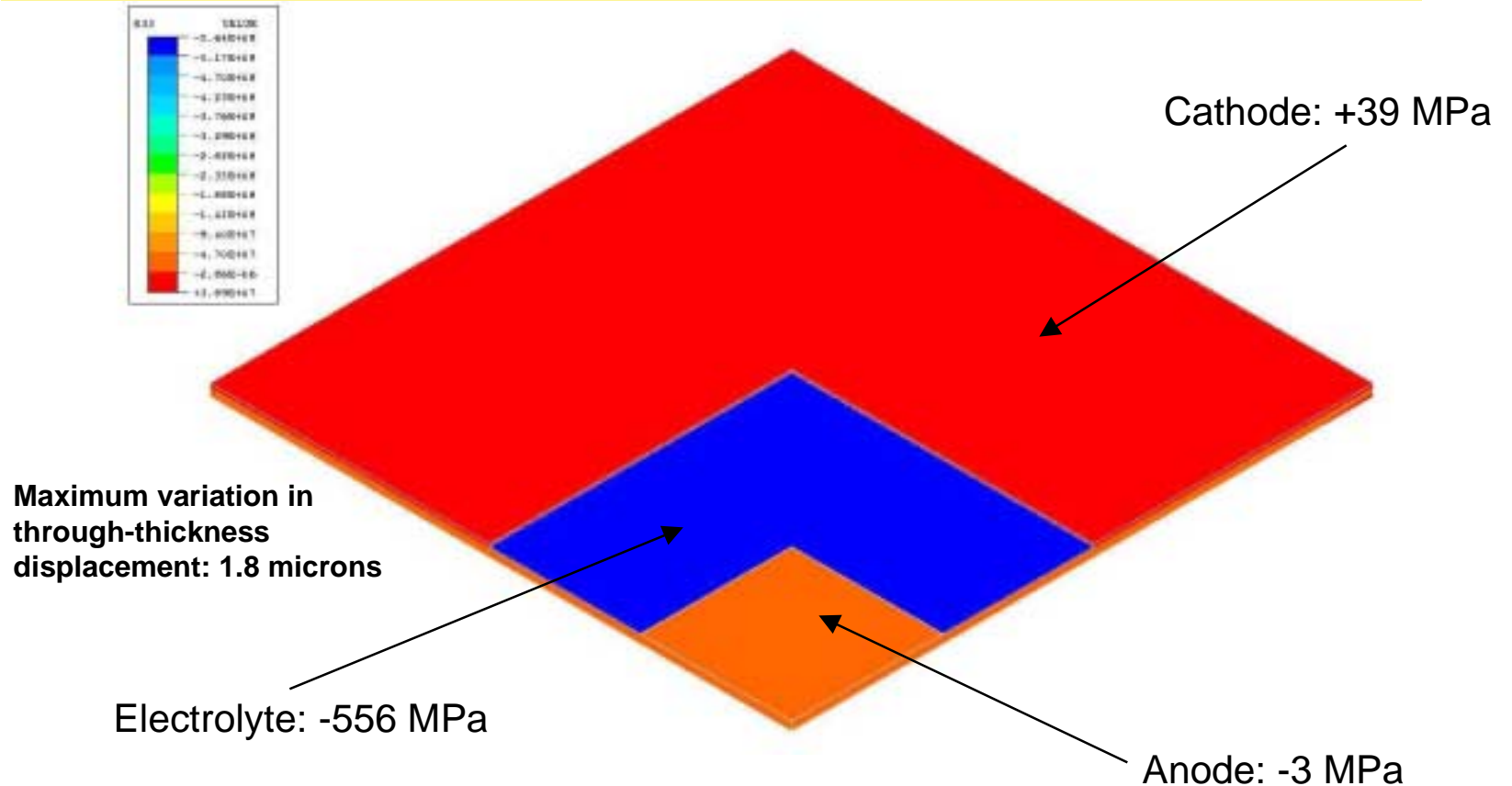


Note: displacements magnified 40 times. Total warping of the cell layers equals 0.28 mm.



After applying the confining pressure, the stresses and deflections in the MEA are identical to those observed in the 6.4-cm model.

Stress in the ceramic MEA layers after 'flattening' between interconnects at room temperature



**Increasing the cell size increases the total CTE-mismatch-related strains but does not significantly affect the stress state or flatness of the MEA.**

- To test the effects of cell area, the results of models representing 3.2-cm, 6.4-cm, and 10-cm square single cells were compared.
- Without application of the confining pressure, the total warping of the ceramic layer varies linearly with the cell area.
- Application of the 0.4 MPa confining pressure reduces the through-thickness displacement variation in the ceramic to below 2 microns for each of the cell sizes examined.
- The most severe stress state for the MEA is at room temperature, rather than under operating conditions, regardless of cell size.
- The average stresses in the MEA layers at room temperature do not depend strongly on the cell area.
- Increasing the cell area produces larger geometric incompatibilities along cell edges, possibly leading to seal failures.

## Outline of Final Report

---

0	Executive Summary
1	Background & Objectives
2	Approach & Scope
3	Model Development
4	Single Channel SOFC Results
5	Multi Channel SOFC Results
6	Limitations for Cell Size
7	Summary
A	Appendix

**In addition to facilitating in the construction of the structural model, the simple performance models provided critical insight into SOFC operation.**

- We have developed 1-d and 2-d, isothermal performance models for planar, anode supported SOFCs, that account for the details of the microstructures of the electrodes.
- The 1-d model calculates cell performance under conditions of low fuel utilization, whereas the 2-d model calculates the performance under high fuel utilization.
- The main results from using these models are:
  - The 1-d model was able to predict the temperature dependence of the performance of an anode-supported SOFC.
  - The cathode overpotential dominated the anode overpotential for operation between 650 - 800 °C, both at low and high fuel utilizations.
  - The higher cathode overpotential at the lower temperatures is a result as much of the poor ionic conductivity of the electrode as of the reduced kinetics.
  - Fuel utilization has a major impact on the power density of the cell mainly due to accumulation of water, which lowers the thermodynamic driving force and the hydrogen mole fraction.

**We verified the successful implementation and debugging of the SOFC performance model in ABAQUS using a single-channel fuel cell geometry.**

- We constructed the SOFC model in ABAQUS and used a simple geometry to verify the successful implementation of the different model elements.
- The model successfully calculated the profiles of temperature, current density, overpotentials, species concentrations, and stress for steady state operation under typical operating conditions.
- We probed the robustness of the model through a sensitivity analysis. The operating conditions were chosen so as to tax the numerical solution scheme:
  - high fuel utilization (85 %);
  - low cell voltage (0.6 V) ;
  - low air inlet temperature (500 C);
  - low flow of air (< 2 x stoichiometry).
- In all of these simulations, the model successfully converged and the resulting profiles of temperature, current density, species concentrations, and overpotentials were consistent with each other.
- In all of these simulations, the error in the mass balance was less than 1 % and error in the energy balance was less than 6 %.



## **The protocols for calculating the stress distribution during operation were also successfully implemented in ABAQUS.**

- The highest levels of stress occur following cool-down from the sintering temperature of 1400 C to room temperature.
  - The thick anode controls the deformation and experiences an in-plane stress of  $-3$  MPa (compression).
  - The compressive stress in the anode is balanced by tensile stress of 38 MPa in the thinner, more compliant cathode.
  - Because of its high coefficient of thermal expansion, the thin electrolyte develops a  $-556$  MPa compressive stress.
- Because the operating temperature is closer to the stress-free sintering temperature, the operating conditions actually relieve the stresses generated during the initial cooling step to room temperature.
- Imposition of ‘no-slip’ conditions along the MEA-interconnect interface increases the tensile stresses in the ceramic by 4 to 16 MPa and produces a shear stress of 5 to 6 MPa at the ends of the cell.
- It is unlikely that such high shear stresses could be sustained without interfacial bonding; simulation of interfacial friction reduces the shear stresses to less than 1 MPa.

**Stress calculations so far show that, absent defects, the ceramics are unlikely to fail due to temperature gradients during cell operation.**

- For conditions we have simulated so far, the most severe stress state for the ceramics occurs at room temperature and not during cell operation.
- Severe residual stresses were built-up in the ceramic layers of the MEA during cool down from the stress-free sintering temperature.
  - Bending stresses, which arose to balance the moments created by anode/cathode TCE mismatch, caused warping of the ceramic MEA layers.
  - The warped MEA was ‘flattened’ by the application of a small confining pressure.
- At the steady state operating temperatures (650 - 850 °C), the residual stresses were relieved to some extent because the temperatures were closer to the stress-free sintering temperature (1400 °C).
- Under conditions simulated in this study, the temperature gradients during steady state operation did not generate severe stresses
  - The high thermal conductivity of the thick metallic interconnect lead only to modest temperature gradients
  - Also, the temperature gradients through the thickness of the ceramic layers were negligible

**Increasing the cell size increases the total CTE-mismatch-related strains but does not significantly affect the stress state or flatness of the MEA.**

- To test the effects of cell area, the results of models representing 3.2-cm, 6.4-cm, and 10-cm square single cells were compared.
- Without application of the confining pressure, the total warping of the ceramic layer varies linearly with the cell area.
- Application of the 0.4 MPa confining pressure reduces the through-thickness displacement variation in the ceramic to below 2 microns for each of the cell sizes examined.
- The most severe stress state for the MEA is at room temperature, rather than under operating conditions, regardless of cell size.
- The average stresses in the MEA layers at room temperature do not depend strongly on the cell area.
- Increasing the cell area produces larger geometric incompatibilities along cell edges, possibly leading to seal failures.

**We are currently exploring more realistic operating conditions (not considered in this study) for determining cell-size limitations.**

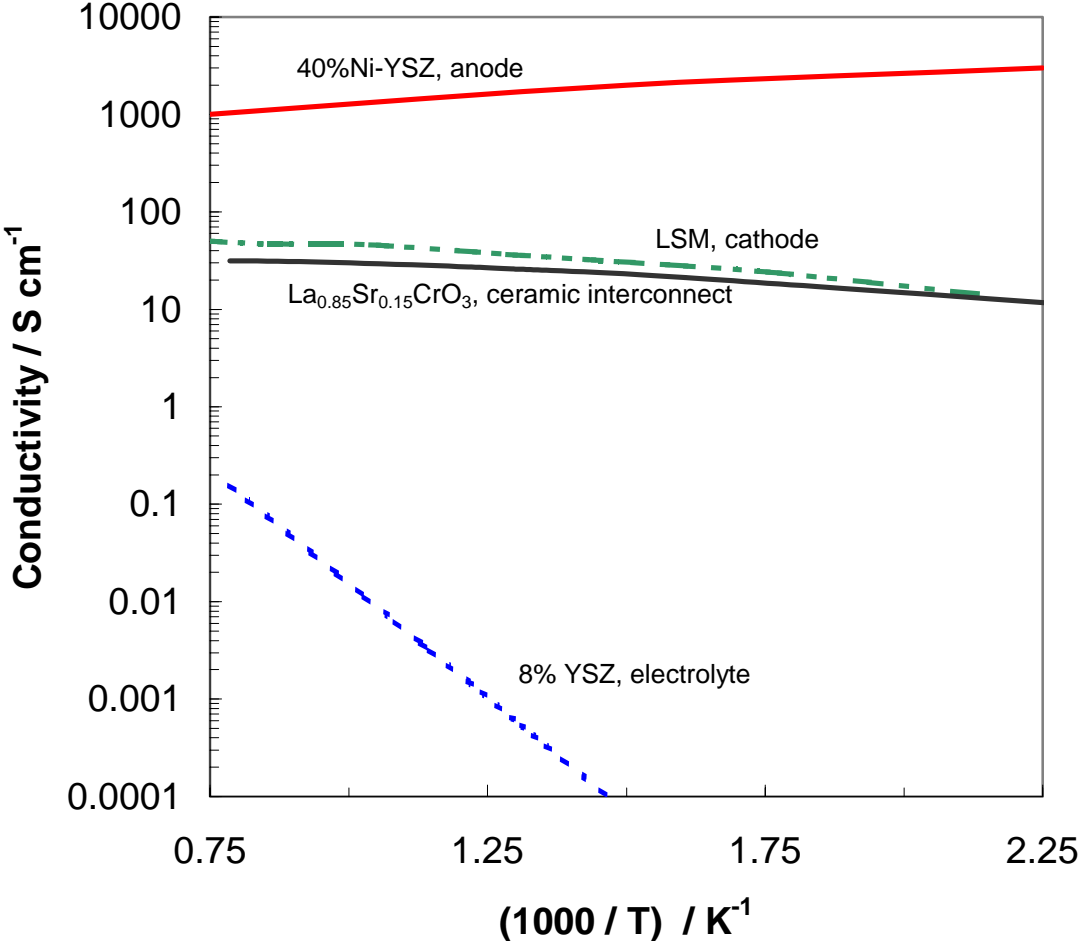
- Potential causes for cell-size limitations not considered in this study:
- **Defects**
  - Ceramic MEAs are known to have defects. The defect density will clearly be higher for larger cells making them prone to failure.
- **Larger temperature gradients**
  - Heat loss from the edges of the stack
  - Internal reforming
- **Seal failure**
  - With larger cells, the total mismatch in strains is also higher, which might increase the probability of seal failure.
- **Unequal application of compressive load**
  - With large area cells it becomes difficult to apply a uniform load on the cell active area.
  - Unequal compressive force can lead to localized high contact resistance, which in turn might lead to local hot-spots because of resistive heating.

## Outline of Final Report

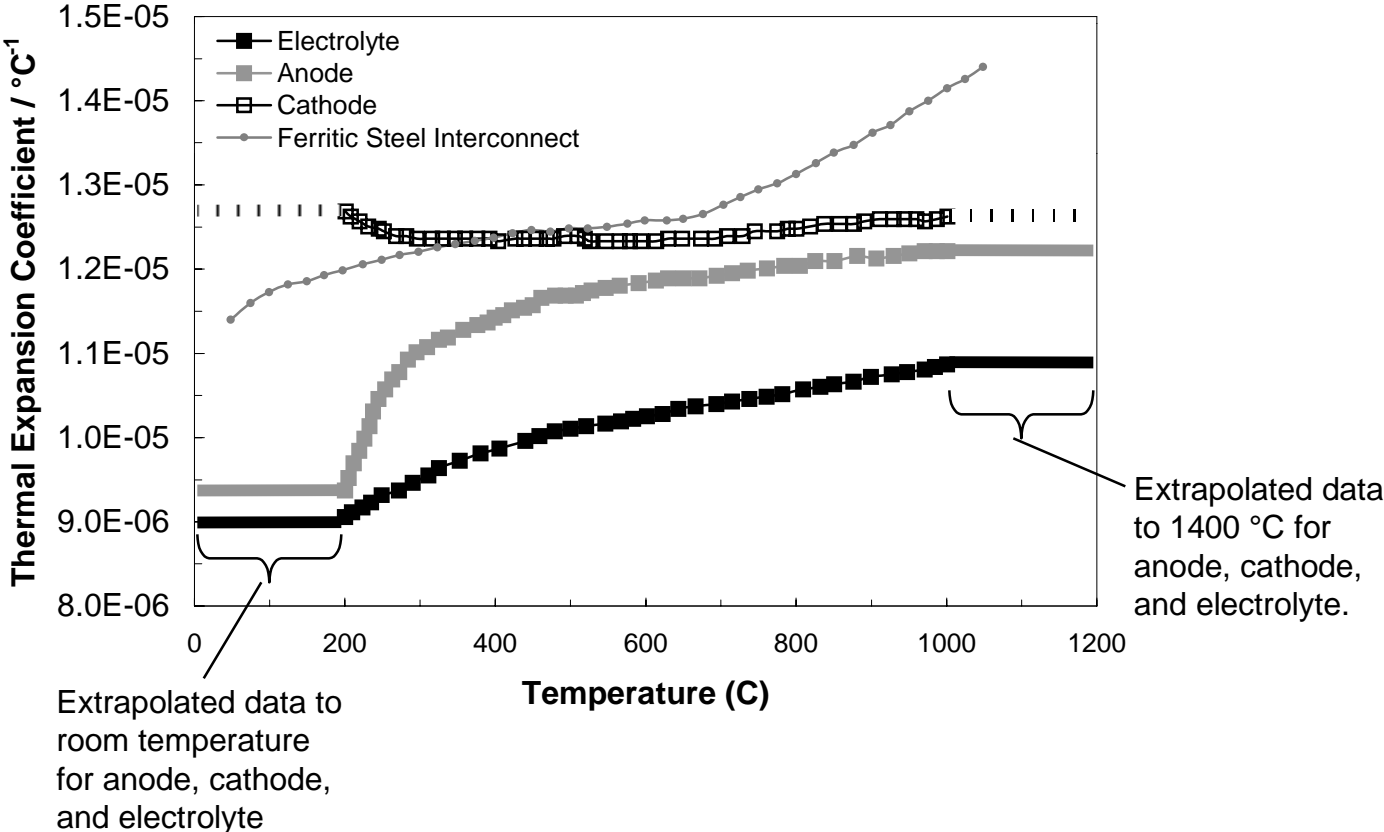
---

0	Executive Summary
1	Background & Objectives
2	Approach & Scope
3	Model Development
4	Single Channel SOFC Results
5	Multi Channel SOFC Results
6	Limitations for Cell Size
7	Summary
A	Appendix

We used the measured temperature dependent conductivities of the anode electrolyte, and cathode.



We used the measured temperature dependent conductivities of the anode electrolyte, and cathode.



\* Data from J. P. Abellan, F. Tietz, L. Singheiser, W. J. Quadackers, A. Gil, in Proceedings of SOFC-V, S. Singhal, U. Stimming, H. Tagawa, W. Lehnert, Eds., Published by The Electrochemical Society (1997) 652.



Following are the parameters used to fit Virkar's data with the 1-d model.

	Units	Anode	Cathode
Exchange Current Density on a Volume Basis <sup>1</sup>	A cm <sup>-3</sup>	4.16 x 10 <sup>6</sup>	2.4x 10 <sup>5</sup>
Activation Energy	kJ/mol	33.2	33.2
Forward Transfer Coefficient <sup>2</sup>	-	0.8	0.67
Tortuosity	-	12.5	3
Thickness of the Reaction Zone	μm	10	10
Porosity	-	0.4	0.4
Fraction of the Solid Phase That is the Ionic Conductor	-	0.5	0.5

<sup>1</sup> The exchange current density is typically given on an area basis and multiplied by the three-phase area per unit volume, to convert to a volume basis. Here, the value reported is after converting to the volume basis.

<sup>2</sup> The transfer coefficient for the reverse reaction was 1-the forward transfer coefficient.